UNIVERSIDAD AUTÓNOMA DE MADRID

Facultad de Ciencias

Departamento de Biología Molecular

Development of *Escherichia coli* cell surface display for selection of single domain antibodies from immune libraries

Doctoral Thesis

Valencio Francis Salema

Madrid 2014

Tesis presentada por D. Valencio Francis Salema para optar al grado de Doctor en Ciencias por la Universidad Autónoma de Madrid.

Director de la Tesis Doctoral:

Dr. Luis Ángel Fernández Herrero, Investigador Científico del Consejo Superior de Investigaciones Científicas.

Este trabajo ha sido realizado en el Departamento de Biotecnología Microbiana del Centro Nacional de Biotecnología (CSIC) gracias a la financiación recibida de la Fundación "La Caixa", el Ministerio de Economía y Competitividad (MINECO), la Comunidad Autónoma de Madrid y el *European Research Council* (ERC).

ACKNOWLEDGEMENTS

First and foremost, I thank my Thesis director, Dr Luis Angel Fernandez, for the excellent supervision and support extended to me during my PhD work. You have facilitated my integration into the lab, and I am very grateful for the time and effort you put in the process. Through everything, you have been patient and supportive, always valuing people above science. You are a brilliant scientist with fantastic ideas and I have been very fortunate to learn as much as I could, from you.

Secondly, I thank all my labmates, both current and former members, for the excellent working environment and friendly atmosphere I have experienced during my stay. It was a joy to come work in everyday, especially knowing how everyone is willing to help each other. In particular: Elvira, Carlos, Carmen Palomino, Gustavo, David and Ana for all the discussions and guidance. You all have helped me think more critically and I wouldn't be where I am today without you. Thank you for all for the help you have offered me through the years, especially teaching me all the basics – like running a gel! Special thanks to Carlos, Carmen Mañas, Lorenza, Massiel, Ariadna, Beatriz and Yago, for always being there to discuss science, but more importantly to discuss everything else. I know I wouldn't have survived the PhD without our morning and afternoon coffee breaks!

I also extend my sincere gratitude to my PhD tutor, Dr José Lopez Carrascosa, for the help, guidance and ideas received during my PhD work, and to Dr Paolo Natale for the review of my thesis manuscript and suggestions for improvement.

Performance of a lot of my PhD work would not have been possible without collaboration with other laboratories in the CNB and outside. First and foremost, I wish to thank the Flow cytometry department, especially Dr Maria del Carmen and Sara, for the help you offered during setting up of the flow cytometry protocols. I also acknowledge the help received from the Protein Tools unit, especially Dr Leonor Kremer and Mayte Martin during the BiaCore experiments. Special thanks to Dr José M. Pingarrón and group, Electroanalysis and Electrochemical Biosensors

Group, UCM for the collaborative work that lead to the development of a biosensor for fibrinogen detection.

I thank all my flatmates, especially Tribhuwan, Praveen, Acharya and Mayank, and special friends, especially Carlos, Gorjana and Daniela. You have all touched my life and made me a better person, and I hope that our friendship lasts the test of time.

I thank God for this wonderful opportunity to carry out my PhD work in Spain. It has been a fantastic experience filled with challenges and learning. I have enjoyed travelling and exploring what this great country has to offer. I have come across so many wonderful people, many of whom have touched my life.

Lastly, I thank my Father (Alex), Mother (Norma) and Brother (Valmiki), for all the love, support and help that I have received all these years. It has been difficult living away from you, and hence I would not have achieved what I have, without your constant love, encouragement and prayers.

TABLE OF CONTENTS

TABLE OF CONTENTS 6
ABBREVIATIONS 12
SUMMARY 16
PRESENTACIÓN 20
INTRODUCTION 26
1. Antibodies and Recombinant antibody fragments 28
1.1 Antibodies and their application in human therapy 28
1.2 Recombinant fragments from conventional antibodies 31
1.3 Heavy-chain only antibodies, single domain antibodies and nanobodies 32
2. Selection of antibodies from libraries using surface display. 35
2.1 Libraries of antibody genes 35
2.2 Surface display methods for screening of Ab libraries 37
2.2.1 Phage display 37
2.2.2 Cell surface display 40
2.2.2.1 Yeast Display 40
2.2.2.2 Bacterial cell surface display 42
2.3 *E. coli* cell surface display of Ab libraries 42
OBJECTIVES 48
MATERIALS AND METHODS 52
1. Bacterial strains 54
2. Conditions of bacterial growth 54
3. Cell lines and Growth conditions 55
4. DNA constructions 55
5. Protein electrophoresis and Western blot 57
6. Protease accessibility assays 59
7. ELISA 59
8. Purification of $TirM_{EHEC}$ 60
9. Magnetic Cell Sorting (MACS) of V_{HH} immune libraries 60
10. Flow cytometry of V_{HH} clones or V_{HH} immune libraries 61
11. Affinity Determination by Flow cytometry 62

12. Purification of VHHs from the periplasm of *E. coli* 62
13. Purification of VHHs from the periplasm as fusions with Maltose binding protein (MBP) 63
14. Surface plasmon resonance (SPR) 64
15. Selection of VHH immune libraries on cells 65
16. Immunofluorescence microscopy (IFM) 65

RESULTS 68

Chapter 1: Display of single domain Ab clones and immune libraries against TirMEHEC and Human fibrinogen on the surface of *E. coli* cells 70

1.1 Comparison of EhaA and Intimin β-domains for display of sdAbs on *E. coli* 70
1.2 Construction of immune libraries against TirMEHEC and Fib, analysis of expression, display levels and cellular toxicity 74

Chapter 2: Selection and characterization of single domain Abs against TirMEHEC from immune libraries displayed on the surface of *E. coli* 80

2.1 Translocated Intimin Receptor domain M (TirM) 80
2.2 Selection of single domain Abs against $TirM_{EHEC}$ by magnetic sorting of *E. coli* bacteria displaying the immune library 81
2.3 Characterization of VTIR1 sdAb and determination of its affinity by Surface Plasmon Resonance (SPR) 86
2.4 Estimation of the affinity of VTIR1 by *E. coli* display 88

Chapter 3: Selection and Characterization of high affinity single domain Abs against Human Fibrinogen from Immune libraries displayed on the surface of *E. coli* cells 91

3.1 Human Fibrinogen (Fib). 91
3.2 Selection of high affinity single domain Abs from the immune library against Fib by MACS 92
3.3 Purification of VFIB1 and VFIB2 VHHs from the periplasm of *E. coli* as fusions to MBP 95
3.3.1 Expression and solubility of the MBP-VHH_{His6} fusions 95
3.3.2 Purification of MBP-VHH_{His6} fusions and antigen binding activity 97
3.3.3 Purification of monomeric VHH_{His6} from MBP-VHH_{His6} fusions 99
3.4 Determination of the affinity of VFIB1 and VFIB2 by Surface Plasmon Resonance (SPR) 102

3.5 Estimation of the affinity of V_{FIB1} and V_{FIB2} by *E. coli* display 103

Chapter 4: Cell Selection and characterization of high affinity single domain Abs against human EGFR from immune libraries displayed on the surface of *E. coli* cells 105

4.1 Epidermal Growth Factor Receptor (EGFR) 105

4.2 Construction of immune sdAb library against Human EGFR 106

4.3 Selection of high affinity sdAbs from the anti-EGFR immune library by MACS 107

4.4 Direct cell selection of high affinity sdAbs against EGFR using *E. coli* display 108

4.5 Binding of selected clones to EGFR+ tumor cells by immunofluorescence microscopy 112

4.6 Binding of selected clones to biotinylated rhEGFR-Fc by flow cytometry 114

4.7 Estimation of the affinity of V_{EGFR1} and V_{EGFR2} by *E. coli* display 116

4.8 Binding of the selected clones to EGFR in the presence of EGF 116

DISCUSSION 118

CONCLUSIONS 128

REFERENCES 134

ANNEXURES 148

LIST OF FIGURES

Figure 1. Structure of conventional antibodies and antibody derived fragments. 28
Figure 2. Chimeric and humanized antibodies. 30
Figure 3. Structure of camelid heavy chain only antibodies and nanobodies. 32
Figure 4. Comparison between conventional V_H/V_L and V_{HH} antibody fragments. 34
Figure 5. Phage display of antibodies. 39
Figure 6. Yeast display of antibodies. 41
Figure 7. *E. coli* display of antibodies. 44
Figure 8. Proposed mechanism of the biogenesis of protein members belonging to the type V secretion system (T5SS). 46
Figure 9. Modular organization and structure of AT and Intimin proteins. 47
Figure 10. *E. coli* cell surface display of V_{HH}s with EhaA and Intimin beta domains. 72
Figure 11. Growth of *E. coli* cultures expressing VgfpA and NVgfp fusions. 73
Figure 12. *E. coli* cell surface display and antigen-binding activity of VgfpA and NVgfp. 74
Figure 13. *E. coli* cell surface display of anti-$TirM_{EHEC}$ and anti-Fib immune libraries. 76
Figure 14. Quantification of the number of molecules of V_{HH}A and NV_{HH} fusions expressed in *E. coli*. 77
Figure 15. Growth of *E. coli* cultures expressing V_{HH}A and NV_{HH} libraries against anti-$TirM_{EHEC}$. 77
Figure 16. The Intimin-Tir interaction between EPEC/EHEC bacteria and host cell plasma membrane. 80
Figure 17. Schematic illustration of Magnetic cell sorting (MACS). 81
Figure 18. Magnetic cell sorting of V_{HH}A and NV_{HH} *E. coli* display libraries with biotinylated antigen, $TirM_{EHEC}$. 83
Figure 19. Binding of *E. coli* cells displaying selected clones from V_{HH}A and NV_{HH} libraries to biotinylated $TirM_{EHEC}$. 84
Figure 20. *E. coli* cell surface display levels of V_{TIR1}A and NV_{TIR1} clones. 85
Figure 21. ELISA of sdAbs selected by *E. coli* display against $TirM_{EHEC}$. 86
Figure 22. Monomeric behaviour and binding activity of the purified sdAb, V_{TIR1}. 87
Figure 23. Determination of the equilibrium dissociation constant (K_D) of V_{TIR1} by SPR. 88
Figure 24. Estimation of the equilibrium dissociation constant (K_D) of V_{TIR1} by *E. coli* display. 89
Figure 25. Structure of Fibrinogen. 91

Figure 26. Magnetic cell sorting of $V_{HH}A$ and NV_{HH} *E. coli* display libraries with biotinylated antigen, Fib. 93
Figure 27. Binding of *E. coli* cells displaying selected clones from $V_{HH}A$ and NV_{HH} libraries to biotinylated Fib. 94
Figure 28. Schematic representation of protein expression vector. 95
Figure 29. Induction and solubility of the MBP-fusions. 96
Figure 30. Purification of the MBP-fusions by Amylose affinity chromatography and their functional analysis by ELISA. 98
Figure 31. Expression and purification of V_{HH}s in *E. coli*. 99
Figure 32. Protease digestion of MBP-V_{HH} fusions, Immobilized Metal Affinity chromatography (IMAC) and Gel filtration. 100
Figure 33. Monomeric V_{HH}s and assay of functional activity by ELISA. 101
Figure 34. Determination of the equilibrium dissociation constant (K_D) of clones V_{FIB1} and V_{FIB2} by SPR. 102
Figure 35. Estimation of the equilibrium dissociation constant (K_D) of clones V_{FIB1} and V_{FIB2} against Fib by *E. coli* display. 103
Figure 36. Schematic of EGFR and the states in which it exists. 106
Figure 37. Magnetic cell sorting of NV_{HH} *E. coli* display libraries with biotinylated rhEGFR-Fc antigen. 108
Figure 38. Direct selection of NV_{HH} *E. coli* display libraries on cells. 109
Figure 39. Flow cytometry analysis of anti-EGFR NV_{HH} *E. coli* display libraries selected on cells. 110
Figure 40. Bright field and immunofluorescence microscopy images of *E. coli* bacteria displaying the indicated V_{HH} clone to HER14 and NIH-3T3 2.2 cells. 113
Figure 41. Bright field and immunofluorescence microscopy images of *E. coli* bacteria displaying the indicated V_{HH} clone to HER14 and NIH-3T3 2.2 cells (continued). 114
Figure 42. Binding of *E. coli* cells displaying selected clones from anti-EGFR NV_{HH} libraries to biotinylated rhEGFR-Fc. 115
Figure 43. Estimation of the equilibrium constant (KD) of V_{EGFR1} and V_{EGFR2} by *E. coli* display. 116
Figure 44. Flow cytometry analysis of binding to EGFR by the clones selected by *E. coli* display in the presence of EGF. 117

LIST OF TABLES

Table 1. Benefits and Limitations of Phage display and Yeast Display. 42
Table 2. Bacterial strains used in this work. 54
Table 3. List of plasmids used in this work. 56
Table 4. List of oligonucleotides. 57
Table 5. Summary of MACS with *E. coli* display libraries against TirM^{EHEC}. 82
Table 6. CDR3 sequences of anti-TirM^{EHEC} clones selected by *E. coli* display. 85
Table 7. Summary of MACS with *E. coli* display libraries against Fib. 92
Table 8. CDR3 sequences of anti-Fib clones selected by *E. coli* display. 94
Table 9. Protein yields after purification from the periplasm of *E. coli* HM140. 101
Table 10. Summary of MACS with *E. coli* display libraries against rhEGFR. 107
Table 11. Summary of Cell selections with NV^{HH} *E. coli* display library against rhEGFR. 110
Table 12. CDR3 sequences of anti-EGFR clones selected by *E. coli* display 111

ABBREVIATIONS

2-ME	2-mercaptoethanol
aa	amino-acid
Ab	antibody
ADCC	Antibody dependent cellular cytotoxicity
Ap	Ampicillin
APEx	Anchored periplasmic expression
AT	Autotransporter
bp	base pair
BSA	Bovine Serum Albumin
CDR	Complementarity determining region
C_H	Constant domain of the heavy chain of an immunoglobulin
C_L	Constant domain of the light chain of an immunoglobulin
Cm	Chloramphenicol
Da	daltons
DAPI	4',6-diamidino-2-fenilindol
DMEM	Dulbecco's modified Eagle´s medium
DNA	Deoxyribonucleic acid
DTT	Dithiotreitol
EDTA	Etylenediamino tetracetic acid
EGFR	Epidermal growth factor receptor
EHEC	Enterohemorrhagic *Escherichia coli*
ELISA	Enzyme-linked immunosorbent assay
EPEC	Enteropathogenic *Escherichia coli*
Fab	Antigen binding fragment
FACS	Fluorescence activated cell sorting
Fc	Crystallizable fragment of an Ab
Fib	Human Fibrinogen
Fv	Variable fragment of an Ab
GFP	Green Fluorescent Protein

h	hour
HCAb	Heavy chain only Ab
His_6	Hexahistidine sequence
Ig	Immunoglobulin
IM	Inner membrane
IPTG	Isopropylthio-β-D-galactoside
kb	kilobase
kDa	kiloDalton
Km	Kanamycin
LB	Luria-Bertani medium
LPS	Lipopolysaccharide
mAb	Monoclonal antibody
MACS	Magnetic cell sorting
MBP	Maltose binding protein
μl	microlitre
μM	micromolar
ml	millilitre
mM	millimolar
min	minute
MOI	Multiplicity of infection
MW	Molecular weight
Nb	Nanobody
nm	nanometer
nM	nanomolar
OD_{600}	Optical density at 600 nm
OD_{490}	Optical density at 490 nm
OM	Outer membrane
ORF	Open reading frame
PBS	Phosphate buffered saline
PCR	Polymerase chain reaction
PG	Peptidoglycan
POD	Peroxidase

PPS	Periplasmic space
rpm	revolutions per minute
rAb	Recombinant antibody
scFv	Single chain fragment variable
sdAb	Single domain antibody
SDS	Sodium dodecyl sulphate
SPR	Surface plasmon resonance
T5SS	Type V secretion system
Tir	Translocated intimin receptor
TirM	Extracellular domain of Tir
$\mathbf{V_H}$	Variable domain of the heavy chain of an Ig
$\mathbf{V_{HH}}$	Variable domain of the heavy chain of a HCAb, also called *nanobody*
$\mathbf{V_L}$	Variable domain of the light chain of an Ig
wt	Wild type

SUMMARY

Screening of antibody (Ab) libraries by direct display on the surface of *E. coli* cells is hampered by the presence of the outer membrane (OM). In this work, we demonstrate that the native β-domains of EhaA autotransporter and Intimin, two proteins from enterohemorrhagic *E. coli* O157:H7 (EHEC) with opposite topologies in the OM, are effective systems for the display of immune libraries of single domain Abs (sdAbs) from camelids (nanobodies or VHH) on the surface of *E. coli* K-12 cells and for the selection of high affinity sdAbs using magnetic cell sorting (MACS). We analyzed the capacity of EhaA and Intimin β-domains to display individual sdAbs and sdAb libraries obtained after immunization of camelids with different proteins of biomedical interest, i.e. the extracellular domain of the translocated intimin receptor from EHEC (TirMEHEC), human fibrinogen (Fib) and A431 cells displaying human epidermal growth factor receptor (EGFR). We demonstrated that both systems displayed functional sdAbs on the surface of *E. coli* cells with little proteolysis and cellular toxicity, although *E. coli* cells displaying sdAbs with the β-domain of Intimin showed higher antigen-binding capacity. The sdAb libraries against TirMEHEC and Fib cloned in both *E. coli* display platforms were screened for antigen binding clones by MACS using purified biotinylated antigen. High affinity binders were selected by both display systems, although more efficiently with the Intimin β-domain. The specificity of the selected clones against their respective antigen was demonstrated by flow cytometry of *E. coli* cells, along with ELISA and surface plasmon resonance with purified sdAbs. In addition, we employed the *E. coli* cell display systems to provide an estimation of the affinity of the selected sdAb by flow cytometry analysis under equilibrium conditions. Further, we used the β-domain of Intimin to display a sdAb library against human EGFR and developed a method for the direct selection of this sdAb library on cells. Bacteria displaying the anti-EGFR sdAb immune library were subjected to consecutive rounds of selection on EGFR-negative cells (i.e. murine fibroblast cell line, 3T3 2.2) and EGFR-positive cells HER14 (i.e. 3T3 2.2 transfected cells expressing human EGFR) to enrich for EGFR-specific binding clones. EGFR-specific clones that bound HER14 cells and not 3T3 2.2 cells were identified and their specific binding to EGFR confirmed by flow

cytometry analysis using biotinylated EGFR-Fc fusion. In addition, we used *E. coli* display to characterize the affinity and binding of these sdAbs to EGFR-Fc in the presence or absence of an excess of EGF, a natural ligand of EGFR. Our data demonstrates that *E. coli* display allows the selection of sdAbs against relevant tumor-associated antigens from libraries generated by cell immunization and performance of direct selection on tumor cells without the need for purified antigens.

PRESENTACIÓN

Introducción

Los anticuerpos (Abs, del ingles “antibodies”) o inmunoglobulinas (Igs) son proteinas globulares plasmáticas producidas por los linfocitos B y utilizadas por el sistema inmune para identificar moléculas ajenas al organismo llamadas antígenos (Ags). Los anticuerpos convencionales están formados por dos cadenas pesadas (H, del ingles “heavy”) y dos cadenas ligeras (L, del inglés “light”) idénticas. Cada una de estas cadenas se componen de regiones variables (V_H y V_L) y regiones constantes (C_H y C_L). La especificidad de cada anticuerpo se encuentra definida por las regiones determinantes de complementariedad (CDRs, del inglés “complementarity determining regions”) localizadas en las regiones VH y VL, mientras que la región Fc media funciones efectoras. Los Abs han sido ampliamente utilizados tanto para detectar antígenos así como en terapias. Los Abs convencionales monoclonales (mAbs) son producidos mediante hibridomas utilizando ratones, pero estos mAbs producen una respuesta inmune no desada en humanos lo que restringe su potencial terapéutico. Por ello, se han desarrollado estrategias alternativas para producir mAbs completamente humanos como son la producción de mAbs en animales transgénicos con loci de Ig humanos y la utilización de genotecas de Abs que se expresan en la superficie de bacteriófagos de *E. coli* y de células de levadura. Además, se han dedicado grandes esfuerzos en el desarrollo de reactivos de tipo anticuerpo basados en fragmentos de estos. Los fragmentos de Ab más comúnmente utilizados incluyen los fragmentos Fv monocadena (scFv, consisten en los dominios V_H y V_L unidos con un conector peptídico), los fragmentos Fab (generados mediante la fusión del dominio C con dominios V), y los anticuerpos monodominio (sdAbs, del inglés “single domain antibodies”) que son fragmentos de pequeño tamaño (peso molecular de aproximandamente 12-15 kDa), totalmente capaces de unirse a antígenos y formados por un único dominio variable (V). El tipo más común de sdAbs, también conocidos como “nanobodies” o V_{HH}s, es generado a partir de dominios V_H de anticuerpos que poseen únicamente cadenas pesadas (HCAbs, del inglés “heavy-chain-only antibodies”) y que se encuentran de forma natural en camélidos (llamas,

dromedarios, etc.). Su tamaño pequeño, sus propiedades biofísicas y su capacidad de unión a los antígenos hacen de los "nanobodies" unas moléculas muy atractivas para múltiples aplicaciones. Además, las secuencias de sdAbs son muy similares a las secuencias de los dominios V_{H3} humanos, por lo que pueden ser utilizados en terapia y en diagnóstico *in vivo* con un riesgo menor de efectos adversos.

Las genotecas de anticuerpos pueden ser obtenidas después de una inmunización del organismo donante con el antígeno de interés (en inglés "immune libraries"), a partir de donantes no inmunizados (colecciones naïve) o generadas artificialmente mediante el ensamblaje *in vitro* de los genes V (colecciones sintéticas). La técnica de la presentación de anticuerpos en fagos (en inglés "phage display") es el método más común de presentación y selección de anticuerpos. Una de las principales ventajas del "phage display" es la posibilidad de realizar colecciones de gran tamaño (hasta 10^{10} clones) debido a la alta eficiencia del clonaje de genes V en vectores fágicos en *E. coli*. Sin embargo, este sistema tiene algunas limitaciones como la alta probabilidad de aislar clones no específicos de unión al antígeno por la tendencia de los fagos de adherirse inespecíficamente, la necesidad de infectar bacterias para generar partículas fago-Ab y la imposibilidad de analizar los clones obtenidos mediante citometría de flujo (FACS, del inglés "fluorescence activated cell sorting") debido al pequeño tamaño de las partículas víricas. Un sistema alternativo utiliza células de levadura para la exposición de anticuerpos en la superficie celular y su posterior selección. Entre las ventajas de este método se encuentran la posibilidad de utilizar la técnica de citometría de flujo para la selección y caracterización de los anticuerpos aislados, la capacidad de las levaduras de realizar modificaciones post-traduccionales que pueden ser relevantes para la funcionalidad de los anticuerpos y la posibilidad de determinar directamente la afinidad de los anticuerpos expuestos. Sin embargo, las levaduras tienen menor eficiencia de transformación y tasa de crecimiento en comparación con *E. coli*.

La presentación de anticuerpos en *E. coli* ofrece una alternativa atractiva a los sistemas de exposición de anticuerpos anteriormente descritos, ya que se obtienen altas eficiencias de transformación, tasas de crecimiento elevadas y la posibilidad de utilizar métodos de citometría de flujo para la selección y caracterización de los clones de anticuerpos aislados. A pesar de todas estas ventajas, la presencia de la membrana externa (OM, del inglés "outer membrane") en *E. coli* interfiere con la correcta exposición del anticuerpo y ha dificultado el desarrollo de sistemas eficientes de presentación de anticuerpos en este microorganismo. Estudios realizados anteriormente en nuestro laboratorio con modelos de V_{HH} demostraron que los dominios β de anclaje a la OM pertenecientes al autotransportador EhaA y de la intimina de la cepa enterohemorrágica *E. coli* O157:H7 (EHEC) son sistemas muy prometedores para la exposición de sdAbs en la superficie de la cepa *E. coli* K-12.

Objetivos

Los objetivos del presente trabajo son:

1) Evaluar y comparar los dominios β de EhaA e intimina como sistemas de exposición de sdAbs funcionales en la superficie de *E. coli*.
2) Utilizar los sistemas de presentación de anticuerpos basados en los dominios β de EhaA e intimina para la expresión de genotecas de sdAbs de animales inmunizados y posterior selección de clones con alta afinidad por antígenos proteicos de origen bacteriano y humano.
3) Caracterizar los sdAbs seleccionados mediante la técnica de presentación en la superficie *E. coli*, determinar su afinidad de unión y especificidad mediante citometría de flujo, y comparar los resultados con aquellos obtenidos con tecnologías bioquímicas estándar como el ensayo por inmunoabsorción ligado a enzimas (ELISA, del inglés "enzyme-linked immunosorbent assay") y la resonancia de plasmones de superficie (SPR, del inglés "surface plasmon resonance").
4) Utilizar la plataforma de presentación de anticuerpos en *E. coli* para la selección directa de sdAbs utilizando células tumorales vivas que expresan un antígeno tumoral relevante en su superficie, como el receptor de factor

de crecimiento epidérmico (EGFR, del inglés “epidermal growth factor receptor“).

Resultados

En primer lugar analizamos la capacidad de los dominios β de EhaA e intimina (pertenecientes a EHEC) para exponer sdAbs individuales y colecciones post-inmunización de sdAbs originados a partir de V_{HH}s de camellos dirigidos contra el dominio extracelular del receptor translocado de intimina de EHEC ($TirM_{EHEC}$) y contra fibrinógeno humano (Fib). Demostramos que ambos sistemas pueden ser utilizados para exponer sdAbs funcionales en la superficie de células de *E. coli* con poca proteolisis y toxicidad celular, aunque las células de *E. coli* que exponían los sdAbs con el dominio β de intimina mostraron una mayor capacidad de unión al antígeno. Se examinaron ambos tipos de sistemas de presentación de *E. coli* con colecciones de sdAbs para buscar clones específicos de antígeno mediante separación magnética de células (MACS, del inglés “magnetic cell sorting”) utilizando antígenos biotinilados. Se aislaron clones con alta afinidad por sus respectivos antígenos utilizando los dos tipos de presentación de sdAbs, aunque el proceso fue más eficiente con el sistema del dominio β de intimina. Se determinó la especificidad de los clones seleccionados contra $TirM_{EHEC}$ y Fib mediante análisis por citometría de flujo de células de *E. coli*, y con las técnicas ELISA y SPR utilizando sdAbs purificados. A continuación, utilizamos los sistemas de presentación de sdAbs en células de *E. coli* para estimar la afinidad de los sdAbs seleccionados mediante análisis de citometría de flujo en condiciones de equilibrio.

Adicionalmente, la plataforma de presentación de sdAbs con el dominio β de intimina fue empleada para la selección de V_{HH}s a partir de una genoteca inmune generada contra EGFR mediante la inmunización de llamas (*Lama glama*) con la línea celular humana de origen tumoral A431. Las bacterias que presentaban la colección de sdAbs en su superficie fueron sometidas a rondas sucesivas de selección sobre células negativas para EGFR (línea celular fibroblástica murina, NIH-3T3 2.2) y células positivas para EGFR, como HER14 (células NIH-3T3 2.2 transfectadas que expresan EGFR humano) para el enriquecimiento de clones que

unían específicamente EGFR. Se identificaron clones EGFR-específicos que se unían a células HER14 pero no a células NIH-3T3 2.2, y se confirmó su capacidad de unión específica a EGFR a través de análisis por citometría de flujo utilizando fusiones biotiniladas EGFR-Fc. Además, utilizamos el sistema de presentación de sdAbs en *E. coli* para determinar la afinidad de la unión de estos sdAbs a EGFR-Fc en presencia de un exceso de EGF, el ligando natural de EGFR. Nuestros datos demuestran que el sistema de presentación de sdAbs en *E. coli* permite la selección de sAbs contra antígenos relevantes asociados a tumores a partir de colecciones generadas mediante inmunización con células. Esta selección se puede realizar directamente sobre células tumorales sin la necesidad de utilizar el antígeno purificado.

Por último, desarrollamos un método alternativo para la producción y purificación de sdAbs del periplasma de *E. coli* basado en fusiones de sdAbs con la proteína de unión a maltosa (MBP, del inglés “maltose binding protein”) en el extremo N-terminal y con una cola de histidinas (His_6) en el extremo C-terminal (MBP-V_{HH}-His6). Se produjeron consistentemente niveles elevados de fusiones solubles MBP-V_{HH}-His_6 (>12 mg/L de cultivo inducido en matraces) en el periplasma de *E. coli* HM140, una cepa que carece de varias proteasas periplásmicas. Se recuperaron fusiones MBP-V_{HH}-His_6 de gran pureza y fusiones libres V_{HH}-His6 (después de una proteolisis especíifica de sitio de las fusiones), tras realizar dos procesos de cromatografía de afinidad a amilosa y a metales. Se determinó la naturaleza monomérica de los V_{HH}-His_6 mediante cromatografía de filtración en gel. También demostramos mediante ELISA que las fusiones monoméricas V_{HH}-His_6 y MBP-V_{HH}-His_6 retenían su capacidad de unión al antígeno y su especificidad, facilitando su utilización directa en ensayos de reconocimiento de antígeno.

INTRODUCTION

1. Antibodies and Recombinant antibody fragments

1.1 Antibodies and their application in human therapy

Antibodies (Abs) or Immunoglobulins (Igs) are proteins that play a very important role in the immune system of humans and animals. These proteins are produced by B-lymphocytes and are deployed by the immune system to identify and target foreign or non-self molecules (Nelson et al., 2000; Ohlin and Zouali, 2003). Every human being has on an average, about one to two billion different Abs continuously flowing through his or her bloodstream, patrolling and fighting infections or diseases. The basic structure of an Ab consists of two identical light and heavy chains, linked by disulfide bonds. Each heavy and light chain contains a variable sequence (V_H and V_L respectively) in the amino terminal and constant sequences (C_H and C_L) in the remaining portion of the chain. Variability of the Abs, which accounts for their different specificities, is located in the V_H and V_L, clustered in several hypervariable regions: the complementarity determining regions (CDRs). The CDRs determine the specificity of the Ab for its cognate antigen, thus allowing the detection of millions of different antigens present in nature. The Fc region of the Ab, on the other hand, is essential for mediating effector functions like antibody-dependent cytotoxicity (ADCC), Ab-dependent cellular phagocytosis, complement mediated lysis and regulation of cell activation or proliferation. Thus, the structure of the Ab (Figure 1A) determines its binding specificity and biological activity (Birch and Racher, 2006).

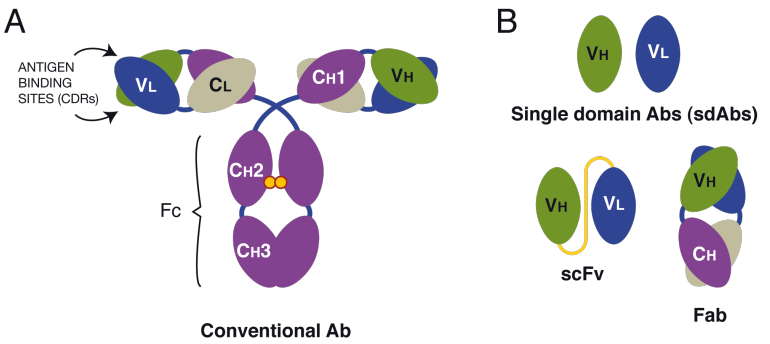

Figure 1. Structure of conventional antibodies and antibody derived fragments.

(A) Structure of conventional IgGs with heavy chain (H) and light (L) chains indicating the crystallizable fragment (Fc) region and antigen binding sites or CDRs. **(B)** Common antibody-derived antigen-binding fragments: single-chain Fv (scFv) and Fab are shown along with single domain V_H and V_L fragments.

Abs have been widely used for antigen detection as well as in therapeutics, and their specificity combined with low toxicity make them promising pharmaceutical molecules (Berger et al., 2002). At present, they comprise the second-largest category of biological medicines in clinical development, after vaccines (Seymour, 2004). However, therapeutic use of antibodies was initially limited by methodological constraints in raising them. Conventional monoclonal antibodies (mAbs) were commonly obtained by immunization of experimental animals, usually mice, with target antigens. Fusions of B-cells from immunized animals with myeloma cell lines produced hybridomas able to grow in culture and that could be screened for specific Ab-producing clones (Kohler and Milstein, 1975). Although well established, this technology is laborious and biased by the immune system of the experimental animal, which limits the ability to obtain high affinity Abs against conserved mammalian proteins of interest. Additionally, the heterologous character of these murine mAbs make them immunogenic to humans and elicit “Human anti-mouse antibody” (HAMA) response, which restricts their use in therapy (Schroff et al., 1985). Hence, human antibodies are of particular interest due to a lower immunogenic response. Human hybridomas were initially evaluated, but were found to be unstable, difficult to prepare and secreted low levels of mAbs of the IgM class with low affinities. Two other approaches to produce fully human mAbs from phage display libraries (McCafferty et al., 1990) or transgenic animals (Bruggemann et al., 1991) have been possible since the early 1990s. At present, about 30 mAbs produced by these methods have already been approved by the Food and Drug Administration (FDA) for therapy (Scott et al., 2012; Pandey and Mahadevan, 2014).

In order to be successful as therapeutic molecules, Abs need to have properties like high binding affinities, reduced immunogenicity, increased half-life in the human body and the ability to adequately recruit human effector functions. These factors combined with the knowledge that the segmented structure of the Ab molecule allows functional domains (carrying antigen-binding or effector functions) to be exchanged, has led to the construction of either, chimeric antibodies i.e. by coupling of the animal antigen-binding variable (V) region with the human constant domains or humanized antibodies, i.e. by grafting of the CDRs derived from murine antibodies with desired specificity onto carefully chosen human V_H and V_L

frameworks (FRs) (Figure 2). Six chimeric, fifteen humanized and ten fully human mAbs are currently on the market, including some Fabs.

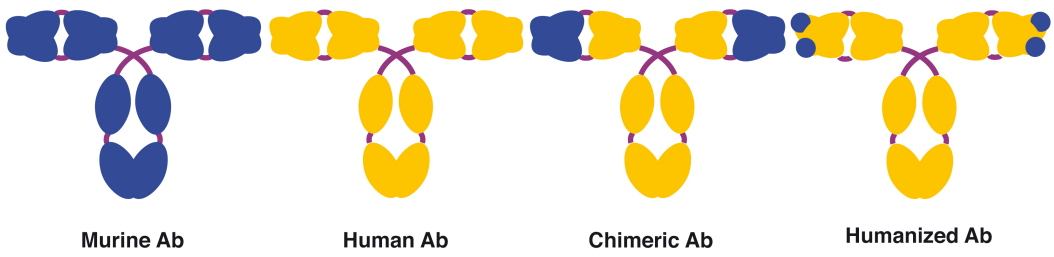

Figure 2. Chimeric and humanized antibodies.

(From left to right) A murine antibody (blue), a human antibody (yellow), a chimeric antibody (with murine variable domains and human constant domains) and a humanized antibody (a human antibody with CDRs of murine origin).

Despite the general success of whole IgGs in therapy, the large size of these molecules leads to practical drawbacks such as lower tumor or tissue penetration, long serum half-life and subsequent low tumor-to-blood ratio; all or some of which makes difficult their use in applications like radioimmunotherapy and *in vivo* diagnostic imaging. Secondly, conventional mAbs have specificity for a single antigen epitope, and since most diseases are multifactorial, involving multiple ligands, receptors and signalling cascades, it would be beneficial to have bivalent or multivalent molecules that could target two or more epitopes. Lastly, the structural properties of a full-length Ab require sophisticated folding mechanisms as well as an oxidizing environment for the generation of disulfide bonds; since most traditional expression hosts do not provide such an environment, the industrial production of full length IgGs is mostly restricted to mammalian cells leading to slow production at high cost.

To circumvent these limitations of mAbs, substantial efforts have gone in to the development of the next wave of therapeutic and diagnostic reagents based on Ab fragments. In many cases, efforts have been made to improve or even delete some characteristics. For example, to achieve better tumor penetration or a better tumor-to-blood ratio for visualizing metastases, it would be preferable to have a relatively small Ab fragment with a fairly short half-life. On the other hand, the molecule should not be too small, in order to avoid rapid clearance from the body

immediately after its application. In addition, it would be advantageous in certain applications to improve the effector functions, while in others, such as in radioimmunotherapy or *in vivo* imaging, it is imperative that Fc mediated cellular effects and prolonged half life do not exist.

1.2 Recombinant fragments from conventional antibodies

It is striking to note that the use of Ab fragments started as early as in the late 1950s after the pioneering work of Porter (Porter, 1958), which made possible the better understanding of the topology of IgGs and the functions associated with the different Ab fragments obtained after controlled proteolytic cleavage. Conversion of monovalent Ab fragments into multivalent formats increases functional affinity; decreases dissociation rates when bound to cell-surface receptors or polyvalent antigens and enhances biodistribution (Holliger and Hudson, 2005). These molecules are particularly useful in applications, where epitope binding is sufficient for the desired effect, including therapeutic applications such as virus neutralization or receptor blocking. The smallest antigen-binding fragment of IgGs maintaining its complete antigen-binding site is the Fv fragment, which consists only of V regions. However, the expression of an individual variable domain of a Fv, either V_H or V_L domain, exposes a large hydrophobic side to the aqueous environment that render these types of molecules difficult to handle. This shortcoming is overcome by introducing a soluble and flexible amino acid peptide linker linking the V_H and V_L domains, to form a scFv fragment, which leads to stabilization of the molecule (Bird et al., 1988). Also common is to add the constant (C) domains to the V regions to obtain a Fab fragment.

Till date, scFvs and Fabs are the most widely used Ab fragments produced in bacteria (Figure 1B). Other formats that have been produced in prokaryotic and eukaryotic cells include disulfide-bond stabilized scFvs (ds-scFv) (Schmiedl et al., 2000), single chain Fab fragments (scFab) (Hust et al., 2007) which combines properties of scFv and Fab, as well as di- and multimeric Ab formats like dia-, tria-, tetra-bodies (Hudson and Kortt, 1999; Carter, 2006), minibodies (Hu et al., 1996; Holliger and Hudson, 2005) or trimerbodies (Cuesta et al., 2012).

1.3 Heavy-chain only antibodies, single domain antibodies and nanobodies

In the early 1990s, a novel type of Abs lacking light chains was discovered in the serum of camelids (Hamers-Casterman et al., 1993). This unique class of heavy chain only antibodies (HCAbs) are apparently the outcome of recent adaptive changes occurring in conventional antibodies within the Camelidae lineage (Flajnik et al., 2011) and play a role in the immune response of these animals. A second type of HCAbs is found in sharks (Greenberg et al., 1995). The structure of camelid HCAbs is illustrated in Figure 3A. The homodimeric HCAbs lack light chains and thus antigen recognition is possible solely through the variable domain of the heavy chain, referred to as VHH for VH of HCAbs. The recombinant expression of VHHs yields a soluble single domain Ab (sdAb) fragment with dimensions of 2-4 nm, and has been referred to as Nanobody (Nb). Nbs have a molecular weight of ~15 kDa, which is at least half the size of the intact antigen-binding site of a conventional Ab (i.e, the VH-VL pair) and are the smallest, intact antigen-binding fragments derived from a functional immunoglobulin (Figure 3A and 3B).

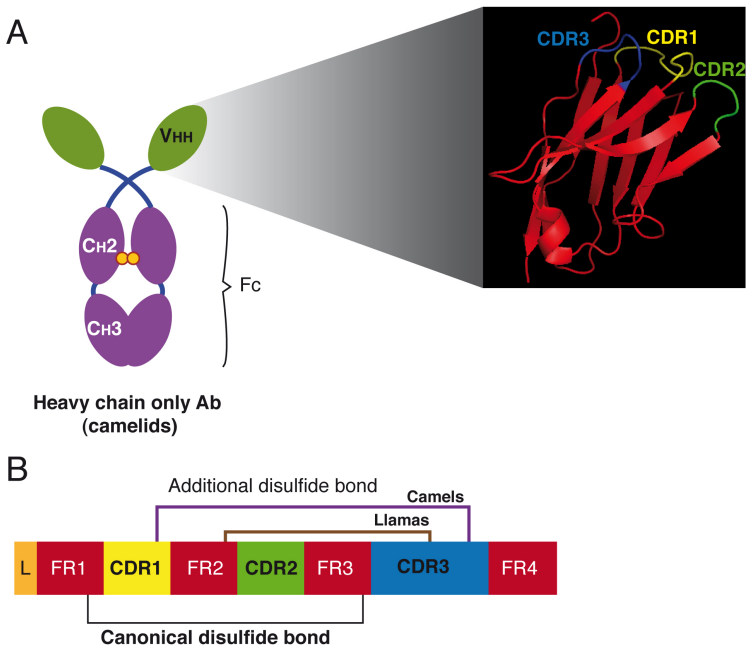

Figure 3. Structure of camelid heavy chain only antibodies and nanobodies.

(A) Schematic representation of a heavy chain only antibody with the structure of the VHH domain highlighted. The CDRs are labelled in different colours: CDR1 in yellow, CDR2 in green, CDR3 in blue and the framework regions (FR) are indicated in red. **(B)** The linear structural diagram of a VHH domain. CDRs are labelled with the same colour scheme as in part A and also the disufide bonds in the molecule, i.e. canonical and additional are illustrated.

These molecules have naturally acquired important adaptations to remain soluble and functional in the absence of the associated light chain variable domain. Further, they have evolved long CDRs with novel conformations for antigen recognition, subtle amino acid adaptations including substitutions of conserved hydrophobic residues in classical VHs (V37, G44, L45, and F47/W47) for more hydrophilic amino acids (Y37/F37; E44/Q44; R45/C45; G47/R47/L47/S47) (Muyldermans, 2013), that confer them strict monomeric behaviour, reversible folding properties, resistance to proteolysis and thermal degradation when compared with the VH from conventional antibodies (van der Linden et al., 1999; Dumoulin et al., 2002). Furthermore, VHHs often contain, besides the canonical disulfide bond of Ig domains, an extra-disulfide bond connecting CDR3 and CDR1 (in camels) or CDR3 with CDR2 (in llamas) that assist in stabilizing the conformation of these CDRs and the overall stability of the domain (Figure 3B) (Govaert et al., 2012).

The small size and long CDRs of VHHs allow them to recognize epitopes located in clefts and protein cavities (Figure 4A) such as active sites of enzymes, conserved inner regions of surface proteins from pathogens, which are frequently less accessible to large molecules and conventional Abs (Desmyter et al., 1996; Lauwereys et al., 1998; Stijlemans et al., 2004). In addition, they share high sequence identity with human VH sequences of family 3 (Figure 4B), which opens the possibility of their use in human therapy and in *in vivo* diagnosis (Wesolowski et al., 2009; Vaneycken et al., 2011). Apart from these advantages, the recombinant expression of VHHs turned out to be favourable as well, as is validated in various expression systems. They are preferentially expressed in *E. coli*, where they can be produced economically as soluble and non-aggregating recombinant proteins with an incorporated histidine tag for easy purification (Arbabi-Ghahroudi et al., 2005), though the levels of soluble VHHs produced are highly variable (Alvarez-Rueda et al., 2007). Higher production levels of VHH can be obtained using high-density cultures in yeast systems like *Pichia pastoris* and *Saccharomyces cerevisiae* (Frenken et al., 2000) or in tobacco plants (Rajabi-Memari et al., 2006).

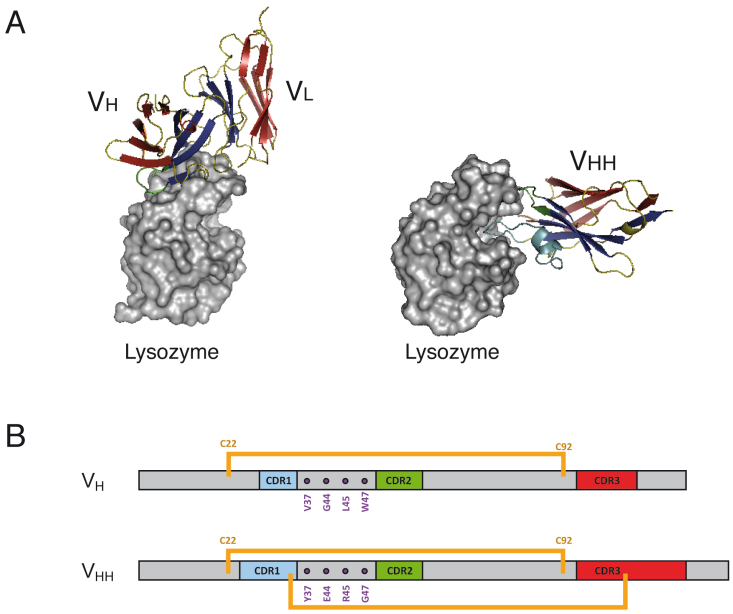

Figure 4. Comparison between conventional VH/VL and VHH antibody fragments.

(**A**) Three-dimensional structure of chicken lysozyme recognized by an scFv (VH/VL domains) (left; PDB code 1mlc) or by a VHH domain of camelid HCAb (right; PDB code 1mel). The CDRs of VH, VL and VHHs are shown in different colors (CDR1 in orange, CDR2 in green, CDR3 in cyan). The long CDR3 loop of the VHH protrudes as a finger-like structure toward an epitope located in the cavity of the active site of lysozyme (right), whereas the flat VH/VL paratope binds to an epitope located at the exposed surface of lysozyme (left).(**B**) Cartoon showing the polypeptide chains of conventional VH and camelid VHHs, indicating the amino acids of framework region 2 of classical VHs (V37, G44, L45, W47) that are substituted by more hydrophilic amino acids (e.g. Y37, E44, R45, G47) in VHHs. Other distinct features shown are the different length of CDR1 and CDR3 in VHs and VHHs, the presence of the conserved canonical disulfide bond between residues C22 and C92, and the extra-disulfide bond between Cys residues of CDR1 and CDR3 in VHHs.

Because of their single domain nature, VHHs, offer several advantages for biotechnological applications. Libraries of VHHs from immunized camels and llamas can be generated through a straightforward cloning procedure in various display systems and selected using antigen immobilized in plates or on cells (Arbabi Ghahroudi et al., 1997; Roovers et al., 2007; Ahmadvand et al., 2009; Ryckaert et al., 2010; Fleetwood et al., 2012). VHHs within these libraries retain full functional diversity resulting in isolation of high-affinity antigen-binding clones. The short serum-life due to renal clearance may limit the efficacy of VHHs in therapeutic applications. Therefore, bispecific VHHs recognizing long-lived serum proteins like albumin or immunoglobulins and the therapeutic target have been generated, thus resulting in increased half-lives (Tijink et al., 2008; Vosjan et al., 2012). The binding and stability properties portrayed by natural VHHs has led to considerable interest in the development of human sdAbs based on human VH (or VL) sequences that could

mimic natural VHHs. Murine VH sdAbs against lysozyme were isolated from phage display in *E. coli* before the discovery of natural HCAbs in camels (Ward et al., 1989). However, most VH sequences from conventional Abs tend to aggregate in solution and show low affinity for antigens. Introduction of 'camel' mutations G44E, L45R, and W47G, in a human VH3 sequence significantly increased its solubility (Davies and Riechmann, 1994). Human VH clones with low tendency to aggregate were isolated by repeated cycles of heating and cooling of phages with displayed VH sequences (Jespers et al., 2004). Based on these findings, synthetic libraries of human VHs have been developed by randomizing CDRs in 'camelized' and/or selected human VH sequences and used for isolation of functional sdAbs with nanomolar affinity (Davies and Riechmann, 1994; Dumoulin et al., 2002; Holt et al., 2008; Arbabi-Ghahroudi et al., 2009). sdAbs based on human VL domains have also been reported and expressed in *E. coli*. These include VL domains from conventional IgGs and naive scFv libraries (Colby et al., 2004; Martsev et al., 2004; Cossins et al., 2007; Schiefner et al., 2011) and sdAbs isolated from synthetic libraries (van den Beucken et al., 2001; Holt et al., 2008)

2. Selection of antibodies from libraries using surface display.

2.1 Libraries of antibody genes

Combinatorial Ab engineering or directed evolution is an efficient approach for generation of Abs with new or improved properties (e.g. affinity) and is based on the generation of molecular libraries containing up to hundreds of billions of different Abs, from which specific binders might be isolated by display and high-throughput screenings or selections. One of the considerations to be taken in to account when constructing a library is the size. A larger library covers a larger part of the theoretical repertoire and results in a higher probability of containing and isolating high-affinity clones. This correlation has been supported by experimental data generated in different studies (Bradbury and Marks, 2004). Equally important is that the Abs in the library are functional. Ab libraries can be classified into three main types, namely immune, naïve and synthetic libraries.

Immune libraries are generated from the V genes of B-cells isolated from the lymph nodes, spleen, or peripheral blood of immunized animals or human donors (Clackson et al., 1991) and takes advantage of the diversity created *in vivo* by the immune system of the donor. These types of libraries are enriched in antigen-specific Abs, some of which have already been affinity matured by the immune system of the donor, and thus serve as a rich source of Abs with higher affinities than those obtained from other sources. In addition, large-sized immune libraries are not necessary in order to obtain high-affinity antibodies. Multiple immune libraries have been constructed and reported, including mouse (Clackson et al., 1991; Chester et al., 1994; Kettleborough et al., 1994), human (Barbas et al., 1993), chicken (Yamanaka et al., 1996), rabbit (Lang et al., 1996) and camel (Arbabi Ghahroudi et al., 1997). The amplified V genes of an immune library are then cloned into a display vector for selection of binders with high affinity and specificity to the target antigen. Despite these advantages, immune libraries also have some limitations. Firstly, active immunization is not always possible due to ethical constraints, or is not effective due to toxicity to or tolerance mechanisms towards the antigen used. Secondly, immune libraries require repeated antigen immunization and library construction for each antigen used. Ideally, universal and antigen-unbiased libraries should be screened to select high affinity Abs to any chosen antigen independent of the immune history. At present, a few such libraries have already been described, either naïve or synthetic (depending upon the source of the immunoglobulin genes), and are particularly useful for the selection of human Abs.

A naïve library, if sufficiently large and diverse, can be used to generate Abs for a large panel of antigens, including self, non-immunogenic and relatively toxic antigens. The murine naïve repertoire has been estimated to contain $<5x10^8$ different B-lymphocytes, while the human repertoire maybe a hundred to a thousand times bigger (Winter et al., 1994). The affinity of Abs selected from a naïve library is proportional to the size of the library, ranging from $10^{-6 \text{ to } -7}$ M for a library with 10^7 clones (Griffiths et al., 1994), to $10^{-8 \text{ to } -10}$ M for a large repertoire of about 10^{10} clones (Vaughan et al., 1996). Synthetic Ab repertoires contain Abs built artificially by the *in vitro* assembly of V-gene segments and D/J segments. V-genes may be assembled by introducing a predetermined level of CDR randomization into

germline V-gene segments or re-arranged V-genes. The regions and degree of diversity may be chosen to correspond to areas of highest natural diversity of the Ab repertoire, like in the loop central to the antigen-combining site i.e. the CDR3 of the heavy chain. Several synthetic libraries have been constructed and been used to select Abs against different antigens like haptens (Barbas et al., 1992; Hoogenboom and Winter, 1992), proteins (Nissim et al., 1994) and cell-surface markers (de Kruif et al., 1995), but their affinities are typically around $10^{-6 \text{ to } -7}$ M.

2.2 Surface display methods for screening of Ab libraries

In vitro display technology is based on the linkage of phenotype to genotype and is currently one of the major technologies for creating mAbs for human therapy, in addition to the use of transgenic mice carrying human Ig genes (Jakobovits et al., 2007) and the humanization of mAbs (Lee et al., 2014). It involves the display and screening of Ab gene libraries on the surface of a biological entity e.g. bacteriophages, yeasts or ribosomes (Hoogenboom, 2005). Selection systems include the *in vitro* display technologies as well as protein complementation-based strategies. The function of a selection system is to enable isolation of specific affinity proteins from the majority of non-binding background proteins present in the library, as well as to co-select the encoding DNA in order to simplify amplification and identification. It is important that selection pressure is dominated by high affinity for the antigen, while potential biases like differences in expression levels or amplification rate are minimized. Many different selection methods have been widely used, including selection on antigen immobilized on polystyrene plates or columns, selection on biotinylated antigen in solution, selection on mammalian cells expressing a surface antigen (Cai and Garen, 1995; de Kruif et al., 1995), enrichment on tissue sections (Van Ewijk et al., 1997) and selection *in vivo* using living animals (Zou et al., 2004; Deramchia et al., 2012).

2.2.1 Phage display

In 1985, George Smith reported the use of recombinant DNA technology for display of heterologous peptides on the surface of filamentous phages, laying the ground for the “phage display” technology (Smith, 1985). This technology has proven to be a very powerful technique to display libraries containing billions of different peptides

and proteins, including Abs and is the most common Ab display method in use. DNA encoding Ab fragments is cloned in phagemids as a fusion to the phage coat proteins (e.g. pIII, pVIII). Upon expression of the Abs, the coat protein fusion is incorporated into new phage particles that are assembled in bacteria. Expression of the phage coat protein fusion product, and its subsequent incorporation into the mature phage coat results in the Ab or Ab fragment being presented on the phage surface. Bacteriophages displaying relevant Abs or Ab fragments on the surface (Figure 5A and 5B) are retained during selection methods, while non-adherent phages are washed away (Figure 5C). Bound phages are recovered by elution, reinfected into *E. coli* and re-grown for further enrichment and eventually analysis of binding. The most commonly used phage for display is the non-lytic filamentous phage, M13 and the most extensively used phage coat protein is the pIII (present in three to five copies per phage particle), which is involved in recognition of F-pilus and Tol-proteins in the bacterial cell envelope during infection (Winter et al., 1994; Vodnik et al., 2011). The vast majority of reports using phage display utilize scFv libraries (Hust and Dubel, 2004), since the smaller size and the composition from a single polypeptide facilitate production and folding in *E. coli*, thus allowing a more efficient presentation of the Ab repertoire on the phage surface. More complex proteins like Fab fragments or full-length Abs have also been expressed, but the necessity to produce two different polypeptide chains, has led to construction of bicistronic expression vectors with increased complexity (Hust and Dubel, 2005; Mazor et al., 2010). The major advantages of phage display include the large library sizes that can be attained in *E. coli*, i.e. 10^{10} members, and the high titres that can be produced (>10^{13} phage particles/ml) thus accounting for a good representation of all clones in the library. Secondly, purification of soluble Ab fragments is possible directly, after selection by phage display, without the need for re-cloning in a different protein expression vector. However, phage display suffers limitations such as high background binding due to the sticky nature of phages, the need for bacterial infection to produce phage-Ab particles in each round of selection, including titre of the phage particles produced, leading to longer experimental procedures, and the unfeasibility of fluorescence activated cell sorting (FACS) or flow cytometry for analysis due to the small size of the phage particles.

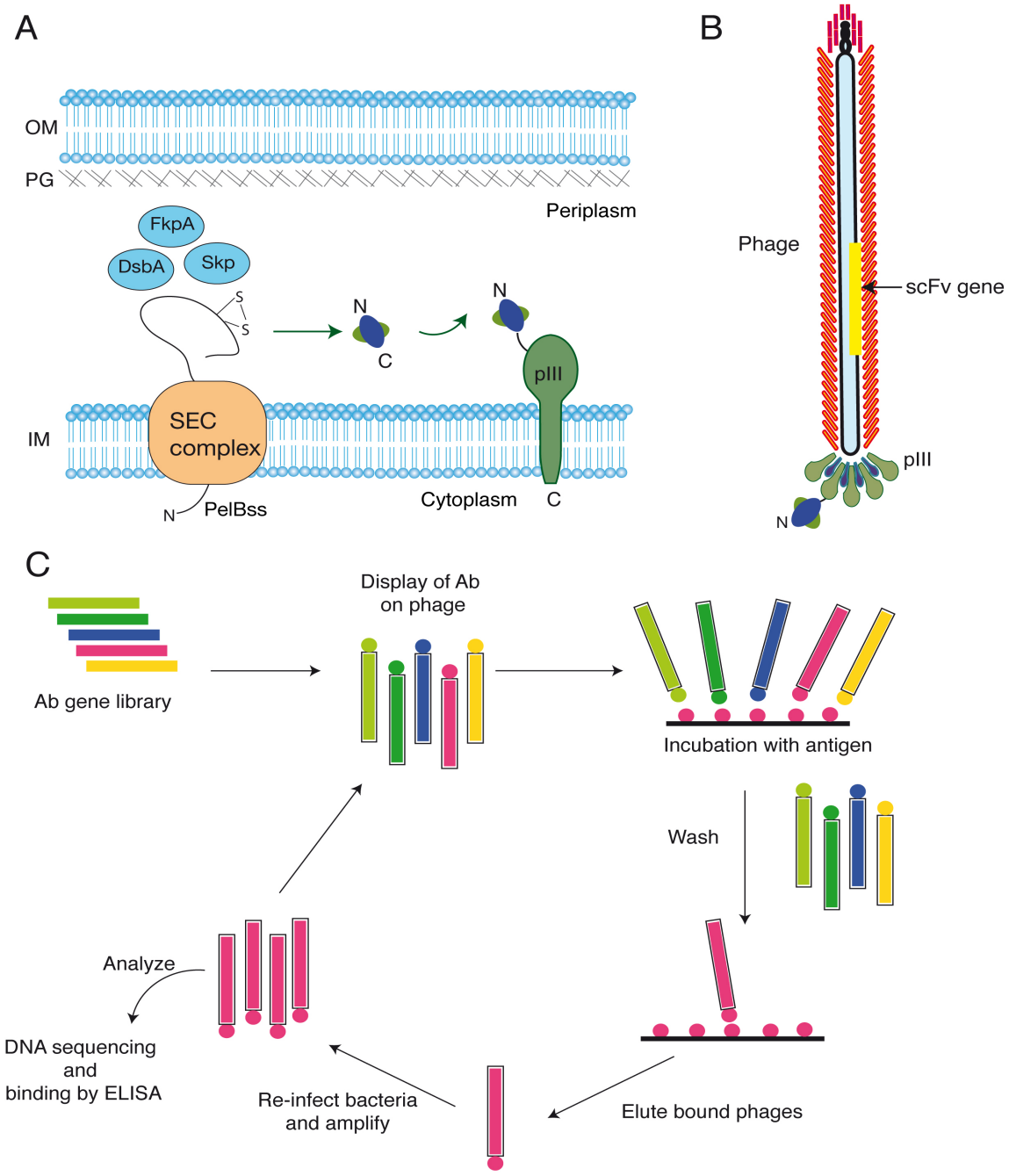

Figure 5. Phage display of antibodies.

(A) Soluble Ab fragments, depicted as a scFv , are exported to the periplasm with an N-terminal signal peptide (e.g. PelBss). The Ab fragment can also be fused at its C-terminus to the minor coat protein III (pIII) of filamentous phages for phage display. In this case, the Ab fragment is exposed to the periplasm but tethers to the inner membrane (IM) of *E. coli* by pIII. (**B**) Phage-scFV particles assembled upon infection of *E. coli* cells expressing Ab-pIII fusions with a helper phage. The Ab-pIII fusion is displayed on the phage capsid (usually one copy per phage), which contains the phagemid DNA with the Ab gene. (**C**) Scheme of the steps involved during panning of phage display libraries on plates coated with antigen.

2.2.2 Cell surface display

Cell surface display systems are effective alternative methods for Ab engineering by directed evolution, and show great promise in both medical and industrial applications. Various cell surface display systems have been developed in a range of host organisms, including Gram negative bacteria (Daugherty, 2007; Mazor et al., 2007), Gram positive bacteria (Wernerus and Stahl, 2004; Fleetwood et al., 2012), yeast (Boder and Wittrup, 2000; Feldhaus and Siegel, 2004; Wen et al., 2011; Boder et al., 2012), insect cells/baculovirus (Makela and Oker-Blom, 2008) and mammalian cells (Ho et al., 2006; Beerli et al., 2008). These systems complement phage display and cell-free protein engineering systems. Currently, yeast and bacteria are the most commonly used cell surface display platforms for protein engineering.

2.2.2.1 Yeast Display

The eukaryotic secretory pathway, coupled with protein folding and quality control mechanisms of yeast allows a wide variety of proteins to be displayed, including many proteins with complex folds like single-chain T-cell receptors (scTCRs) (Richman et al., 2009; Aggen et al., 2011), human major histocompatibility (MHC) class II molecules (Wen et al., 2011), human epidermal growth factor (EGF), cytokines, extracellular domains of epidermal growth factor receptor (EGFR), scFvs (Feldhaus and Siegel, 2004) and Fabs (Blaise et al., 2004; Weaver-Feldhaus et al., 2004; Lin et al., 2012). Proteins are displayed on the yeast *Saccharomyces cerevisiae* cell surface via fusion to the α-agglutinin yeast adhesion receptor, which is located in the yeast cell wall (Figure 6A). The display level on the cell is variable (on an average about $3x10^4$ fusions per cell for a scFv), but the intrinsic avidity of this display system is counteracted by the power of cell sorting. By staining cells with both fluorescently labelled antigen and anti-epitope tag reagent, the yeast cells can be sorted according to the level of antigen binding and Ab expression on the surface (Figure 6B). Non-immune human scFv libraries with over 10^9 members have been generated and efficiently selected using magnetic beads (Yeung and Wittrup, 2002; Feldhaus et al., 2003; van den Beucken et al., 2003) and then sorted by flow cytometry to yield Abs with nanomolar affinities (Feldhaus et al., 2003).

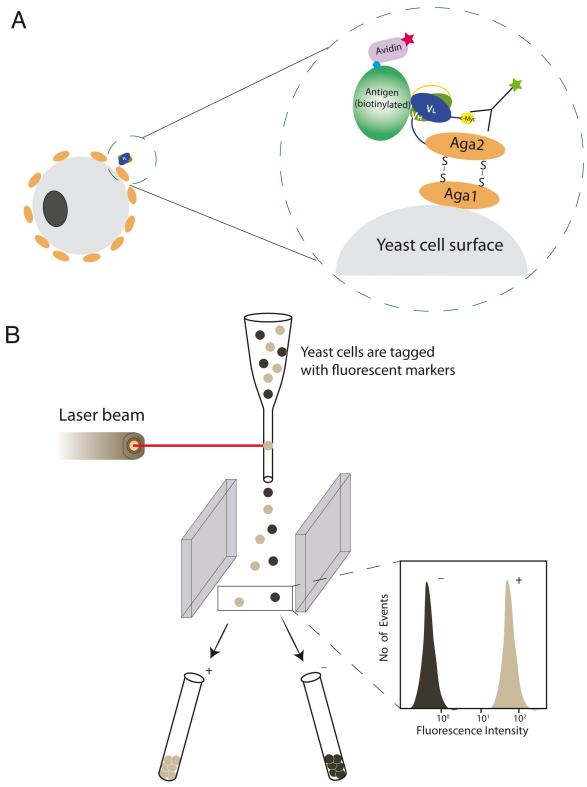

Figure 6. Yeast display of antibodies.

(A) Ab fragments, depicted as a scFv in this scheme, are fused at its C-terminus to the Yeast agglutinin receptor (Aga) present on the yeast surface for display. **(B)** A schematic of Fluorescence assisted cell sorting (FACS) using yeast-displayed Ab fragments is depicted.

Yeast display has been used with a much more diverse range of proteins than prokaryotic hosts. A comparative study carried out using phage and yeast display; with a HIV-1 immune scFv library against the HIV-1 gp120 envelope glycoprotein showed that although both libraries yielded the same six scFvs, yeast display identified an additional twelve clones. Only five of these twelve clones could be displayed on the phage particle, likely due to the greater protein folding capabilities of yeast (Bowley et al., 2007). Limiting factors of yeast display include the smaller library sizes due to the low transformation efficiency of yeast, longer experimental time due to slower culture growth and low speed of fluorescent cell sorting (FACS).

A table comparing the two most common Ab display methods in use i.e phage display and yeast display is illustrated in Table 1.

Table 1. Benefits and Limitations of Phage display and Yeast Display.

Phage Display		Yeast Display	
Benefits	Limitations	Benefits	Limitations
1) A highly robust Ab display system. Phages can be produced and handled in high densities (upto 10^{13} phages/ml)	1) High background levels due to sticky nature of phage particles.	1) Presence of eukaryotic post-translationary machinery.	1) Difficult to obtain large library sizes due to low transformation efficiency of yeast.
2) Large library sizes can be commonly obtained (upto 10^{10} members).	2) Sticky nature of phages makes difficult the use of complex antigenic surfaces such as cells for selection.	2) Larger size of yeast makes possible the use of flow cytometry based methods for selection and screening.	2) Slower growth of yeast leads to increased experimental times.
3) Use of stringent conditions of wash and elution is possible.	3) Use of high throughput methods based on flow cytometry is not possible due to the small size of phages.	3) Direct affinity analysis of Abs displayed on yeast cells is possible by flow cytometry.	3) Slow speeds of cell sorting due to large size.

2.2.2.2 Bacterial cell surface display

Although both phage display and yeast display are good Ab display systems, they suffer from some limitations (Table 1). Hence, it would be beneficial to develop an Ab display system that could combine the major advantages of both methods, while improving on the limitations. Bacterial display could be an alternative to these existing platforms of Ab display. Firstly, the larger size of bacteria than phages allows the use of flow cytometry based methods for selection, screening and characterization of clones. Secondly, bacteria are less sticky than phages, could result in lower background levels and selection could be carried out more easily using complex antigenic surfaces such as cells. Lastly, the faster growth of bacteria such as *E. coli* compared to that of yeast, greatly reduces experimental times and this fact combined with the highly versatile protein expression systems and methods available in *E. coli*, makes this method of Ab display very attractive. *Escherichia coli* is currently the most commonly used host for protein engineering by bacterial surface display, though a few reports used Gram-positive bacteria for display of enzymes and Ab fragments (Kronqvist et al., 2008; Fleetwood et al., 2012).

2.3 *E. coli* cell surface display of Ab libraries

The expression of Abs in *E. coli*, both full-length IgGs molecules and smaller antigen-binding fragments, provides a set of powerful technologies for the

generation of Abs with novel specificities and improved properties (Holliger and Hudson, 2005; Beck et al., 2010). A major advantage of this display platform is that the relatively high transformation efficiencies of *E. coli* allow Ab libraries with up to 10^{10} members to be constructed. Moreover, *E. coli* remains a suitable microorganism for the generation, amplification and maintenance of large Ab repertoires owing to its versatile protein expression and secretion systems.

Although *E. coli* lacks eukaryotic protein folding and post-translational modification machineries, it allows expression of many eukaryotic proteins or protein domains in functional form, including the V domains of Igs. *E. coli* cells have an inner membrane (IM) and an outer membrane (OM) separated by periplasmic space. The presence of the OM in *E. coli* has hindered the development of effective cell surface display methods for Ab selection. In addition, display of heterologous proteins on the surface of *E. coli* often affects cell physiology, resulting in growth arrest, cell lysis and poor display performance. In order to be displayed on the surface, the polypeptides produced in the cytoplasm have to traverse the IM, the periplasm and be inserted into the OM. Thus, OM proteins native to the organism have served as convenient targeting and anchoring portions and are widely used for display, though heterologous anchor proteins have also been evaluated. Several *E. coli* surface display systems have been described for display of peptides, enzymes and other proteins (Bessette et al., 2004; Rice et al., 2006; Hall et al., 2007; Dane et al., 2009; Kenrick and Daugherty, 2010; Little et al., 2011; van Bloois et al., 2011), but very few of these are focussed on the surface display of Abs, either full length or Ab fragments (Figure 7).

Georgiou and co-workers demonstrated in a proof-of-principle experiment that scFvs could be functionally displayed on the surface of *E. coli* and that FACS could be employed to isolate target-binding bacteria spiked in the background of non-binding cells (Francisco et al., 1993), and performed the first cell sorting of a library of scFv mutants. Both these experiments displayed anti-digoxin scFv libraries containing up to 4×10^6 scFvs on *E. coli* as N-terminal fusions to a chimeric lipoprotein (Lpp-OmpA'). Lpp-OmpA' is composed of the N-terminal signal peptide and the first nine residues of the mature Lpp fused to the residues 46 to 159 of

OmpA, which is a truncated fragment of its native 8-stranded β-barrel. The Lpp-OmpA´ format was the first bacterial display system to be combined with flow cytometry for library screening and used in protein engineering applications (Daugherty et al., 1998). scFv variants that bound digoxin with a K_D of <1 nM were identified. However, Lpp-OmpA' fusions were found to be toxic to the host cells primarily due to membrane disruption, and resulted in lysed cultures following protein induction (Christmann et al., 1999; Daugherty et al., 1999).

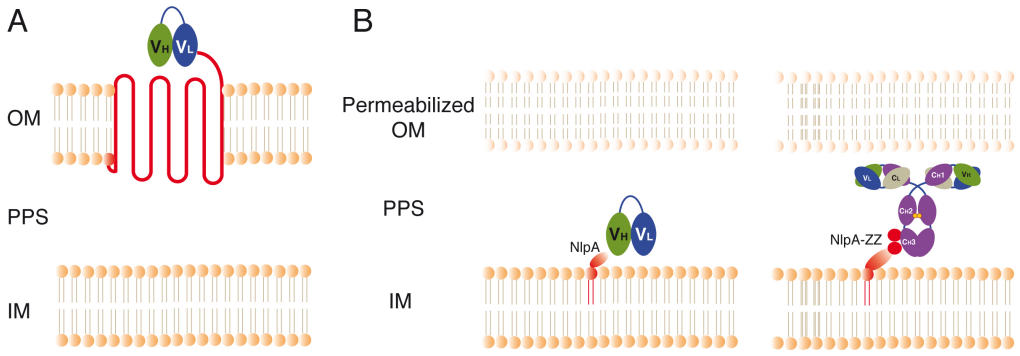

Figure 7. *E. coli* display of antibodies.

(**A**) Lpp-OmpA´ display (**B**) Anchored Periplasmic Expression (APEx) of scFvs and IgGs.

Displaying proteins of interest on the periplasmic side of the IM of *E. coli* s also a valuable display system for protein engineering. Advantages of this system include the lack of complex carbohydrates like LPS, that could sterically interfere with protein binding to large targets, and that the protein of interest is required to traverse only one membrane, which avoids factors that may restrict export. The anchored periplasmic expression (APEx) system anchors the protein of interest to the inner membrane, either as an N-terminal fusion to a six-residue sequence derived from the native *E. coli* lipoprotein NlpA or as a C-terminal fusion to the pIII gene that codes for the minor coat protein of M13 (Harvey et al., 2004). A slight modification of the APEx system enabled the display of full-length Abs. Abs are secreted into the bacterial periplasm, where they are captured by an inner membrane protein that binds their Fc domain. After permeabilization of the outer membrane, the displayed antibodies could interact with fluorescently labeled antigen, and binding clones were selected by flow cytometry. As the anchoring protein is not encoded by the plasmid carrying the antibody genes, soluble, full-length, aglycosylated IgG molecules can subsequently be produced by transformation of a bacterial strain devoid of the Fc-binding anchor protein (Mazor

et al., 2007). However, library screening involves the permeabilization of the OM (to permit access of the fluorescently labelled antigen to the periplasm) generating spheroplasts followed by sorting using FACS of these spheroplasts. Disruption of the OM and spheroplast production decreases dramatically the viability of bacteria and the isolated clones after FACS cannot be amplified by simple growth, thus requiring amplification of the enriched Ab genes by PCR and subcloning for the next round of sorting. Hence, although both the Lpp-OmpA' and APEx are good technologies for Ab selection, alternative methods that enable direct display of Abs or Ab libraries on the outer surface of *E. coli* cells, with little cellular toxicity and without the need for generation of Phabs or spheroplasts, would be of great interest.

Integral OM proteins and secreted proteins with OM-anchoring domains have also been used for display of Abs on the surface of *E. coli* (Lofblom, 2011), of which the autotransporters (AT) and Intimins stand out by their apparent simplicity and modularity as attractive systems (Wentzel et al., 2001; Rutherford and Mourez, 2006; Jose and Meyer, 2007; Wilhelm et al., 2011; Leo et al., 2012; Leyton et al., 2012b; Nicolay et al., 2013; Zude et al., 2013). These proteins play important roles in the virulence and survival of both pathogenic and environmental Gram-negative bacteria. Protein members of the AT and Intimin families are a part of the type V secretion system of Gram-negative bacteria (Leo et al., 2012). Intimins and ATs are large, secreted polypeptides that contain three functional regions: i) a N-terminal SP, that drives their Sec-dependent translocation across the IM; ii) a β-domain, that is anchored into the OM by a 12-stranded β-barrel with an internal peptide linker; and iii) a *passenger* region, that is secreted to the extracellular milieu (Leyton et al., 2012a). The passenger domains are highly diverse and carry the specific AT functions which maybe enzymatic, proteolytic, cytotoxic or adhesive (in the case of Intimin), and contribute to colonization, immune evasion and biofilm formation. Although, their mechanism of secretion remains uncertain, both AT and Intimin appear to use the β-barrel assembly machine (BAM) complex of the OM for insertion and translocation of the *passengers* to the cell surface (Figure 8) (Bernstein, 2007; Bodelon et al., 2009; Leyton et al., 2012a; Gruss et al., 2013; Noinaj et al., 2013).

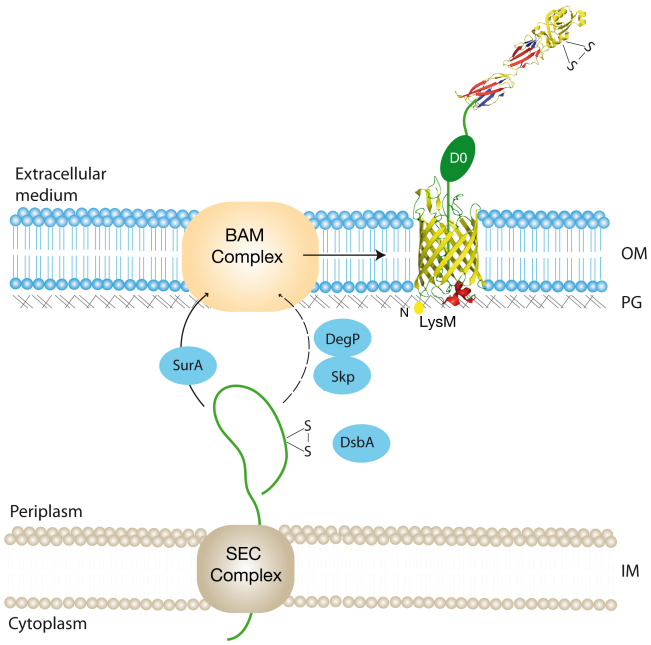

Figure 8. Proposed mechanism of the biogenesis of protein members belonging to the type V secretion system (T5SS).

Autotransporters and Intimins are members of the T5SS and their secretion to the extracellular medium shares a common mechanism. Secretion of Intimin is shown in the Figure. Intimin is translocated across the IM via the Sec-translocon. In the periplasm, DsbA catalyzes the formation of the disulfide bond (S-S) present in the D3 domain of Intimin. Intimin mostly follows the SurA pathway for its delivery to to the BAM complex, which is responsible for folding and OM insertion of its β-barrel domain. The alternate DegP/Skp pathway is used less frequently and is depicted with a dashed line. The LysM domain is predicted to bind the peptidoglycan (PG) layer. Translocation of the secreted domains D0 (green oval), D1, D2 and D3 is believed to take place concomitantly with insertion of the β-domain in the OM via the BAM complex. Based on (Bodelon et al., 2009; Fairman et al., 2012)

Despite their similarities, AT and Int/Inv proteins have important differences. They have opposite topological organization in the OM, the exposed *passenger* being located in the N-terminal region in AT, whereas is found at the C-terminus in the case of Int/Inv proteins (Figure 9). The distinct topologies are also reflected in their β-domains. In the case of AT, the first strand of the β-barrel is preceded by an α-helix linker that fills the lumen and connects its N-terminus with the *passenger* region (Oomen et al., 2004; Barnard et al., 2007). In contrast, the last strand of the β-barrel of Int/Inv proteins is followed by a peptide linker that runs through the lumen in an extended conformation connecting its C-terminus to the *passenger* region (Fairman et al., 2012). In addition, the natural *passenger* domains of AT and Int/Inv have distinct structures, i.e. β-helical rods in most ATs and tandems of Ig-like domains in Int/Inv proteins (Luo et al., 2000; Otto et al., 2005).

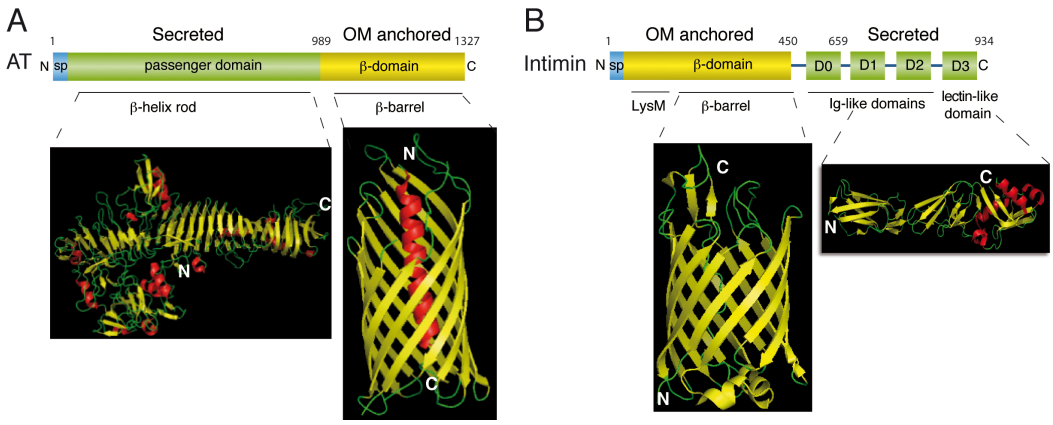

Figure 9. Modular organization and structure of AT and Intimin proteins.

(A) Scheme of AT proteins, showing the N-terminal SP, a secreted passenger domain, and an OM anchored C-terminal β-domain. Crystal structures of the passenger domain of Hbp (an AT protein from *E. coli*) (Otto et al., 2005) and β-domain of NalP (an AT protein from *N. meningitidis*) are shown. **(B)** Scheme of Intimin, showing the N-terminal SP, an OM anchored β-domain and a C-terminal passenger domain. The passenger consists of three Ig-like domains (D0, D1 and D2) and a lectin-like domain (D3). Crystal structures of the passenger domain (Luo et al., 2000) and the OM β-barrel (Fairman et al., 2012) of Intimin are shown.

Previous studies from our laboratory showed that the AT protein, IgA protease (IgAP) from *Neisseria gonorrhoeae* could display model scFv and sdAb clones on the surface of *E. coli* fused to its β-domain (Veiga 2004). In addition, improved display levels of a model sdAb on *E. coli* cells were observed when the β-domain of EhaA, an AT from enterohemorrhagic *E. coli* (EHEC) O157:H7 was used (Marin et al., 2010). The displayed sdAb was correctly folded with the canonical disulfide bond of V domains formed by the action of DsbA (Veiga et al., 2004; Marin et al., 2010). In a different study, the expression of Intimin from EHEC and enteropathogenic *E. coli* (EPEC) strains was demonstrated in *E. coli* K-12 cells with the display of its native Ig-like and lectin-like domains on the bacterial surface with a disulfide bond formed by DsbA (Bodelon et al., 2009). However, the utility of the β-domains of EhaA and Intimin for the display of Ab libraries had not been investigated. Hence, in this work we have evaluated these systems for display and selection of sdAbs from immune libraries raised against diverse antigens of biomedical importance, viz. a protein involved in the infection of enteropathogenic and enterohemorrhagic *E. coli* strains (i.e. Tir); a human serum protein that plays an important role in the blood coagulation (i.e. fibrinogen); and a tumor antigen overexpressed on the cell surface of many epithelial tumors, i.e. Epidermal growth factor receptor 1 (EGFR/HER1).

OBJECTIVES

The objectives of this work were as follows:

1) To evaluate and compare the β-domains of Intimin and EhaA proteins from EHEC for the display of functional sdAbs on the surface of *E. coli*.

2) To utilize the *E. coli* display systems based on the β-domains of Intimin and EhaA proteins for expression of immune libraries of sdAbs and selection of high-affinity clones binding protein antigens of bacterial and human origin.

3) To characterize sdAbs selected by *E. coli* display and determine their binding affinities and specificity using flow cytometry of *E. coli* cells, as well as compare the data with that obtained with standard biochemical technologies (ELISA and SPR).

4) To apply the *E. coli* display platform for direct selection of sdAbs on live tumor cells expressing a relevant antigen such as EGFR on their surface.

MATERIALS AND METHODS

1. Bacterial strains

The bacterial strains used in this work are described in Table 2.

Table 2. Bacterial strains used in this work.

Name	Genotype / Characteristics	References
BL21 (DE3)	F$^-$ *omp*T *hsd*S_B(rB–, mB–) *gal dcm lon* λ(DE3) [*lacI* lacUV5-T7 *gene1 ind1 sam7 nin5*])	Novagen
DH10B-T1^R	F$^-$ *mcrA* Δ*mrr-hsdRMS-mcrBC φ80lacZDM15* Δ*lacX74 recA1 endA1 araD139* Δ*(ara,leu) 7697 galU galK rpsL (StrR) nupG tonA* λ$^-$	Invitrogen
MG1655	K-12 (F$^-$ λ$^-$)	(Blattner, 1997)
EcM1	MG1655Δ*fim*A-H	(Blomfield et al., 1991)
UT5600	K-12 (F$^-$ λ$^-$) Δ*(ompT-fepC)266*	(Grodberg and Dunn, 1988)
WK6	Δ (*lac-proAB*), *galE*, *strA*, *nal*, F'[*lacI^q*ZDM15, *proAB*]	(Zell and Fritz, 1987)
HB2151	K-12 Δ(*lac-proAB*), *ara*, *nal^R*, *thi*, F'[*lacI^q*ZDM15, *proAB*]	(Carter et al., 1985)
HM140	*F$^-$ ΔlacX74 galE galK thi rpsL (StrA) ΔPhoA (PvuII) degP ptr ompT eda tsp rpoH15*	(Meerman and Georgiou, 1994)

2. Conditions of bacterial growth

The *E. coli* DH10B-T1^R strain was used in the preparation of electrocompetent cells for use in the cloning experiments. Bacteria carrying plasmids with V_{HH} were grown at 30 °C in Luria–Bertani (LB) liquid medium or on agar plates with the appropriate antibiotic for plasmid selection. LB plates and pre-inoculum media prior to induction contained 2% (w/v) glucose for repression of the *lac* promoter. The preinocula cultures were started from individual colonies (for single clones) or from a mixture of clones (in case of libraries), freshly grown and harvested from plates, diluted to an initial OD_{600} of 0.5, and grown overnight (o/n) under static conditions. For induction, bacteria (corresponding to an OD_{600} of 0.5) were harvested by centrifugation (4000

xg, 5 min), and grown in the same media with 0.05 mM isopropylthio-β-D-galactoside (IPTG), but without glucose for 3 h with agitation (160 rpm), unless indicated otherwise. For over-expression of soluble V_{HH} in the periplasm, *E. coli* WK6 cells with the corresponding pCANTAB6-V_{HH} plasmid (Ap^R) were induced with 0.3 mM IPTG for 3 h at 30 ºC. Secretion of V_{HH} into the culture media was performed using the hemolysin (Hly) secretion system of *E. coli* HB2151 cells carrying pVDL9.3 (HlyBD; Cm^R) and the corresponding pEHlyA4SD-VHH (Ap^R) plasmids, induced with 0.3 mM IPTG for 6 h. Over-expression of soluble $TirM_{EHEC}$ with N-terminal His-tag was induced in *E. coli* BL21 (DE3) cells carrying the pET28a-$TirM_{EHEC}$ plasmid (Km^R) and grown at 37 ºC in LB medium containing 1.0 mM IPTG for 2 h. For over-expression of soluble V_{HH} as MBP fusions in the periplasm, *E. coli* HM140 strain with the corresponding pMAL1-V_{HH} plasmid (Ap^R) was induced with 0.3 mM IPTG for 3 h with agitation (250 rpm).

3. Cell lines and Growth conditions

Frozen aliquots of mouse fibroblast cells, viz. NIH 3T3 2.2 and HER14 were thawed and seeded into culture flasks (BD Falcon) containing 25 ml DMEM (Sigma) supplemented with 10% Fetal bovine serum (FBS, Sigma), 2 mM Glutamine, and grown in an incubator (Thermo Scientific) at 37° C with 5% CO_2. Cells were subcultured periodically, when the cultures attained a confluency of ~80%. In experiments of selection of VHH libraries on cells, growing cells in culture were trypsinized and seeded in 6-well plates (Falcon) containing growth media to a confluency of ~20%, the day before the experiment. For Immunofluorescence microscopy (IFM) experiments, cells were seeded and grown on circular coverslips (previously irradiated with UV for 30 mins) present in 24-well plates (Falcon), prior to infection with bacteria, staining and analysis under the microscope.

4. DNA constructions

The plasmid constructions used in this work were carried out using standard techniques of DNA amplication and modification as described by Ausubel et al, 1997.

Table 3. List of plasmids used in this work.

Name	Characteristics	References
pAK-Not	(Cm^R), $lacI^q$-P*lac* promoter, pBR322 ori	(Veiga et al., 1999)
pHEA	pAK-Not derivative; for fusions to C-EhaA (pelB-His-E-tag-EhaA$_{989-1327}$)	(Marin et al., 2010)
pVgfpA	pHEA-derivative; Vgfp fused to C-EhaA (pelB-Vgfp-E-tag-EhaA$_{989-1327}$)	(Salema et al., 2013)
pVTIR_nA	pHEA-derivative; V$_{TIR}$ (n clone) fused to C-EhaA (pelB-V$_{TIR}$n-E-tag-EhaA$_{989-1327}$)	(Salema et al., 2013)
pVFIB_nA	pHEA-derivative; V$_{FIB}$ (n clone) fused to C-EhaA (pelB-V$_{FIB}$n-E-tag-EhaA$_{989-1327}$)	This work
pNeae	pAK-Not derivative; Neae[Intimin$_{EHEC}$ (1-659)-E-His-tag]	(Bodelon et al., 2009)
pNeae2	pNeae-derivative; for fusions to Neae-myc [Intimin$_{EHEC}$ (1-659)-E-His-myc tag]	(Salema et al., 2013)
pNVgfp	pNeae-myc-derivative; NVgfp fusion [Intimin$_{EHEC}$ (1-659)-E-Vgfp-myc tag]	(Salema et al., 2013)
pNVTIR_n	pNeae-myc-derivative; NV$_{TIR}$ (n clone) fusion [Intimin$_{EHEC}$ (1-659)-E-V$_{TIR}$n-myc tag]	(Salema et al., 2013)
pNVFIB_n	pNeae-myc-derivative; NV$_{FIB}$ (n clone) fusion [Intimin$_{EHEC}$ (1-659)-E-V$_{FIB}$n-myc tag]	This work
pNV$EGFR_n$	pNeae-myc-derivative; NV$_{EGFR}$ (n clone) fusion [Intimin$_{EHEC}$ (1-659)-E-V$_{EGFR}$n-myc tag]	This work
pCANTAB6	(Ap^R), pUC-ori, for pIII fusions or soluble expression of sdAb with His-myc-tags	(McCafferty et al., 1996)
pCANTAB6-V$_{TIR1}$	pCANTAB6-derivative; for expression of sdAb V$_{TIR1}$ with His-myc-tags	(Salema et al., 2013)
pCANTAB6-Vgfp	pCANTAB6-derivative; for expression of sdAb Vgfp with His-myc-tags	(Salema et al., 2013)
pCANTAB6-VFIB_n	pCANTAB6-derivative; for expression of sdAb V$_{FIB}$ (n clone) with His-myc-tags	This work
pET28-a	(Km^R), pBR322-ori, T7 promoter; for N-terminal His-tag protein fusions	Novagen
pET28-a-TirM_{EHEC}	pET28-a derivative; His-tagged TirM_{EHEC} (residues 252 to 360 of Tir$_{EHEC}$)	(Salema et al., 2013)
pVDL9.3	(Cm^R), pSC101-ori, *lac* promoter, for production of HlyB and HlyD transporters	(Fernandez et al., 2000)
pEHlyA2SD	(Ap^R), pUC-ori, *lac* promoter, C-terminal E-tagged HlyA signal	(Fernandez et al., 2000)
pEHlyA4SD	pEHlyA2SD derivative with modified polylinker having unique *Sfi*I and *Not*I sites	(Salema et al., 2013)
pEHlyA4SD-V$_{TIR}$n	pEHlyA4SD derivative; V$_{TIR}$ (n clone) fused to C-terminal E-tagged HlyA signal	(Salema et al., 2013)

pMAL-p2E	(Ap^R), pUC-ori, contains multiple cloning sites (MCS) for cloning of recombinant proteins in fusion to maltose binding protein (MBP) and soluble expression in the periplasm of *E. coli*	New England Biolabs
pMAL1	pMAL-p2E derivative; for sdAb fusion to MBP [MalE-PreScission protease site-sdAb-His tag]	(Salema and Fernandez, 2013)
pMAL1-V_{FIB_n}	pMAL-p2E derivative, VFIB (n clone) fused to C-terminal of MBP, for soluble expression of sdAb, VFIB (n clone) in *E. coli* periplasm	(Salema and Fernandez, 2013)
pMAL1-Vgfp	pMAL-p2E derivative, Vgfp fused to C-terminal of MBP, for soluble expression of sdAb, Vgfp in *E. coli* periplasm	(Salema and Fernandez, 2013)

Table 4. List of oligonucleotides.

Name	Nucleotide sequence (5'-3')
RSP -48	AGCGGATAACAATTTCACACAGGA
pAK-directo	GTGACGCAGTAGCGGTAAACGGCAGAC
eae4	CGTAATGGCAATAGCTCTAACAATGTA
eae5	GACTTCAGCACTTAATGCCAGTGCGG
VHH-*Sfi*2	GTCCTCGCAACTGCGGCCCAGCCGGCCATGGCTCAGGTGCAGCTGGTGGA
VHH-*Not*2	GGACTAGTGCGGCCGCTGAGGAGACGGTGACCTGGGT
VTIR1_CDR3_up	GAGAGTAGGGATGGGCGTGTG
VFIB1_CDR3_up	GTAGTTATACTTTCCCATATCGTAC
VFIB2_CDR3_up	GGACTCGGGTGCACAGCGTCTCCA
VEGFR1_CDR3_up	CCAGTAGTCATAGTCAACGCTCCG
VEGFR2_CDR3_up	CTCAGTGGTCATGCGCGGGAAGT
VEGFR3_CDR3_up	CCCCAGTAGGCATATCTTTCTG
VEGFR4_CDR3_up	GGCCCACTTTGTAAAGATAGTATC
VEGFR6_CDR3_up	GTCATACTTCTCGGACGTTGTAG
MalE-3'_down	GCCAGCGGTCGTCAGACTGTCGATG
pMAL-up	TTGTAAAACGACGGCCAGTGCCAAGCT
EcoRI-PreScission-*SfiI*	CCGGAATTCCTGGAAGTTCTGTTCCAGGGGCCCGGGGCCCAGCCGGCCATGGCTCAGGTGCAGCTGGTGGA
HindIII-stop-myc	CGGGCAGGAAGCTTTTACTATGCGGCCCCATTCAGATCCTC

5. Protein electrophoresis and Western blot

Whole cell protein extracts were prepared by harvesting bacteria after induction (1 ml of OD_{600} 1.5), resuspended in 50 µl of 10 mM Tris HCl pH 8.0, mixed with the

same volume of SDS-sample buffer (2X) or urea-SDS sample buffer (2X) and boiled for 10 min (pHEA constructs) or 30 min (pNeae constructs). The SDS-sample buffer (1X) consists of 60 μM Tris-HCl pH 6.8, 1% w/v SDS, 5% (v/v) glycerol, 0.005% (w/v) bromophenol blue and 1% (v/v) 2-mercaptoethanol (2-ME). The urea-SDS-sample buffer (1X) contains 60 μM Tris-HCl pH 6.8, 2% w/v SDS, 4 M urea, 5 mM EDTA, 5% (v/v) glycerol, 0.005% (w/v) bromophenol blue and 1% (v/v) 2-mercaptoethanol (2-ME). The boiled samples were sonicated (5 sec; Labsonic B Braun), centrifuged (14,000 x*g*, 5 min) to pellet insoluble material, loaded onto 8% or 10% SDS-PAGE gels and run using a Miniprotean III electrophoresis system (Bio-Rad). For Western blot, the gels were transferred to a polyvinylidene difluoride membrane (PVDF, Immobilon-P, Millipore) using a semi-dry electrophoresis transfer apparatus (Bio-Rad) and the membranes were blocked in phosphate buffered saline (PBS; 8 mM Na_2HPO_4, 1.5 mM KH_2PO_4, 3 mM KCl, 137 mM NaCl, pH 7.0) with 3% (w/v) skimmed milk (Milk-PBS) for 1 hour at RT. For immunodetection of the E-tagged proteins, membranes were incubated for 1 h at room temperature (RT) in the same buffer with anti-E-tag mAb (Phadia), while for immunodetection of the myc-tagged proteins anti-c-myc-POD mAb (clone 9E10; Roche) was used. Membranes were washed three times with PBS containing 0.1% Tween 20 to remove unbound Abs. Bound anti-E-tag mAb was developed using anti-mouse IgG conjugated with peroxidase (POD) (Sigma). Streptavidin-POD conjugate (Roche) was employed to detect the biotinylated broad range SDS-PAGE protein markers (Bio-Rad). All mAbs and POD conjugates were used in a 1:5000 dilution. For developing, a chemiluminescence reaction was prepared using a mixture of 1.25 mM luminol (Sigma) and 200 μM p-coumaric acid (Sigma) in 10 ml of 100 mM Tris–HCl (pH 8.0). Following a rapid rinse in PBS, the membranes were soaked in the chemiluminiscence mixture and H_2O_2 (Sigma) was added at 0.02% (v/v), followed by one minute incubation in the dark and the PVDF-membranes were either exposed to an X-ray film (Curix, Agfa) or scanned in a Chemi-Doc XRS (Bio-Rad). To quantify the total number of V_{HH} fusions expressed in *E. coli*, Western blots of whole cell protein extracts and dilutions of a purified E-tagged V_{HH} of known concentration (hereafter referred to as “unknowns” and “standard”, respectively) were visualized on a ChemiDoc XRS and analyzed using the Quantity One software (Bio-Rad). The

intensity of bands from standard and unknown samples was measured and the local background was corrected. The total number of molecules in the various dilutions of the standard protein was calculated and was plotted against the corresponding values of density of its band (Intensity/mm^2) to generate a standard curve. Based upon the standard curve plot, the number of molecules of V_{HH} fusions in the unknown samples was estimated, assuming that ~$1.5x10^8$ bacteria (0.15 units of OD_{600}) were loaded per lane. Two independent experiments were done with each sample in duplicates.

6. Protease accessibility assays

Induced bacteria (1 ml, OD_{600}=1.5) were harvested by centrifugation (4000 xg, 3 min) and resuspended in 100 ml of 10 mM Tris HCl pH 8.0. This bacterial suspension was incubated with trypsin (10 mg/ml; Sigma) or with proteinase K (ProtK; 40 mg/ml; Roche) as indicated, for 20 min at 37 °C. Next, the trypsin inhibitor (5 mg/ml; Sigma) or the serine proteases inhibitor (PMSF 1 mM; Sigma) was added to stop further proteolysis. The cell suspension was centrifuged (14,000 xg, 1 min), the cell pellet resuspended in 50 ml of 10 mM Tris HCl pH 8.0, lysed with one volume of SDS-sample buffer (2X) or urea-SDS-sample buffer (2X), boiled and analyzed by Western blot.

7. ELISA

$TirM_{EHEC}$ or BSA (Sigma) proteins were adsorbed at 4°C o/n onto 96-well immunoplates (Maxisorb; Nunc) at a concentration of 5 μg/ml in PBS. Next, immunoplates were washed in PBS and blocked by incubation with 200 μl of 3% (w/v) Milk -PBS for 2 h at RT. The sdAbs (secreted or purified) were diluted in 3% (w/v) Milk-PBS, added at the indicated concentrations (0.1-100 nM) in duplicates and incubated for 1 h at RT. After incubation, the wells were washed three times with PBS (Immunowash 1575, Bio-Rad) and the bound sdAbs was detected by the addition of anti-c-myc-POD mAb (clone 9E10; Roche; 1:1000), or anti-E-tag mAb (Phadia; 1:1000) followed by anti-mouse-POD (Sigma; 1:1000) for E-tagged sdAb, and incubation of the plates for 1 h at RT. The plates were washed three times with PBS and developed with H_2O_2 and o-phenylenediamine (OPD; Sigma) as previously

described (Jurado et al., 2002). The plates were read at 490 nm using the iMark ELISA plate reader (Bio-Rad).

8. Purification of $TirM_{EHEC}$

500 ml cultures of induced *E. coli* BL21(DE3) cells carrying pET28a-$TirM_{EHEC}$, were centrifuged (4000 xg, 15 min, 4ºC) and the pellet was resuspended in 25 ml of PN3 buffer (50 mM sodium phosphate pH 7.4, 300 mM NaCl) containing DNase (0.1 mg/ml; Roche) and a cocktail of protease inhibitors (Complete EDTA-free; Roche). The cells were lysed in a French Press at 1200 psi (3 cycles) and the whole cell lysate was ultracentrifuged (40000 xg, 1 h, 4ºC). The supernatant was loaded (flow rate of 1 ml/min) onto a column packed with 3 ml of a Cobalt-containing resin (Talon, Clontech) pre-equilibrated with 30 ml PN3 buffer. The column was subsequently washed with 10 ml of PN3 buffer, followed by a wash with 10 ml of PN3 buffer containing 5 mM imidazole and the protein was finally eluted in 1 ml fractions with the PN3 buffer containing 150 mM imidazole. The eluted fractions were dialyzed against HEPES-buffer (20 mM HEPES pH 7.4, 200 mM NaCl, sterile filtered and degassed). Dialyzed fractions were concentrated 10 fold in a 3-kDa centrifugal filter unit (Amicon Ultra-15) and loaded onto a gel filtration column (HiLoad 16/600 Superdex 75 preparative grade, GE Healthcare), pre-equilibrated with HEPES-buffer and calibrated with protein markers (Gel Filtration Standards, Bio-Rad) and Blue dextran (for exclusion volume V_0; Sigma). Fractions of 1 ml containing $TirM_{EHEC}$ were collected and checked for purity by SDS-PAGE. Protein concentration was estimated using the Bicinchoninic acid (BCA) Pierce protein assay kit (Thermo Scientific).

9. Magnetic Cell Sorting (MACS) of VHH immune libraries

Induced *E. coli* cells (equivalent to a final OD_{600} of 5.0) were harvested by centrifugation (4000 xg, 3 min), washed three times with 2 ml PBS (sterile filtered and degassed), and resuspended in a final volume of 1 ml of PBS. Biotinylated antigen ($TirM_{EHEC}$, hFib or rhEGFR, at concentrations indicated) was added to 100 µl of bacteria, the final volume was adjusted to 200 µl with PBS-BSA (PBS supplemented with 0.5% w/v BSA, sterile filtered and degassed), and incubation was carried out for 1 h at RT. After incubation, bacteria were washed three times

with 1 ml of PBS-BSA, resuspended in 100 ml of the same buffer containing 20 μl of anti-biotin paramagnetic beads (Miltenyi Biotec) and incubated at 4 ºC for 20 min. Next, bacteria were washed three times with 1 ml of PBS-BSA, resuspended in 500 μl of the same buffer, of which 10 μl was kept aside to calculate the input bacteria before the procedure, while the rest (490 μl) was applied onto a MACS MS column (Miltenyi Biotec), previously equilibrated with 500 μl of PBS-BSA and placed on the OctoMACS Separator (Miltenyi Biotec). The flow through of unbound cells was collected and the column was washed three times with 500 μl of PBS-BSA. The wash was combined with the flow-through as "Unbound fraction". Next, the column was removed from the OctoMACS Separator and placed onto a new collection tube, 2 ml of LB was added and the cells were eluted out. This fraction was labeled as the "Bound fraction". Serial dilutions of Unbound and Bound fractions were plated to determine CFU and to harvest the bound bacteria.

10. Flow cytometry of VHH clones or VHH immune libraries

For standard flow cytometry, induced bacterial cells (equivalent to a final OD_{600} of 1.0; ~10^9 CFU) were harvested by centrifugation (4,000 xg, 3 min), washed twice with 500 μl of PBS (filter-sterilized) and resuspended in a final volume of 400 μl of PBS. Next, 190 μl of this cell suspension (~$3x10^8$ CFU) was incubated with the primary Ab or antigen (as indicated) and PBS was added to adjust the total volume to 200 μl. The primary Abs (for assay of expression levels) were anti-E-tag mAb (1:200; Phadia) or anti-c-myc mAb (1:200; 9B11 clone; Cell Signalling), while biotinylated antigens (GFP, $TirM_{EHEC}$, hFib, rhEGFR or BSA) were used at 50 nM for assay of antigen binding, unless otherwise indicated. The samples were incubated at RT for 1h. After incubation, the cells were washed once with 500 μl of PBS, and resuspended either in 500 μl of PBS containing 1 μl of anti-mouse-IgG1 conjugated to Alexa 488 Fluor (2 mg/ml, Invitrogen) or in 200 ml of PBS containing 30 μl of 1:200 dilution of Streptavidin-phycoerythrin (PE) (0.5 mg/ml, Beckman Coulter). The mixture was incubated 30 min at 4 ºC in the dark. The cells were washed once with 500 μl of PBS and resuspended in a final volume of 1 ml in PBS. For each experiment at least 100,000 cells were analyzed in a cytometer (Gallios, Beckman Coulter).

11. Affinity Determination by Flow cytometry

Induced *E. coli* cells (equivalent to final OD_{600} of 1) were centrifuged (4000 xg, 3 min), washed twice with 1 ml of PBS (filter-sterilized) and resuspended in a final volume of 1 ml of PBS. Next, 50 µl of this cell suspension (~$3x10^7$ CFU) was incubated at room temperature for 90 min with a fixed amount of biotinylated $TirM_{EHEC}$ and hFib (2 pmols) or rhEGFR (1 pmol) and increasing volumes of PBS (from 0.1 to 1.5 ml) to attain a final concentration range between 20 nM to 1 nM or 100 nM to 0.8 nM respectively. After incubation, cells were centrifuged (4000 xg, 3 min), washed twice with 1 ml of PBS (filter-sterilized) and labeled with Streptavidin-PE as described for standard flow cytometry. After a final washing step with PBS, the mean fluorescence intensity (MFI) of Phycoerythrin (PE) was quantified in a cytometer (Gallios, Beckman Coulter). Data of MFI (relative values to maximum MFI) obtained from the cytometer were plotted against the concentration of biotinylated antigen to obtain the dissociation constant (K_D). Curve was fitted according to non-linear least squares regression method and one site - specific binding saturation kinetics model using the data analysis tool in Prism software (GraphPad).

12. Purification of VHHs from the periplasm of *E. coli*

Soluble VHHs with His_6 and myc tags in their C-termini were induced in *E. coli* WK6 cells carrying pCANTAB6-V_{TIR1} or pCANTAB6-Vgfp. Cells were pelleted by centrifugation (4000 xg, 12 min, 4ºC) from 1 L cultures, resuspended in 22.5 ml Periplasmic Extraction buffer [50 mM Sodium phosphate pH 7.4, 200 mM NaCl, 5 mM EDTA and 1 mg/ml polymyxin B sulphate (Sigma)] and stirred at 4ºC for 2 h using a magnetic stirrer. The periplasmic extract was obtained by ultracentrifugation (40000 xg, 30 min, 4ºC) and dialyzed o/n at 4ºC against 5 L of PN2 buffer (50 mM sodium phosphate pH 7.4, 200 mM NaCl). Dialyzed extract was loaded onto a Cobalt-containing affinity resin (Talon, Clontech), washed, and bound protein eluted in PN2 with 150 mM imidazole. Eluted sdAb was dialyzed, concentrated, and loaded onto a calibrated gel filtration column (HiLoad 16/600 Superdex 75 preparative grade, GE Healthcare) as described previously for $TirM_{EHEC}$. The fractions corresponding to the monomeric sdAb were collected and concentrated in a 3-kDa centrifugal filter unit (Amicon Ultra-15). Protein concentration was

estimated using the Bicinchoninic acid (BCA) Pierce protein assay kit (Thermo Scientific).

13. Purification of VHHs from the periplasm as fusions with Maltose binding protein (MBP)

Frozen pellets of *E. coli* cells (ca. 3 grams of wet weight), harvested from induced 1 L cultures, were thawed in 25 ml of buffer NaPi (50 mM sodium phosphate pH 7.4, 200 mM NaCl) containing DNaseI (0.1 mg/ml, Roche) and a cocktail of protease inhibitors (Complete EDTA-free, Roche). Bacteria were lysed using the French Press at 1200 psi (3 cycles). All of the following steps were carried out at 4ºC. The cell lysate was clarified by a low-speed centrifugation (5000 x*g*, 15 min), to pellet non-lysed bacteria and cell debris, followed by a high-speed centrifugation (20000 x*g*, 60 min) using the supernatant obtained from the previous step. The final supernatant was filtered through a 0.22 μm syringe filter (PVDF, Durapore, Merck Millipore) and loaded (at a flow rate of 1 ml/min) onto a chromatography column packed with 2 ml of amylose resin (New England Biolabs) pre-equilibrated with 20 ml (10 column volumes) of buffer NaPi. All steps were performed in a BioLogic LP chormatography system (Bio-Rad). The column was washed with 20 ml of buffer NaPi, followed by elution of the MBP-fusion protein with 20 ml of buffer NaPi containing 10 mM D-maltose (Sigma), in 1-ml fractions. The collected fractions were analyzed for purity by SDS-PAGE and total protein content by the Bicinchoninic assay (BCA, Piercenet) with BSA as protein standard. Selected fractions of high protein content and purity were pooled together and dialyzed o/n against 5 L of buffer NaPi. Dialyzed protein samples were loaded at a flow rate of 1 ml/min onto a chromatography column packed with 2 ml IMAC resin (Talon, Clontech), pre-equilibrated with 20 ml of buffer NaPi. The column was washed with 10 ml of buffer NaPi followed by 10 ml of buffer NaPi containing 10 mM imidazole (Sigma). MBP-fusions were eluted with 20 ml of buffer NaPi containing 150 mM imidazole in 1-ml fractions. The eluted protein fractions were analyzed for protein content by BCA assay and purity by SDS-PAGE analysis. Selected fractions of high purity and protein content were concentrated 10-fold and the buffer was exchanged to NaPi in a 3-kDa centrifugal filter unit (Amicon Ultra-15, Merck Millipore) to remove imidazole.

In cases when VHH free from the MBP was desired, enzymatic cleavage of the MBP-VHH_{His6} fusions was carried out using dialyzed protein samples (from above). Fifty units of PreScission protease® (GE Healthcare) were added to 5 mg samples of MBP- VHH_{His6} fusions in buffer NaPi and incubated at 4 ºC for 16 h on a rolling wheel. Digested samples were loaded onto a chromatography column packed with 2 ml amylose resin (New England Biolabs) in order to remove free MBP and undigested MBP- VHH_{His6} fusions. The VHHs with C-terminal His_6- and myc- tags were collected in the flow-through fraction and loaded directly onto a chromatography column packed with 2 ml IMAC resin (Talon, Clontech), as described above with MBP-fusions. The column was washed and VHHs were eluted as previously described with MBP-fusions. All steps were performed in a BioLogic LP chormatography system (Bio-Rad) at 4 °C. The eluted protein fractions were analyzed for protein content by BCA assay and purity by SDS-PAGE analysis. Selected fractions of high purity and protein content were concentrated 10-fold and the buffer was exchanged to 20 mM HEPES pH 7.4, 200 mM NaCl in a 3-kDa centrifugal filter unit (Amicon Ultra-15, Merck Millipore). The concentrated protein was loaded at a flow rate of 1 ml/min onto a Gel-filtration column (HiLoad 16/600 Superdex 75 pg, GE Healthcare Life Sciences) pre-equilibrated with 360 ml of 20 mM HEPES pH 7.4, 200 mM NaCl and pre-calibrated with Gel-filtration protein standards (Bio-Rad) and Blue Dextran (Sigma). The fractions corresponding to the size of monomeric VHHs were collected, concentrated 10-fold in a 3-kDa centrifugal filter unit (Amicon Ultra-15, Merck Millipore) and analyzed for purity by Western blot and SDS-PAGE. Total protein concentration was determined by the microBCA protein assay (Piercenet) with BSA as the protein standard.

14. Surface plasmon resonance (SPR)

SPR measurements were performed using a Biacore 3000 instrument (GE Healthcare). All proteins solutions were dialyzed against HEPES-buffer [20 mM HEPES 200 mM NaCl (pH 7.4) sterile filtered and degassed] at 4ºC o/n. Biotinylated $TirM_{EHEC}$ (0.1 μg/ml) or Human fibrinogen (60 μg/ml) was immobilized on a Streptavidin SA chip (GE Healthcare) at 150 response units (RU) or 18000 response units (RU) at a flow rate of 10 μl/min in HEPES-buffer containing 0.005% (v/v) of the

surfactant Polysorbate 20 (P20, GE Healthcare). For determination of binding kinetics, dilutions of purified sdAb (analyte) from 32 nM to 200 pM (in case of V_{TIR1}), from 40 nM to 2.5 nM (in case of V_{FIB1}) or from 80 nM to 5 nM (in case of V_{FIB2}) were flown at 30 µl/min in HEPES-buffer and sensograms were generated. The biotinylated antigen surface on the Streptavidin SA chip was regenerated after every cycle using three injections (10 µl) of 10 mM Glycine-HCl (pH 1.7) or 10 mM Glycine-HCl (pH 2.5) in case of $TirM_{EHEC}$ and Human fibrinogen respectively. Sensograms with the different concentrations of analyte were overlaid, aligned and analyzed with BIAevaluation 4.1 software (GE Healthcare). All data were processed using a double-referencing method.

15. Selection of V_{HH} immune libraries on cells

Mouse fibroblast cell lines i.e. NIH-3T3 2.2 ($EGFR^-$)and HER14 ($EGFR^+$), growing in monolayers in 6-well culture plates (BD Falcon) containing culture media and at a confluency of ~40-50% i.e. ~$6X10^5$ cells were washed with Hank´s balanced salt solution (HBS, Sigma) solution. Induced *E. coli* cells (equivalent to a final OD_{600} of 1) were harvested by centrifugation (4000 xg, 3 min), washed with 2 ml HBS. 300 µl of washed bacteria (containing ~$6X10^7$ cells) were added to wells with NIH-3T3 2.2 cells and incubation was carried out for 1 h at 37ºC. After incubation, the unbound bacteria were recovered, added to wells containing HER14 cells and further incubation was carried out for 15 min at 37ºC. Next, HER14 cells were washed three times with 1 ml of HBS, to remove any non-specific binders and lysed by addition of HBS supplemented with 0.2% SDS and 0.1% DNAse. Serial dilutions of the cell lysate containing bacteria were plated to determine the CFU of bacteria recovered after the procedure. All experiments were carried out in duplicates.

16. Immunofluorescence microscopy (IFM)

~$5X10^4$ cells of the mouse fibroblast cell lines viz. NIH-3T3 2.2 and HER14 (in DMEM supplemented with FBS and Glutamine), were seeded onto circular coverslips (previously UV irradiated for 30 mins, placed in 24 well tissue culture treated plates), and grown in an incubator at 37º C and 5% CO_2 for 36 hours. Induced *E. coli* cells (1 OD_{600}) were washed in HBSS and used to infect the cells at a Multiplicity of Infection (MOI) of 100:1 for 20 mins at 37ºC. The coverslips were

washed by immersion in a beaker containing PBS (1X). Washed cells were fixed with 4% paraformaldehyde (PFA, Sigma) for 20 mins and subsequently washed ten times in PBS to remove excess of PFA. The coverslips were incubated at room temperature with the primary Ab for 45 mins (as described below), washed ten times in PBS and incubated with the secondary Ab (as described below) for 30 mins. Upon incubation, the coverslips were washed ten times in PBS, mounted on slides using ProLong Gold anti-fade reagent (Life technologies, Ref: P36930) and visualized using a Zeiss Axioimager immunofluorescence microscope.

Different primary and secondary Abs, diluted in PBS and 10% goat serum, were used to stain the eukaryotic cell and the bacteria respectively. EGFR present on the surface of eukaryotic cells was stained with an anti-EGFR mAb (EMD Millipore, Ref: GR01, dilution 1:750), while *E. coli* cells were stained with a rabbit anti- *E. coli* all antigens polyclonal Ab (Amsbio, Ref: B65001R, dilution 1:1500). In case of secondary Abs used, a rabbit anti-mouse mAb conjugated to the fluorophore Alexa 488 (Life technologies, Ref: A-11059, dilution 1:500) stained the EGFR in green, a goat anti-rabbit Ab conjugated to the fluorophore Alexa 594 (Life technologies, Ref: A-11012, dilution 1:500) stained the bacteria in red and DAPI (4',6-diamidino-2-phenilindole, Life technologies, Ref: D3571) stained the DNA in the microscopy preparations in blue.

RESULTS

Chapter 1: Display of single domain Ab clones and immune libraries against TirMEHEC and Human fibrinogen on the surface of *E. coli* cells

1.1 Comparison of EhaA and Intimin β-domains for display of sdAbs on *E. coli*

To compare the potential of Intimin and EhaA β-domains for the display of sdAbs we employed camelid V_{HH} (nanobodies) (Muyldermans et al., 2009). Initial assays were conducted using a model V_{HH} clone binding GFP (Vgfp) (Rothbauer et al., 2008) fused to the β-domains of EhaA and Intimin for comparison of the two systems before cloning of an immune library of sdAbs. Vgfp was cloned in pHEA vector (Table 2) in frame with the N-terminal SP of PelB (Keen and Tamaki, 1986) and the C-terminal fragment of EhaA (residues 989-1327; named as C-EhaA), bearing its native β-barrel with α-helix linker, and including the E-tag epitope between the VHH and C-EhaA (Figure 10A) (Marin et al., 2010). The Vgfp sequence was cloned in pNeae2 (Table 2) in frame with the N-terminal fragment of Intimin (residues 1-659; named as Neae), comprising its N-terminal SP, periplasmic LysM domain (expected to bind the peptidoglycan), native β-barrel with C-terminal linker, the first Ig-like domain (D0); and in addition, the E-tag and myc-tag (EQKLISEEDL) epitopes flanking the VHH for detection of expression and binding (Figure 10B). Both *E. coli* display vectors contain unique *Sfi*I and *Not*I restriction sites flanking the VHH in the same frame as those of conventional phagemids (e.g. pHEN6, pCANTAB6) (McCafferty et al., 1994). The resulting fusion proteins were referred to as VHHA (fusions to C-EhaA) and NVHH (fusions to Neae).

The expression of VgfpA and NVgfp fusions in *E. coli* K-12 cells (strain UT5600; Table 1) was analyzed by Western blot after induction with 0.05 mM IPTG at 30 °C for 3 h (see Materials and Methods). Discrete protein bands corresponding to VgfpA and NVgfp were detected with anti-E or anti-myc mAbs in whole cell protein extracts from the induced cells (Figure 10C and Figure 10D). Both fusion proteins, i.e. VgfpA and NVgfp, showed a shift in their electrophoretic mobility (Figure 10C

and Figure 10D), a characteristic of native OMPs with correctly folded β-barrels, which makes them resistant to SDS denaturation at low temperatures and hence migrate faster than the unfolded polypeptides due to the compact structure of the β-barrel (Schnaitman, 1973; Koebnik et al., 2000).

Interestingly, NVgfp was resistant to 2% SDS and 4 M urea at low temperatures (i.e. 22 °C) and required boiling in this buffer to unfold, as previously reported for full-length Intimin and its β-domain (Bodelon et al., 2009). The major protein bands detected with anti-E mAb in the boiled samples corresponded to full-length VgfpA and NVgfp fusions (Figure 10C and 10D; labelled with arrows). Detection of NVgfp with anti-myc mAb confirmed the integrity of its C-terminal end (Figure 10D). Minor bands of lower MW were also detected in Western blot with anti-E mAb, which likely represent proteolytic fragments of the full-length fusions (Figure 10C and 10D; labelled with asterisks).

The accessibility of VgfpA and NVgfp fusions to the external milieu was initially compared by incubation of intact *E. coli* cells with externally added proteases. Trypsin digested full-length VgfpA leaving some weakly detectable proteolytic fragments with a size similar to C-EhaA and Vgfp domains (Figure 10C, lane 3). The NVgfp fusion was resistant to Trypsin (data not shown) and sensitive to Proteinase K (ProtK) (Figure 10D, lane 3) but ProtK digestion of NVgfp fusion left a resistant fragment comprising Neae.

The induced *E. coli* cultures expressing VgfpA or NVgfp fusions showed only a slight decrease in their growth rate compared to control cultures having the empty vector (pAK-Not), or expressing the β-domains C-EhaA (pHEA) or Neae (pNeae2), and reached final optical densities at 600 nm (OD_{600}) identical to controls (Figure 11A and 11B). Hence, both the β-domains display the sdAb to the extracellular milieu, in a way that is accessible to externally added proteases but C-EhaA fusions are more sensitive to digestion than the Neae fusions. Resistance to proteolysis was also previously observed for full-length Intimin (Bodelon et al., 2009).

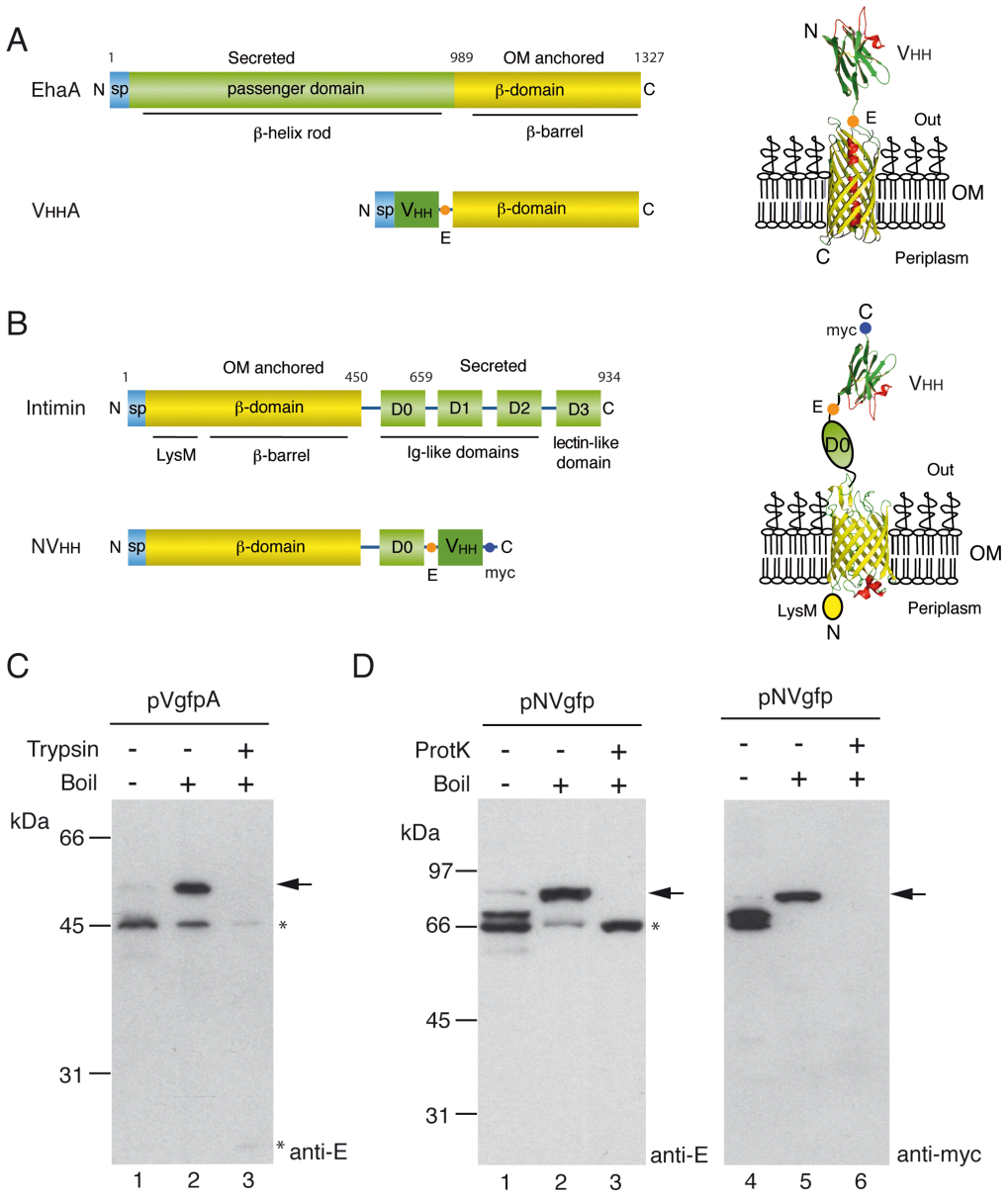

Figure 10. *E. coli* cell surface display of VHHs with EhaA and Intimin beta domains.

(A) Scheme of EhaA autotransporter and VHHA fusions (left), showing N-terminal SP, secreted passenger or VHH domain, and C-terminal β-domain. Model of VHHA fusion in the OM (right), with N-terminal VHH domain exposed to the extracellular milieu and with C-EhaA β-barrel inserted in the OM. These domains are connected with the E-tag epitope and the internal α-helical linker of the β-barrel. **(B)** Scheme of Intimin and NVHH fusions (left), showing N-terminal SP, LysM and β-domains, and secreted D0-D3 Ig-like and lectin-like domains, or VHH domain replacing D1-D3 in NVHH fusions. Model of NVHH fusion in the OM (right), with N-terminal LysM domain in the periplasm, β-barrel with linker in the OM, and connecting with C-terminal D0 and VHH domains exposed to the extracellular milieu. The E-tag and myc-tag epitopes flanking the VHH domain are indicated. **(C)** and **(D)** Western blots of whole-cell protein extracts from induced *E. coli* UT5600 harbouring pVgfpA **(C)** or pNVgfp **(D)**. Intact *E. coli* cells were incubated with (+) or without (-) the indicated protease, Trypsin or Proteinase-K (ProtK), before lysis. Protein extracts were prepared in SDS **(C)** or SDS-urea **(D)** sample buffers and boiled (+) or not boiled (-) before SDS-PAGE. Western blots were developed with anti-E or anti-myc mAb, as indicated. The positions of full-length VgfpA and NVgfp fusions are labeled with arrows. Asterisks indicate protein bands detected in protease-treated samples. The mass of protein markers (in kDa) is shown on the left.

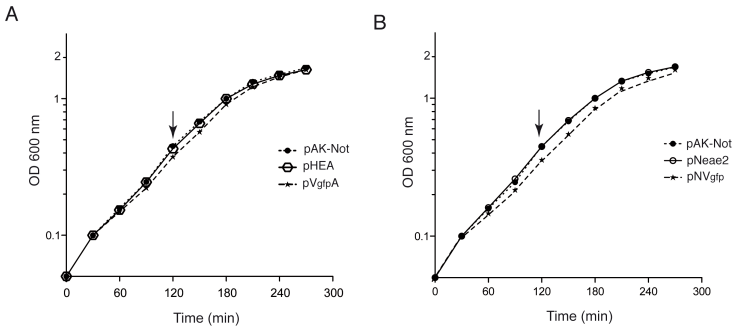

Figure 11. Growth of *E. coli* cultures expressing VgfpA and NVgfp fusions.

A) Growth curve of LB cultures of *E. coli* UT5600 cells carrying plasmids pVgfpA, pHEA (expressing C-EhaA), or pAK-Not (empty vector). (**B**) Growth curve of LB cultures of *E. coli* UT5600 cells carrying plasmids pNVgfp, pNeae2 (expressing Neae), or pAK-Not (empty vector). The cultures were incubated at 30 °C with agitation (160 rpm) and induced with 0.05 mM IPTG at the time indicated by an arrow. The optical density at 600 nm (OD_{600}) of the cultures was monitored at the time points shown.

Surface display of VgfpA and NVgfp was assessed by flow cytometry (Figure 12). Induced *E. coli* cells harboring pVgfpA, pNVgfp, or pAK-Not (control) were stained with anti-E or anti-myc mAbs followed by anti-mouse IgG-Alexa488 (Figure 12, left panels). *E. coli* cells expressing VgfpA or NVgfp were positively bound by anti-E mAb, though cells expressing NVgfp were also positively bound with the anti-myc mAb. Control *E. coli* cells with pAK-Not were negative for both mAbs. Importantly, the presence of a single peak in the flow cytometry histograms indicated that most *E. coli* cells were expressing a homogenous level of the fusion proteins. The mean fluorescence intensity (MFI) of cells with anti-E-tag mAb suggested a higher expression and display level of NVgfp than VgfpA (~3-fold). The antigen-binding activity of the surface displayed Vgfp was compared by flow cytometry after incubation of *E. coli* cells expressing these fusions with 50 nM biotin-labeled GFP (positive antigen) or biotin-labeled BSA (negative antigen), followed by incubation with Streptavidin-Phycoerythrin (PE) conjugate (Streptavidin-PE) (Figure 12, right panels). This analysis showed the specific binding of the *E. coli* cells expressing VgfpA and NVgfp fusions to GFP, whereas control *E. coli* cells did not bind GFP. No significant binding to BSA was observed. Hence, the β-domains of EhaA and Intimin allow the functional display of sdAb on the surface of *E. coli* cells. However, the MFI of GFP binding was clearly higher in *E. coli* cells expressing NVgfp than in those with VgfpA (ca. 8-fold) (Figure 12, right panels). The higher expression level of NVgfp

does not appear to be sufficient to account for this difference in binding, suggesting that the sdAb may have a higher antigen-binding activity when fused to the β-domain of Intimin.

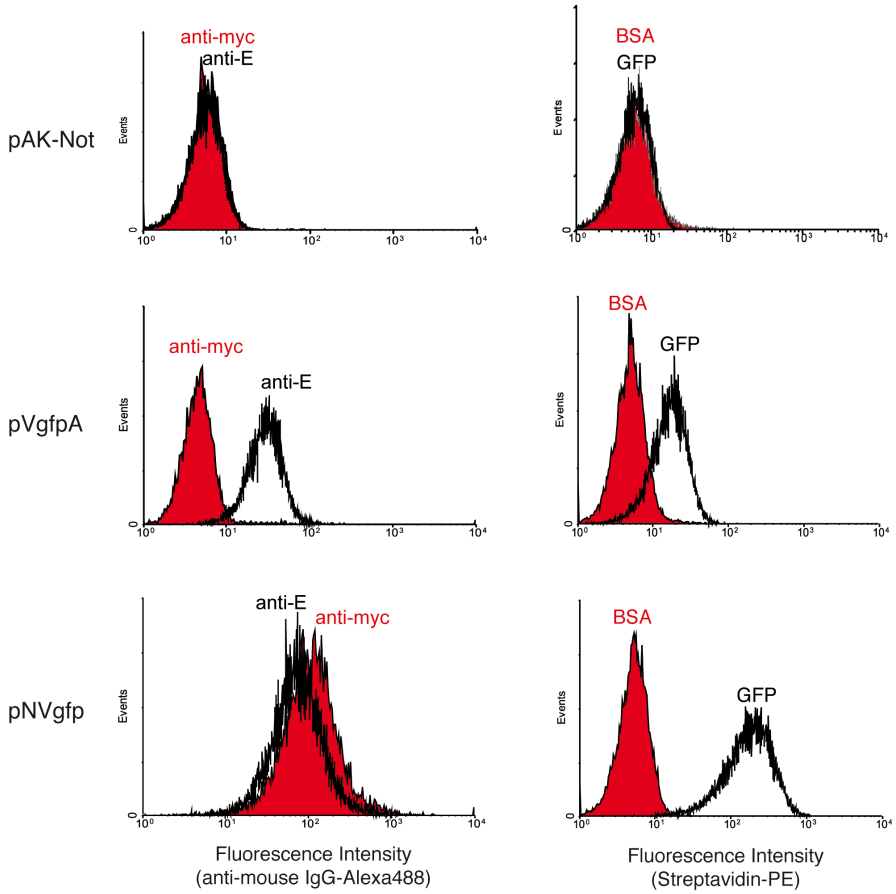

Figure 12. *E. coli* cell surface display and antigen-binding activity of VgfpA and NVgfp.

Fluorescent flow cytometry analysis of induced *E. coli* UT5600 cells bearing the indicated plasmids: pAK-Not (control), pVgfpA, and pNVgfp. Histograms show the fluorescence intensity of bacteria stained with anti-E or anti-myc mAbs (as indicated) and secondary anti-mouse IgG-Alexa 488 (left panels) or incubated with biotinylated antigens (GFP or BSA, as labeled) and secondary Streptavidin-phycoerythrin (PE) (right panels).

1.2 Construction of immune libraries against TirMEHEC and Fib, analysis of expression, display levels and cellular toxicity

Two distinct immune libraries of VHH genes from dromedaries immunized with purified antigens were used to demonstrate the effectiveness of *E. coli* Intimin and EhaA display systems with large sdAb repertoires. An immune library of VHH was generated against the soluble extracellular fragment of the translocated intimin receptor (*tir*) from EHEC (named TirMEHEC, corresponding to residues 252-360 of

full-length Tir$_{EHEC}$) (Frankel and Phillips, 2008) was cloned in vectors pHEA and pNeae2. Similarly, another immune library against Human Fibrinogen (Fib) was also cloned in vectors pHEA and pNeae2. Both VHH libraries were obtained by immunization of a dromedary with purified antigens, i.e. TirM$_{EHEC}$-His$_6$ and Fib, and subsequent amplification of the VHH gene segments from ~2x10^7 lymphocytes isolated from a peripheral blood sample (see Materials and Methods). The amplified VHH gene segments were cloned into the *Sfi*I and *Not*I sites of pHEA and pNeae2 vectors, generating two *E. coli* display immune libraries of similar size (~2-3x10^6 clones). The *E. coli* strain EcM1 (Table 2) was used as host for cell display. This strain is derived from the reference wild type K-12 strain (MG1655) with a deletion in the operon encoding type 1 fimbriae (Δ*fim*A-H) (Munera et al., 2008). Sequencing of 40 clones picked randomly from each of the two libraries in both display systems confirmed the cloning of different VHH sequences in frame with the β-domains of EhaA and Intimin respectively (data not shown). The expression and display of both libraries with the β-domains of EhaA (VHHA) and Intimin (NVHH) were analyzed by flow cytometry with anti-E and anti-myc mAbs, revealing a fairly homogeneous expression of both libraries in *E. coli* EcM1 (Figure 13A and 13C).

The MFI with anti-E mAb indicated a similar expression level of VHHA and NVHH libraries, in contrast to the significantly lower expression of VgfpA observed previously. Western blot analysis of whole-cell protein extracts from induced cultures revealed major protein bands with the expected size for full-length VHHA and NVHH fusions, upon boiling in SDS or SDS-urea buffer, respectively, and which have heat-modifiable electrophoretic mobility indicating the correct folding of their β-barrels (Figure 13B and 13D).

Quantification of the Western blot signals with anti-E mAb using ~1.5x10^8 bacteria (0.15 units of OD_{600}) expressing VHHA or NVHHfusions, was carried out using a standard curve generated with a purified E-tagged VHH of known concentration (Figure 14), and allowed an estimation of ~6.5x10^3 molecules of VHHA and ~7.8x10^3 molecules of NVHH per bacterium.

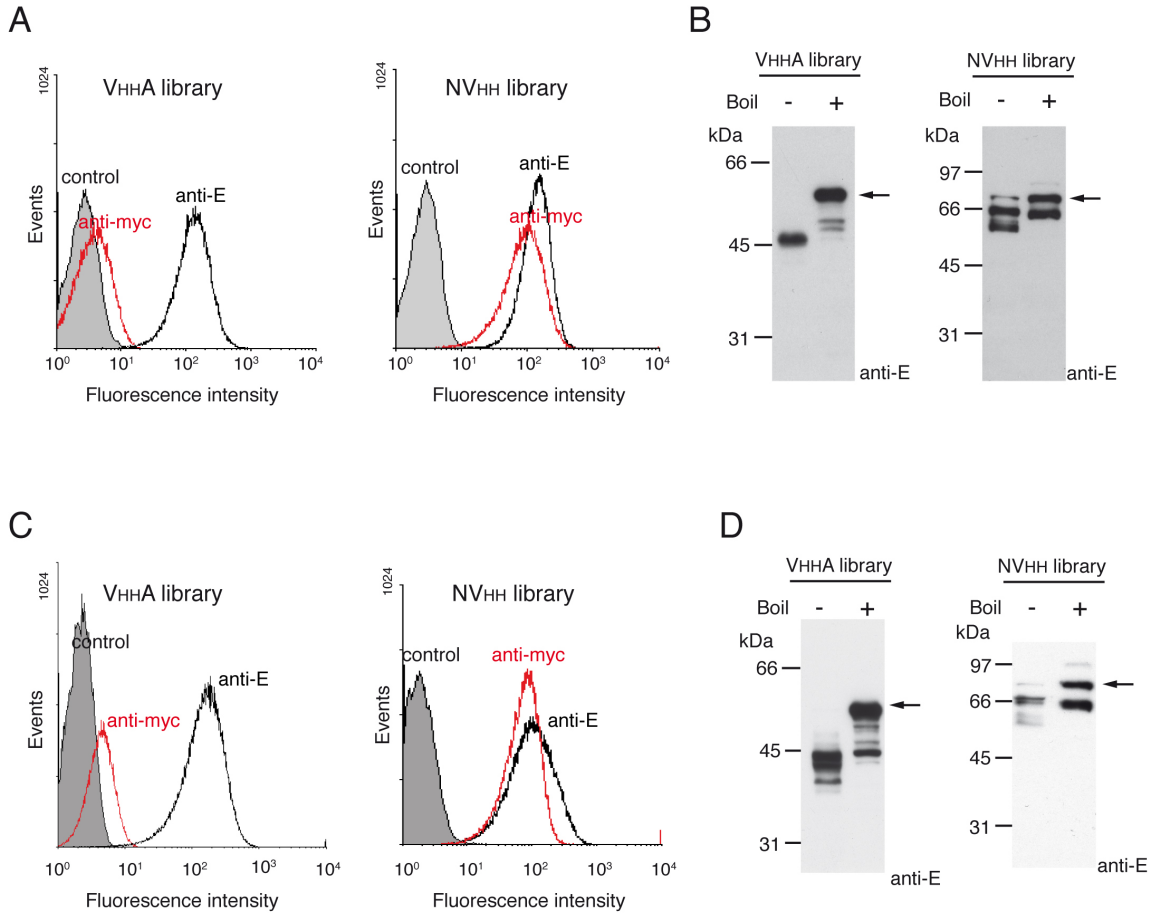

Figure 13. *E. coli* cell surface display of anti-TirMEHEC and anti-Fib immune libraries.

Fluorescent flow cytometry analysis of induced *E. coli* EcM1 cells expressing either **(A)** VHHA or NVHH immune libraries anti-$TirM_{EHEC}$ (as indicated) or **(C)** VHHA or NVHH immune libraries anti-Fib (as indicated). Control cells carried the empty vector pAK-Not. Histograms show the fluorescence intensity of bacteria stained with anti-E or anti-myc mAbs (as labeled) and secondary anti-mouse IgG-Alexa 488. Western blots of whole-cell protein extracts from induced *E. coli* EcM1 cells expressing either **(B)** VHHA or NVHH immune libraries anti-$TirM_{EHEC}$ (as indicated) or **(D)** VHHA or NVHH immune libraries anti-Fib (as indicated). Protein extracts were prepared in SDS (VHHA library) or SDS-urea (NVHH library) sample buffers and boiled (+) or not boiled (-) before SDS-PAGE. Western blots were developed with anti-E mAb. Positions of full-length fusions are labeled with arrows and mass of protein markers (in kDa) is shown on the left.

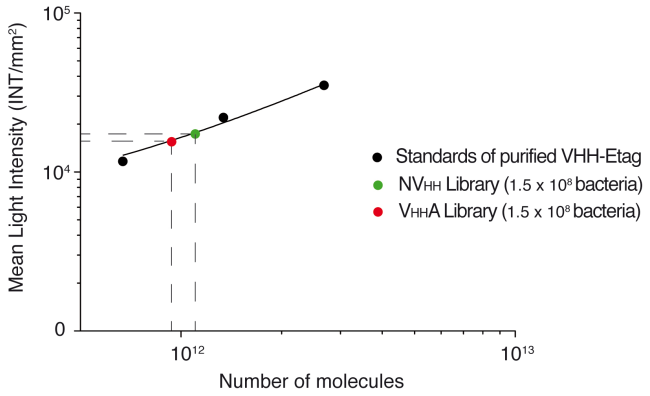

Figure 14. Quantification of the number of molecules of VHHA and NVHH fusions expressed in *E. coli*.

The plot shows the intensity of protein bands from Western blots developed with anti-E-tag mAb and quantified on a ChemiDoc XRS using the Quantity One software (Bio-Rad). Samples analyzed were whole-cell protein extracts from ~1.5x10^8 bacteria (0.15 units of OD_{600}) of induced *E. coli* EcM1 cells carrying the pVHHA or pNVHH anti-$TirM_{EHEC}$ libraries. The standard curve was generated with the values of band intensities (Intensity/mm^2) of a purified E-tagged V_{HH} of known concentration. Two independent experiments were done with similar results.

The growth of *E. coli* cultures expressing VHHA or NVHH libraries against TirMEHEC was only slightly delayed compared to a control with pAK-Not and the cultures reached similar OD_{600} after induction (Figure 15).

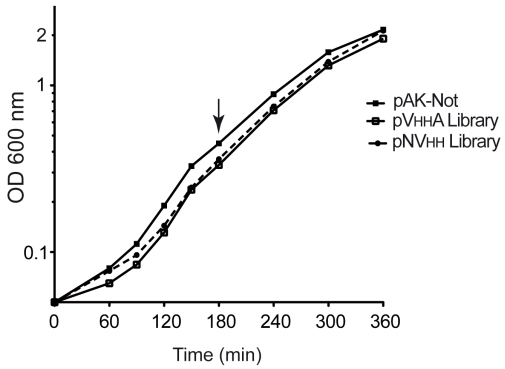

Figure 15. Growth of *E. coli* cultures expressing VHHA and NVHH libraries against anti-TirMEHEC.

Growth curve of LB cultures of E. coli EcM1 cells carrying pAK-Not (empty vector) or plasmids of the pVHHA and pNVHH anti-TirMEHEC libraries. Procedure was carried out as described previously.

Plating of the induced cultures to determine the number of colony forming units (CFU) per OD_{600} gave ~1.0x10^9 CFU/OD_{600} in the control (pAK-Not), ~ 0.9 x10^9 CFU/OD_{600} in the anti-TirMEHEC VHHA library, and ~0.6x10^9 CFU/OD_{600} and anti-

TirMEHEC NVHH library. While for the anti-Fib libraries we found ~ 0.83 x10^9 CFU/OD_{600} in VHHA library and ~0.8x10^9 CFU/OD_{600} in the NVHH library. Hence, growth of bacteria is not overly affected due to expression or transport of the fusions, though expression of some NVHH fusions appear to slightly reduce the viability of *E. coli* cells when compared to control cultures, especially with the anti-TirMEHEC library. Nevertheless, since the CFU/OD_{600} after expression of NVHH fusions remains within the same order of magnitude as the control, the diversity of the sdAb library is not compromised. Cell toxicity during the expression of Intimin constructs has been reported previously in some *E. coli* K-12 strains (Wentzel et al., 2001).

Chapter 2: Selection and characterization of single domain Abs against TirM$_{EHEC}$ from immune libraries displayed on the surface of *E. coli*

2.1 Translocated Intimin Receptor domain M (TirM)

The translocated intimin receptor (Tir) of enteropathogenic and enterohemorrhagic *Escherichia coli* strains (EPEC and EHEC, respectively) is an important protein for the infection of these enteric pathogens, which can result in severe diarrhea, hemorrhagic colitis and the life-threatening hemolytic uremic syndrome (in the case of EHEC). Tir is translocated through the bacterial type III secretion system (Kenny et al., 1997; Gauthier and Finlay, 2003) into the host cell, where it becomes inserted in the plasma membrane through two hydrophobic helices that leave an extracellular region exposed to the surface of the host cell (Figure 16).

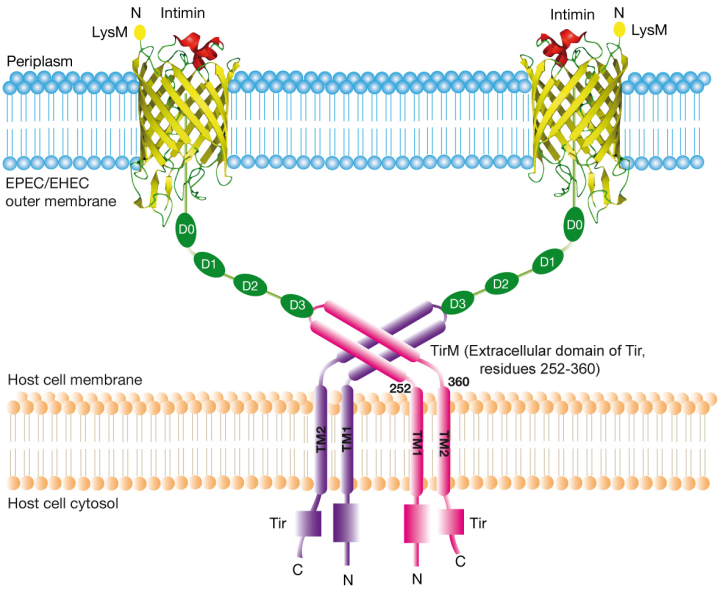

Figure 16. The Intimin-Tir interaction between EPEC/EHEC bacteria and host cell plasma membrane.

The model is based on structural data of the complex of the C-terminal fragment of intimin (domains D1, D2 and D3) and the extracellular domain of Tir (TirM) (Luo et al., 2000). Intimin is shown in green with its domains labelled. The transmembrane domain folds as a β-barrel (Fairman et al., 2012) and is inserted in the outer membrane of EPEC/EHEC.The Ig-like domains D0, D1, D2, and the lectin-like domain D3, which binds to the TirM, are shown as ovals. Tir is shown as a dimer (in pink and purple) in the host-cell membrane, with extracellular domain (residues 252-360) flanked by the two predicted transmembrane (TM) domains. The N-terminal domain of Tir anchors host cytoskeletal components (such as actin) that are needed to form the characteristic attaching and effacing (A/E) lesion on the host-cell surface upon bacterial adhesion.

This extracellular region of Tir, named TirM, which corresponds to amino acid residues 232-360 for Tir of EHEC, serves as anchor for the bacterial adhesin Intimin, responsible for the intimate attachment of these pathogens to the enterocyte. Intimin is an integral OM protein whose extracellular C-terminal domains are displayed on the surface of EPEC and EHEC bacteria and bind TirM region (Kenny et al., 1997). The Intimin-Tir interaction ultimately leads to F-actin polymerization within the epithelial cell at the sites of bacterial attachment, and the formation of actin pedestals beneath the bacterium (Lai et al., 2013). It is postulated that blocking Intimin-Tir interaction could prevent the stable attachment of the bacteria to the intestinal epithelium and thus, reduce the infection process and the disease.

2.2 Selection of single domain Abs against $TirM_{EHEC}$ by magnetic sorting of *E. coli* bacteria displaying the immune library

E. coli EcM1 cells expressing VHHA and NVHH libraries were screened to isolate clones binding to $TirM_{EHEC}$ by magnetic cell sorting (MACS) (Figure 17).

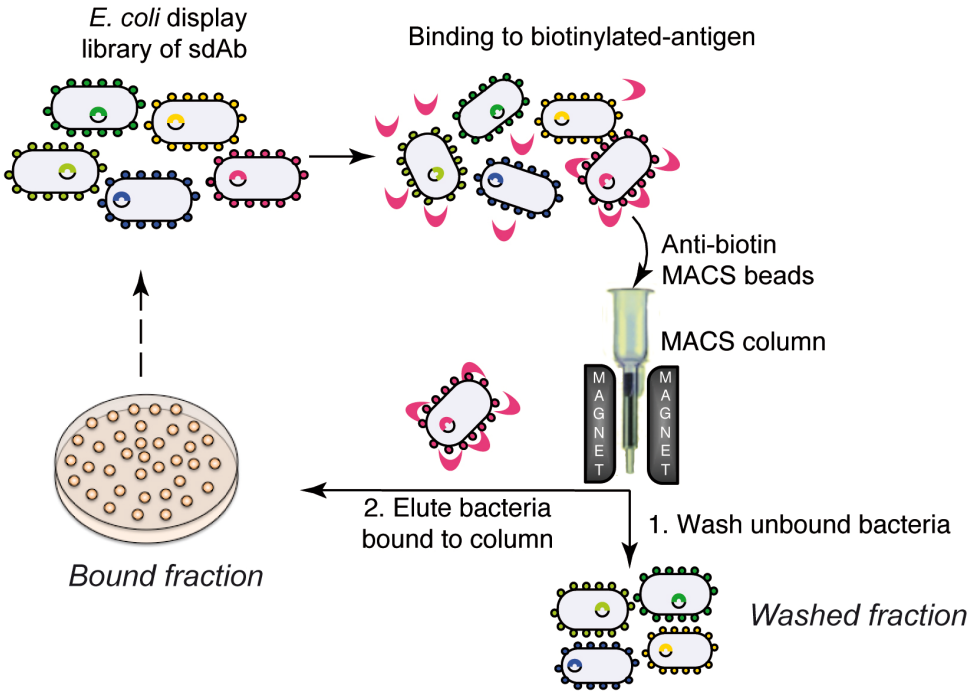

Figure 17. Schematic illustration of Magnetic cell sorting (MACS).

General scheme summarizing the steps followed during MACS of an *E. coli* display library of sdAb with a biotinylated antigen. *E. coli* cells binding the biotinylated antigen are captured in a MACS column held in a magnet, while *E. coli* cells that do not bind the antigen are washed out of the column. Elution of bound bacteria is done with fresh LB media upon column removal from the magnet. The CFU in the Washed and Bound fractions are determined by plating.

The MACS conditions for capturing *E. coli* cells expressing VHHA or NVHH fusions were established using biotin-labeled anti-E mAb. An initial input of 0.1 units of OD_{600} (~6-9x10^7 CFU of each culture) was incubated with 50-250 nM of biotinylated anti-E mAb allowing the recovery of a total of ~2-4x10^7 CFU in the Wash and Bound fractions. The Bound fractions contained ~95-99% of the CFU in the VHHA and NVHH libraries, and only ~0.2-0.5% in control *E. coli* cells with pAK-Not. Using these conditions, the VHHA and NVHH libraries were incubated with biotinylated $TirM_{EHEC}$ (250 nM) for the first selection step (MACS1) and ~0.3-0.6% of the total CFU from both libraries were collected in the Bound fractions (Table 5). The colonies grown from the Bound fractions of each library were pooled independently, their plasmids purified and electroporated into fresh *E. coli* EcM1 cells to obtain VHHA and NVHH sublibraries (≥2x10^6 transformants). Next, the VHHA and NVHH sublibraries were subjected to a new round of selection with biotinylated $TirM_{EHEC}$ using conditions identical to those used in MACS1. Bacteria harvested from Bound fractions were pooled, their plasmids purified and transformed for the following rounds of MACS. Antigen concentration was reduced to 50 nM in the following MACS. The percentage of *E. coli* bacteria recovered in the Bound fractions showed a significant increase from the initial 0.3-0.6% to over 70% in MACS3 of NVHH and MACS4 of VHHA (Table 5), suggesting an enrichment of antigen binding clones in both libraries.

Table 5. Summary of MACS with *E. coli* display libraries against TirMEHEC.

Round	Antigen conc (TirMEHEC)	VHHA library %	NVHH library%
MACS1	250 nM	0.3	0.6
MACS2	250 nM	2.6	12.5
MACS3	50 nM	12.5	75.6
MACS4	50 nM	70.5	-

(%): Percentage of bacteria in Bound fractions with reference to total bacteria in Wash+Bound fractions (ca. 1-5 x 10^7 CFU)

Bacteria from the different rounds of selection were analyzed by flow cytometry to test their binding to biotinylated TirMEHEC (50 nM) (Figure 18), which demonstrated an enrichment of *E. coli* cells binding to TirMEHEC along the selection rounds, from ~0.2 % positives in the original libraries to ~45% after MACS4 of the VHHA library and more than 75% positives after MACS2 and MACS3 of the NVHH library. No

significant binding to biotinylated BSA was detected by flow cytometry in these populations. The expression levels of the VHHA and NVHH fusions in the bacterial pools after the MACS steps were similar to those of the original libraries (data not shown).

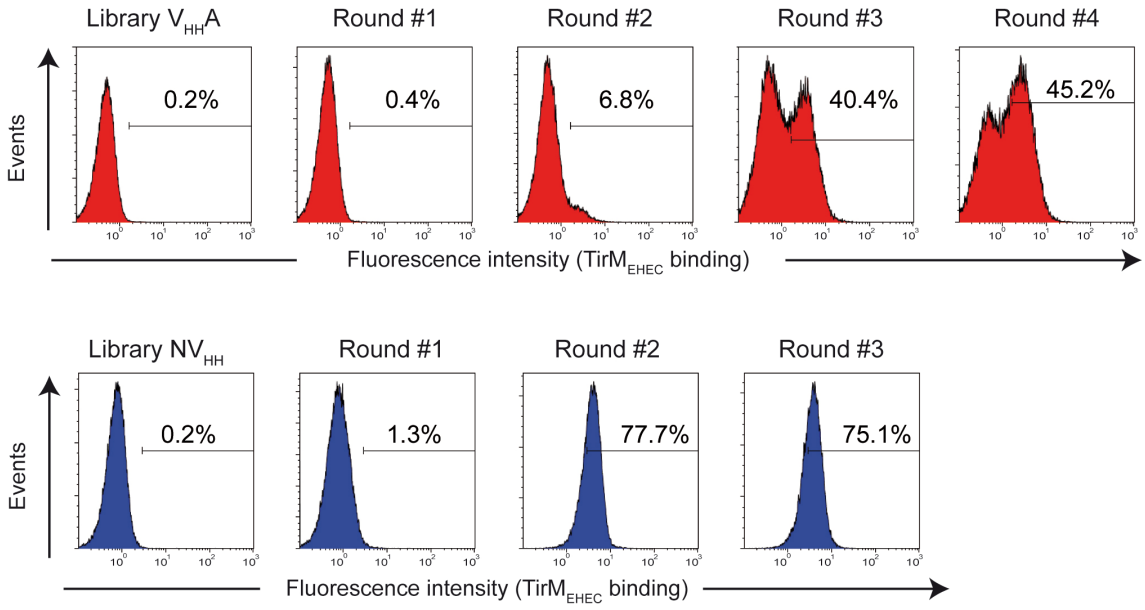

Figure 18. Magnetic cell sorting of VHHA and NVHH *E. coli* display libraries with biotinylated antigen, TirMEHEC.

Fluorescent flow cytometry analysis of IPTG-induced *E. coli* EcM1 cells expressing VHHA (top panel) or NVHH (bottom panel) immune libraries, or their respective sublibraries enriched after the indicated round of MACS with biotinylated $TirM_{EHEC}$. Histograms show the fluorescence intensity of bacteria incubated with biotinylated $TirM_{EHEC}$ and secondary Streptavidin-PE.

Fifty colonies from the final round of selection of each library were randomly picked for plasmid isolation and DNA sequencing. A VHH sequence, named as VTIR1, was found in all NVHH clones and in 36 VHHA clones, while the rest were different VHH sequences. Flow cytometry analysis confirmed the specific binding of biotinylated TirMEHEC (50 nM) by *E. coli* cells displaying VTIR1 fused to EhaA and Intimin β-domains whereas these cells did not bind to biotinylated BSA (Figure 19A and 19B).

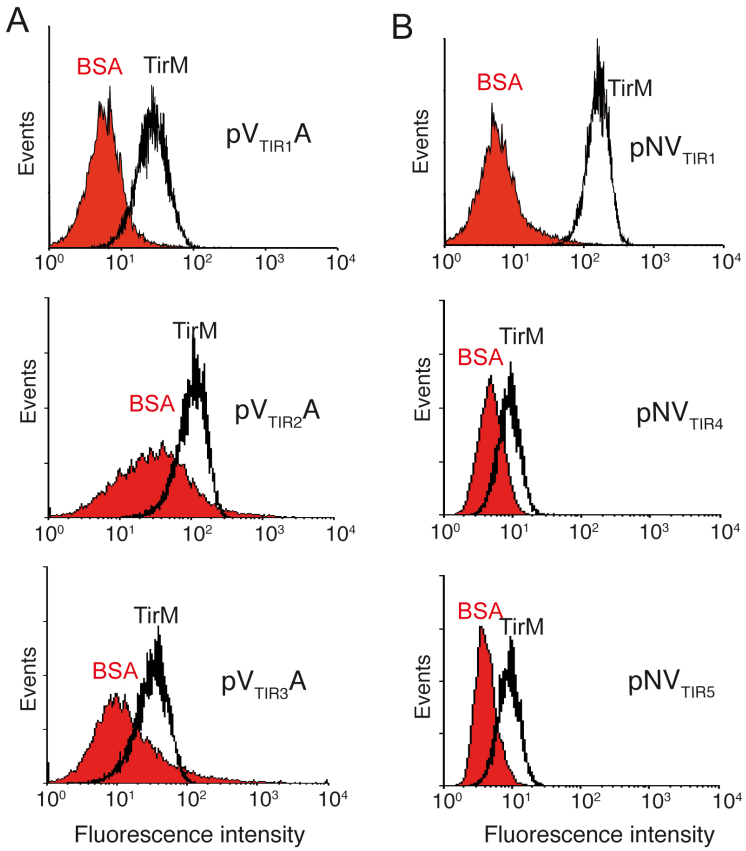

Figure 19. Binding of *E. coli* cells displaying selected clones from VHHA and NVHH libraries to biotinylated TirMEHEC.

Fluorescent flow cytometry analysis of induced *E. coli* EcM1 cells bearing the indicated plasmids selected from **(A)** the VHHA library: pVTIR1A, pVTIR2A, pVTIR3A; and **(B)** from the NVHH library: pNVTIR1, pNVTIR4, pNVTIR5. Histograms show the fluorescence intensity of bacteria incubated with biotinylated antigens (TirMEHEC or BSA, as labeled) and secondary Streptavidin-PE.

The MFI of *E. coli* cells displaying VTIR1 was higher in the NVTIR1 fusion than with VTIR1A fusion (Figure 20), although both were expressed at similar levels (Figure 20). We also conducted a flow cytometry screening of the remaining 14 non-VTIR1 clones from MACS4 of VHHA library, identifying three other VHH sequences that bound to biotinylated TirMEHEC, referred to as VTIR2, VTIR3, VTIR4 (Figure 20A, and data not shown). VTIR4 did not bind biotinylated BSA, but VTIR2 and VTIR3 clones exhibited non-specific binding to biotinylated BSA and were not further analyzed (Figure 19A and 19B).

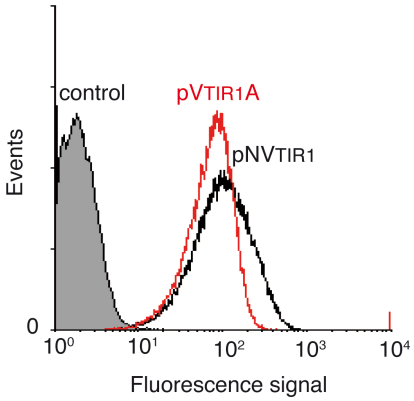

Figure 20. *E. coli* cell surface display levels of VTIR1A and NVTIR1 clones.

Fluorescent flow cytometry analysis of induced *E. coli* EcM1 cells expressing VTIR1A or NVTIR1 clone (as indicated). Control cells carried the empty vector pAK-Not. Histograms show the fluorescence intensity of bacteria stained with anti-E mAb and secondary anti-mouse IgG-Alexa 488.

We sought for additional VHH sequences binding TirMEHEC in the NVHH library by screening 96 colonies picked randomly after the first round of selection (MACS1), in which a higher diversity of binders with low and high affinities are expected. PCR screening with a specific primer hybridizing the CDR3 of VTIR1 enabled us to identify 17 VTIR1 clones out of these 96 colonies. This number fits with the percentage of clones recovered from this population after MACS2 (Table 5). Flow cytometry screening of the remaining clones allowed the identification of two additional VHH sequences that specifically bound biotinylated TirMEHEC, VTIR4 (2 clones), which was found previously in the VHHA library, and VTIR5 (1 clone). The MFI of binding of these clones to 50 nM biotinylated TirMEHEC was low compared to VTIR1 (Figure 19B) and increased at higher antigen concentrations (200 nM) (data not shown) suggesting that these clones had a lower affinity for TirMEHEC. The CDR3 amino acid sequences of the selected VHH clones are shown in Table 6.

Table 6. CDR3 sequences of anti-TirMEHEC clones selected by *E. coli* display.

Clone Name	Amino acid sequence of CDR3	β-domain system
VTIR1	GTAPYWHTPIPTLSEDKYFY	Neae, C-EhaA
VTIR2	GNSGSRGFDY	C-EhaA
VTIR3	AKGPRRCNQGFDY	C-EhaA
VTIR4	PDLSTNCDTVLTNSGALYNY	Neae, C-EhaA
VTIR5	PKYGGTWRWRVEEEKTTI	Neae

The VHHs encoded by VTIR1, VTIR4, VTIR5 and one unrelated VHH binding α-amylase as a control, were secreted into *E. coli* culture media as soluble fragments with the hemolysin system (Fernandez et al., 2000; Fraile et al., 2004) and used in ELISA against TirMEHEC and BSA. This experiment showed that soluble VTIR1, VTIR4, and VTIR5 sdAbs, bound specifically to TirMEHEC (Figure 21). According to ELISA data, VTIR1 was the clone with an apparent higher affinity, as could be also inferred from its strong enrichment in both the *E. coli* display libraries.

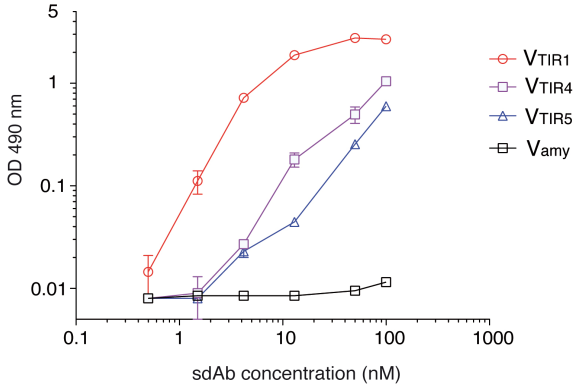

Figure 21. ELISA of sdAbs selected by *E. coli* display against TirMEHEC.

ELISA against TirMEHEC of sdAbs secreted into culture media as E-tagged HlyA fusions from the indicated VTIR clones and one a negative control (Vamy) (Fraile et al., 2004). The plot shows the average OD values at 490 nm with standard error from duplicate experimental samples obtained with the secreted sdAbs at the indicated concentrations. ELISAs were developed with anti-E-tag mAb and anti-mouse-POD. ELISA signals against a control antigen (BSA) are subtracted from the represented values.

2.3 Characterization of VTIR1 sdAb and determination of its affinity by Surface Plasmon Resonance (SPR)

The VTIR1 clone was produced in the periplasm of *E. coli* WK6 cells as soluble sdAb with C-terminal His- and myc-tags and purified by metal-affinity chromatography followed by gel-filtration chromatography (Materials and Methods). As a control, Vgfp was also expressed and purified in the same manner. Both sdAbs behave as monomers with an apparent mass of ~15 kDa in gel filtration chromatography (Figure 22A). The binding activity of the purified VTIR1 was confirmed in ELISA (Figure 22B).

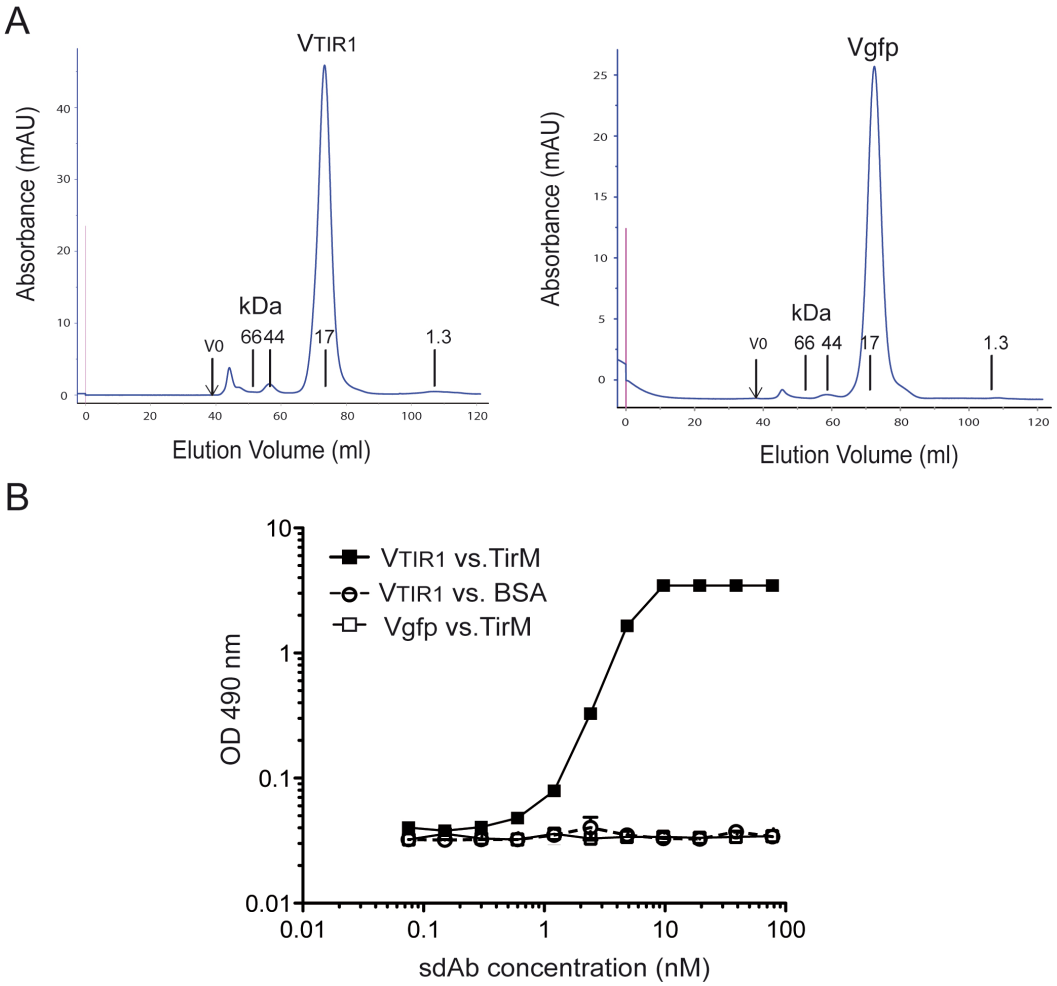

Figure 22. Monomeric behaviour and binding activity of the purified sdAb, VTIR1.

(A) Gel-filtration chromatograms of sdAbs VTIR1 and Vgfp purified from the periplasm of *E. coli* WK6 cells (carrying the corresponding pCANTAB6-derivative) after a metal-affinity chromatography step. Gel-filtration chromatography was performed in a HiLoad 16/600 Superdex 75 column calibrated with protein markers (labeled in kDa) and Blue dextran (for exclusion volume Vo). Both sdAbs have major peaks of ~15 kDa corresponding to their monomeric forms. **(B)** ELISA of purified monomeric VTIR1 and Vgfp (control) against $TirM_{EHEC}$ and BSA. The plot represents the OD values at 490 nm obtained with the indicated concentrations of sdAbs. ELISA developed with anti-myc mAb-POD as secondary.

In order to determine the apparent equilibrium dissociation constant (K_D) between VTIR1 and $TirM_{EHEC}$, their interaction was studied in surface plasmon resonance (SPR) experiments with a Streptavidin (SA) sensor chip coated with biotinylated $TirM_{EHEC}$ (Materials and Methods). The change in resonance units (RU) was recorded with time at different concentrations of purified VTIR1 from 0.2 to 32 nM showing a clear binding to $TirM_{EHEC}$ that reached the steady state equilibrium in ~220 s for the two highest concentrations used, but not for the lower concentrations (Figure 23A). No binding was observed when Vgfp (40 nM) was flown over this sensor surface, or

when VTIR1 (40 nM) was flown over a SA cell lacking biotinylated $TirM_{EHEC}$ (data not shown). Injection of buffer to evaluate the dissociation of VTIR1 (labeled with an arrow in Figure 23A) showed no loss of RU for > 200 s, indicating that VTIR1 remained stably bound to $TirM_{EHEC}$ over long periods of time. Because of the very slow dissociation of VTIR1 from TirMEHEC, we were not able to calculate the value of KD directly from the curves. Hence, kinetic constants were calculated at a time point when the curves reached equilibrium (i.e. 220 s). From the graph, KD was calculated as 2.2 X 10^{-9} M (Figure 23B).

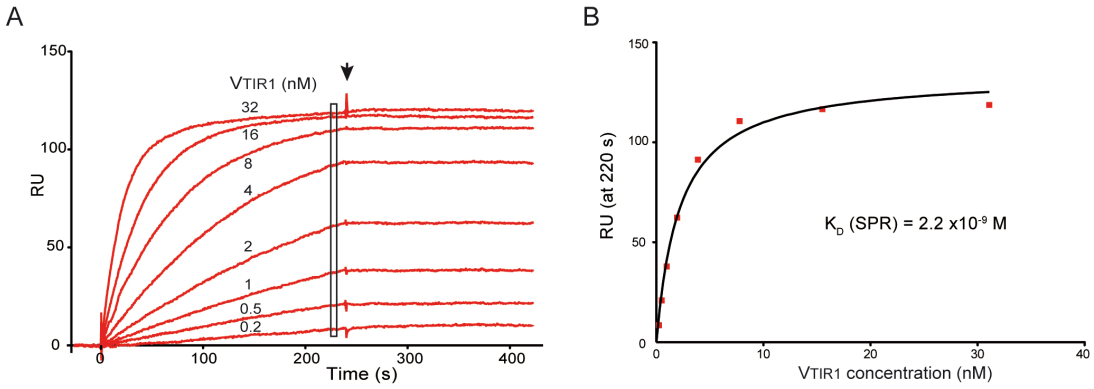

Figure 23. Determination of the equilibrium dissociation constant (KD) of VTIR1 by SPR.

(A) SPR sensograms monitoring real-time association and dissociation of purified sdAb VTIR1 (at the indicated concentrations) to biotinylated $TirM_{EHEC}$ immobilized onto a Streptavidin-SA sensor chip. The increase in resonance units (RU) is recorded along time (in seconds). Dissociation of VTIR1 is evaluated by injection of buffer at the time indicated with an arrow. **(B)** RU values at 220 seconds (labeled with a rectangle in A) are plotted *versus* the different concentrations of VTIR1. The curve was fitted by non-linear least squares regression.

2.4 Estimation of the affinity of VTIR1 by *E. coli* display

Flow cytometry analysis under equilibrium conditions has been used to estimate the apparent KD of Abs and anticalins displayed on the surface of yeast and *E. coli* cells (Daugherty et al., 1998; Boder and Wittrup, 2000; Binder et al., 2010). Thus, we tested whether the affinity of VTIR1 could be estimated by flow cytometry analysis of *E. coli* cells with this sdAb on their surface and incubated with biotinylated TirMEHEC under conditions expected to be close to the equilibrium. We chose the Intimin display system given its superior MFI signals in flow cytometry with the antigen. *E. coli* EcM1 cells displaying NVTIR1 (~3x10^7 CFU) were incubated for 90 min with a fixed amount of biotinylated TirMEHEC (2 pmols) in two-fold increasing volumes of PBS (from 0.1 to 2 ml) to reach a final concentration range from 20 nM to 1 nM.

After this incubation, cells were washed and labeled with Streptavidin-PE as previously described.

The relative MFI of the cells was plotted against the antigen concentration used and the curve fitted by non-linear least squares regression, giving an estimated apparent KD of 1.7x10^{-9} M (Figure 24). This value was consistent with the apparent KD determined by SPR analysis (KD of ~2.2 x 10^{-9} M, Figure 23B), and indicates that the *E. coli* display systems could also be used to estimate the KD of selected sdAbs before purification.

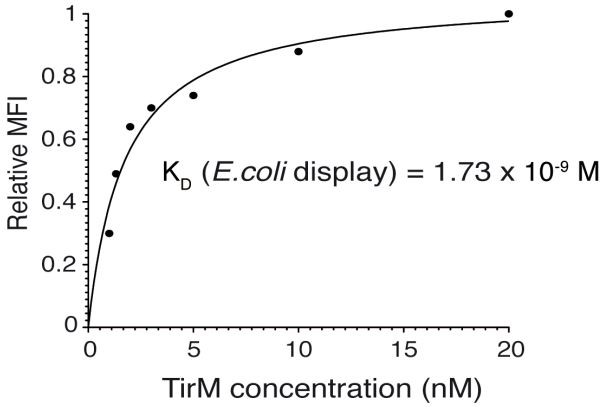

Figure 24. Estimation of the equilibrium dissociation constant (KD) of VTIR1 by *E. coli* display.

The K_D of VTIR1 was estimated by flow cytometry analysis of *E. coli* cells expressing NVTIR1 incubated with different concentrations of biotinylated TirMEHEC under equilibrium conditions. The mean fluorescent intensities (MFI) of bacteria, after labeling with Streptavidin-PE, were plotted *versus* the concentration of TirMEHEC used in the assays. The curve was fitted by non-linear least squares regression.

Chapter 3: Selection and Characterization of high affinity single domain Abs against Human Fibrinogen from Immune libraries displayed on the surface of *E. coli* cells

3.1 Human Fibrinogen (Fib).

Fibrinogen (Fib, Factor I) is a 340 kDa glycoprotein produced by the liver and circulated in plasma at concentrations ranging between 1.5 and 4.5 mg/ml (Lowe et al., 2004). It plays a key role in the hemostatic system, being involved in the final step of blood coagulation. Abnormal Fib concentration in blood has been reported to be associated with cardiovascular diseases, venus thrombosis or myocardial infarction (Smith et al., 1998). There is also increasing evidence that Fib is a biomarker of oxidative stress (Selmeci et al., 2010) and metabolic syndrome (Onat et al., 2009) in human plasma. Lower protein concentrations indicate the risk of bleeding and maybe related to liver diseases, whereas higher Fib concentrations reveal an important risk for ischemic vascular or coronary accidents (Kamath and Lip, 2003), (Lowe et al., 2004), (Dudek et al., 2010). The structure of fibrinogen is illustrated in Figure 25.

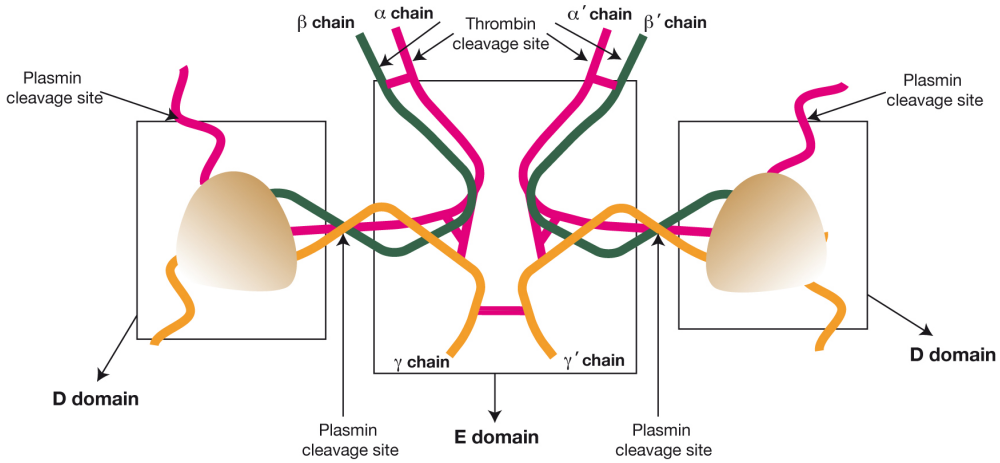

Figure 25. Structure of Fibrinogen.

Fibrinogen is a dimeric glycoprotein composed of three pairs of peptide chains, i.e. α, β and γ chains. The two sub-units are composed of a D domain containing a globular region and an E domain, which contains a disulfide bond which links the two subunits. Fibrinogen is an important acute phase protein that is an important part of coagulation cascade of proteins. Thrombin rapidly hydrolyzes fibrinogen into fibrin and releases fibrinopeptides A and B. The fibrin is further stabilized by Factor XIIa, leading to aggregation of fibrin and blood platelets that block the damaged blood vessel preventing further bleeding. Plasmin is involved in Fibrin degradation into Fragment D and E.

Fib is also an important determinant of the metastatic potential of circulating tumor cells (Palumbo et al., 2000) and a prognostic blood marker for survival in patients with ovarian (Ma et al., 2007), (Polterauer et al., 2009) and gastric cancer (Yamashita et al., 2005).

3.2 Selection of high affinity single domain Abs from the immune library against Fib by MACS

Similar to previous work carried out with the immune libraries against $TirM_{EHEC}$, MACS was used to isolate high affinity clones binding to biotinylated Fib from *E. coli* EcM1 bacteria expressing VHHA and NVHH libraries, generated from dromedaries immunized with purified Fib. Initially, the VHHA and NVHH libraries were incubated with biotinylated Fib (250 nM) for the first selection step (MACS1) and ~0.3-0.4% of the total CFU from both libraries were collected in the Bound fractions (Table 7). The colonies grown from the Bound fractions of each library were pooled independently and their plasmids purified and electroporated into fresh *E. coli* EcM1 cells to obtain VHHA and NVHH sublibraries (≥2x10^6 transformants). Next, the VHHA and NVHH sublibraries were subjected to a new round of selection with 100 nM biotinylated Fib and maintaining the other conditions identical to those used in MACS1. Bacteria harvested from Bound fractions were pooled, their plasmids purified and transformed for the following rounds of MACS. In total, 5 rounds of MACS were performed with both the NVHH and VHHA libraries.

Table 7. Summary of MACS with *E. coli* display libraries against Fib.

Round	Antigen conc (Fib)	VHHA library %	NVHH library%
MACS1	250 nM	0.3	0.4
MACS2	100 nM	0.8	0.7
MACS3	100 nM	1.7	3.3
MACS4	100 nM	2.9	9.6
MACS5	100 nM	26.1	24.5

(%): Percentage of bacteria in Bound fractions with reference to total bacteria in Wash+Bound fractions (ca. 1-5 x 10^7 CFU)

The percentage of *E. coli* bacteria recovered in the Bound fractions showed a very gradual increase from the initial 0.3-0.4% to over 50% in MACS5 of NVHH and VHHA (Table 7), suggesting an enrichment of antigen binding clones in both libraries.

Bacteria from the different rounds of selection were analyzed by flow cytometry to test their binding to biotinylated Fib (50 nM) (Figure. 26A and 26B), which demonstrated an enrichment of *E. coli* cells binding to Fib along the selection rounds, from ~0.25 % positives in the original libraries to ~40% and ~60% after MACS5 of the VHHA library and NVHH library respectively, with no significant binding to biotinylated BSA. The expression levels of the VHHA and NVHH fusions in the bacterial pools obtained after MACS was similar to those of the original libraries (Figure 26A and 26B).

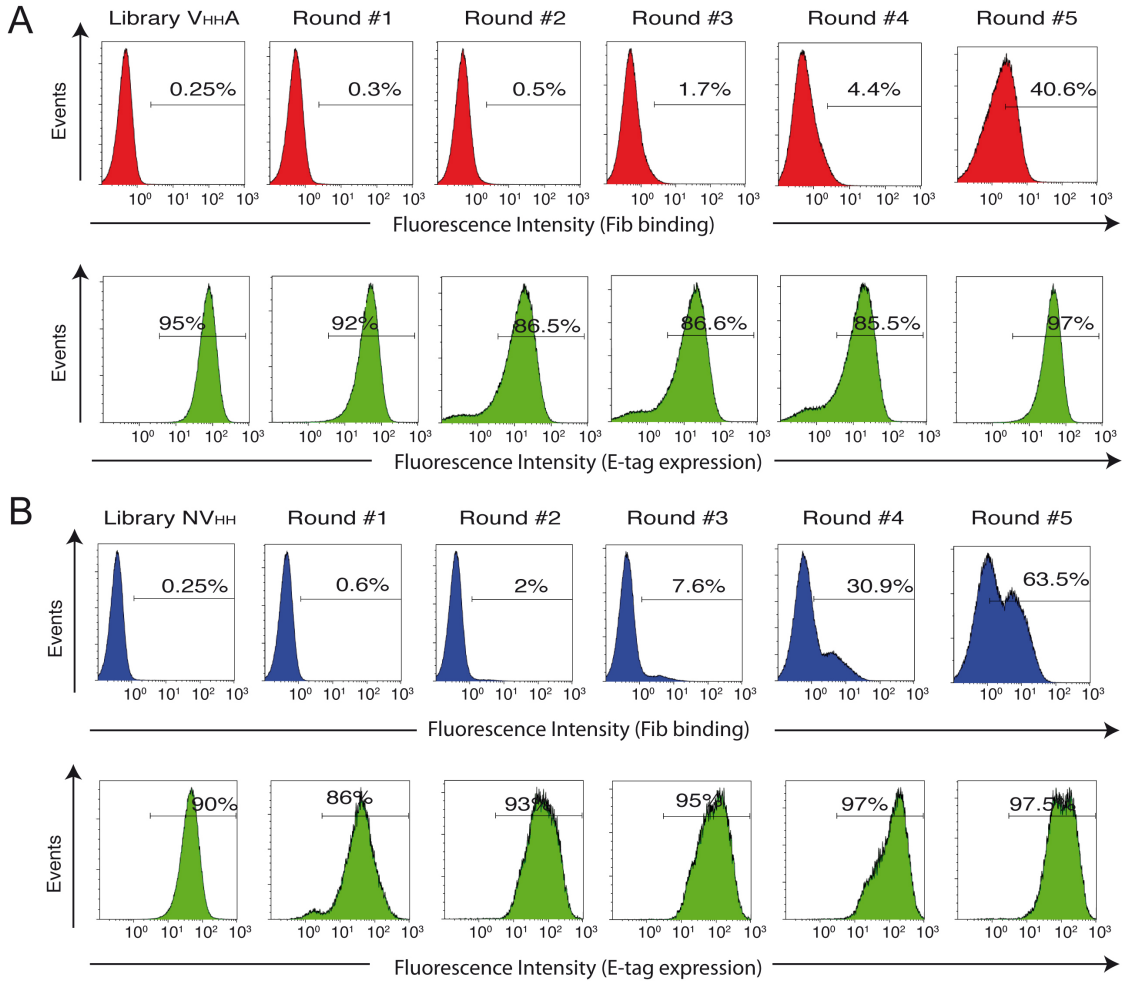

Figure 26. Magnetic cell sorting of VHHA and NVHH *E. coli* display libraries with biotinylated antigen, Fib.

Fluorescent flow cytometry analysis of IPTG-induced *E. coli* EcM1 cells expressing **(A)** VHHA or **(B)** NVHH immune libraries, or their respective sub-libraries enriched after the indicated round of MACS with biotinylated Fib. Histograms show the fluorescence intensity of bacteria incubated with biotinylated Fib and secondary Streptavidin-PE or anti-E tag mAb and anti-mouse conjugated to Alexa 488 fluorophore.

Fifty colonies from the fifth round of MACS selection from both libraries were randomly picked for plasmid isolation and DNA sequencing. Upon DNA sequencing, three different VHH sequences, named as VFIB1, VFIB2 and VFIB3 were identified in both systems. The remaining clones were negative in binding to biotinylated fibrinogen (data not shown). The screening is summarized in Table 8. Flow cytometry analysis confirmed the specific binding of biotinylated Fib (50 nM) by *E. coli* cells displaying each of the three VHH sequences fused to the Intimin β-domains, with negligible binding to biotinylated BSA. The MFI of VFIB1 and VFIB3 were the best and at similar levels (Figure 27).

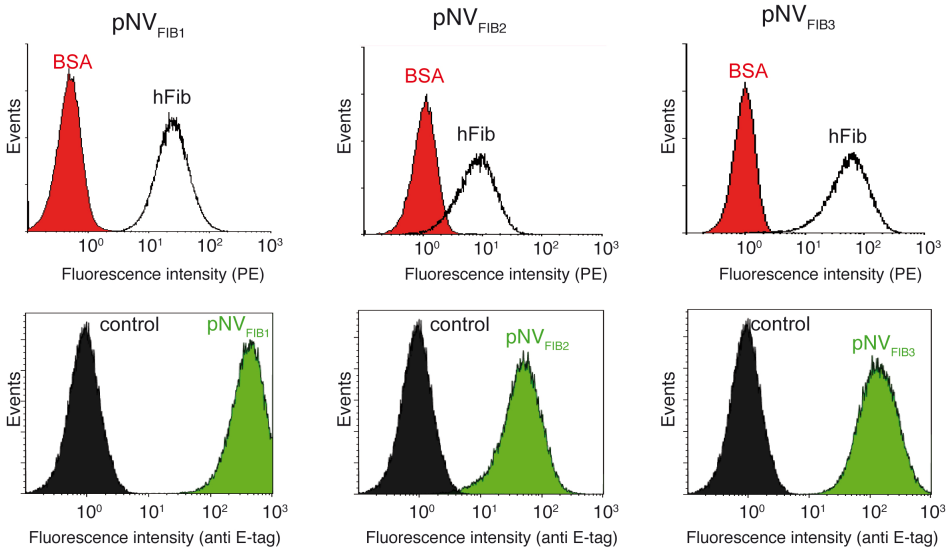

Figure 27. Binding of *E. coli* cells displaying selected clones from VHHA and NVHH libraries to biotinylated Fib.

Fluorescent flow cytometry analysis of induced *E. coli* EcM1 cells bearing the indicated plasmids selected from the NVHH library: pNVFIB1, pNVFIB2 and pNVFIB3. Histograms show the fluorescence intensity of bacteria incubated with biotinylated antigens (Fib or BSA, as labeled) and secondary Streptavidin-PE or anti-E mAb and secondary anti-mouse Alexa 488.

Table 8. CDR3 sequences of anti-Fib clones selected by *E. coli* display.

Clone Name	Amino acid sequence of CDR3	Display system	
		Neae	C-EhaA
VFIB1	RWGWASSSNWYDMGKYNY	15/50	09/50
VFIB2	RCAPES	21/50	26/50
VFIB3	KYYRSCTSLGDYRN	06/50	03/50

3.3 Purification of VFIB1 and VFIB2 VHHs from the periplasm of *E. coli* as fusions to MBP

The two more frequent clones against Fib isolated by *E. coli* display, VFIB1 and VFIB2, were initially produced in the periplasm of *E. coli* WK6 cells as soluble VHHs with C-terminal His_6- and myc-tags, but poor yields were attained (~0.1-0.2 mg/L; data not shown). Similar problems of variability in protein expression have been previously reported during the production of VHHs against methotrexate, (Alvarez-Rueda et al., 2007). Another common issue is that the single IMAC step is generally not sufficient to avoid the presence of protein contaminants in VHH preparations, thus requiring further purification by less efficient chomatographic steps (e.g. gel filtration, ion-exchange). Hence, in order to circumvent these issues, we developed a purification method for VHHs based on their fusion to the *E. coli* maltose binding protein (MBP) in the N-terminus and a His_6-tag in the C-terminus.

3.3.1 Expression and solubility of the MBP-VHH_{His6} fusions

In order to investigate whether fusion to MBP could have a positive effect on expression levels of VHHs and on their purification from the *E. coli* periplasm, we constructed an expression vector, named pMAL1-VHH (Figure 28).

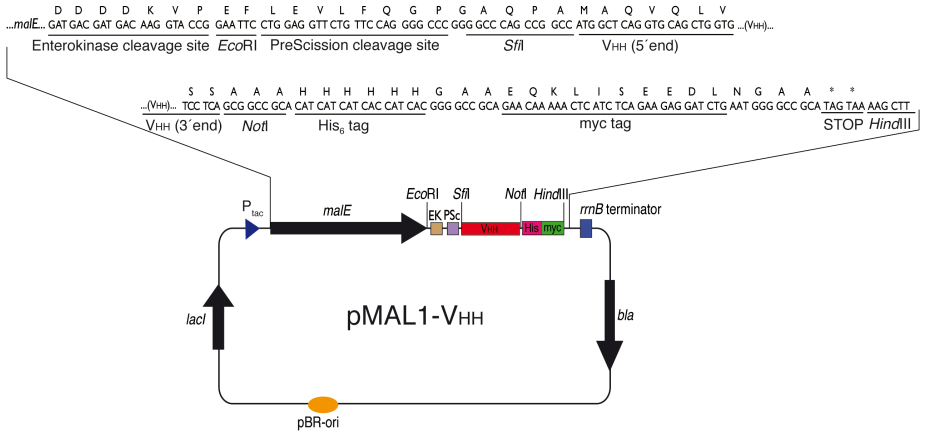

Figure 28. Schematic representation of protein expression vector.

The pMALp2E plasmid vector (New England Biolabs) was modified to include the PreScission protease cleavage site and DNA restriction enzyme sites (*Eco*RI, *Sfi*I, *Not*I, *Hind*III) for cloning of the VHH to the C-terminal end of MBP. This modified vector, pMAL1- VHH also contains the His_6 and myc tags for purification and detection respectively.

pMAL1-VHH is based on the pMAL-p2E backbone (New England Biolabs), and contains in addition, the cleavage site for the site-specific protease PreScission (LEVLFQ/GP) in the linker connecting MBP with the VHH, a C-terminal His_6 and myc tags. The MBP-fusions are under the control of the IPTG-inducible P_{tac} promoter, while the vector also encodes the LacI repressor and contains unique *Sfi*I and *Not*I restriction sites flanking the VHH sequence encoding the VHH. Three characterized VHH genes with different complementarity determining region (CDR) sequences, encoding VHHs that specifically recognized human fibrinogen (VFIB1 and VFIB2), or GFP (VGFP) were cloned and the corresponding pMAL1-VHH derivative was generated. Expression of MBP-VHH_{His6} fusions was initially tested in *E. coli* BL21 strain (Studier and Moffatt, 1986) but high proteolysis of the full-length fusions was observed (data not shown). Hence, we tested protein production in an *E. coli* strain deficient in several periplasmic proteases, *E. coli* HM140 (Meerman and Georgiou, 1994), and high-level accumulation of the full-length MBP-VHH_{His6} (~60 kDa) was obtained after 3 h induction at 30°C with 0.3 mM IPTG (Figure 29A).

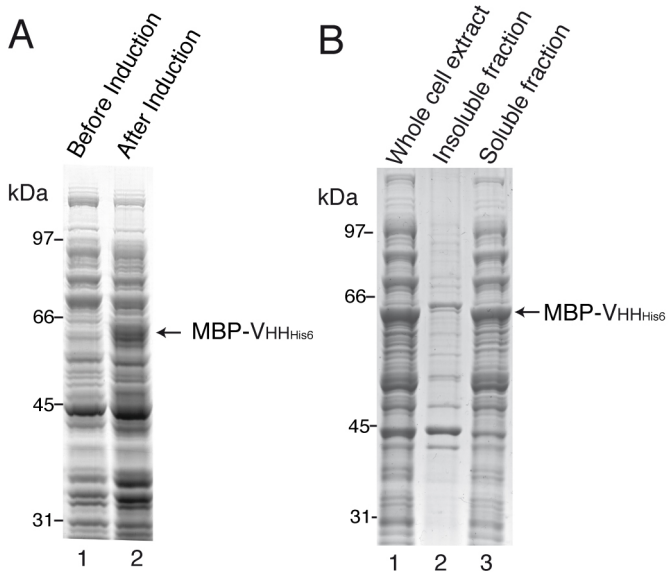

Figure 29. Induction and solubility of the MBP-fusions.

(A) 10% SDS-PAGE gel loaded with pre- and post-induction Whole Cell Extract (WCE) samples to check the induction and expression of the MBP-fusion protein. The MBP-VHH fusion has a size of about 60 kDa (as labelled with the arrow). (**B**) 10% SDS-PAGE gel loaded with (Lane 1) Whole Cell Extract (WCE) obtained after lysis of IPTG-induced *E. coli* HM140 cells expressing the MBP fusion proteins. The WCE sample was centrifuged at 20000 X g for 60 mins in a tabletop centrifuge, and the pellet after centrifugation (Insoluble fraction, Lane 2) and the supernatant (Soluble fraction, Lane 3) were loaded onto the 10% SDS-polyacrylamide gel. The MBP-VHH fusions are found in the soluble fraction of the WCE after centrifugation. Mass of protein standards is shown on the left (in kDa).

Approximately 15-20 mg of MBP-$V_{HH_{His6}}$ fusions were produced per litre of induced culture in shake flasks with a final OD_{600} ~1.0. Importantly, in all cases the majority of the accumulated MBP-$V_{HH_{His6}}$ fusion remained in the soluble fraction after cell lysis and high-speed centrifugation (20000 x*g*, 1 h), as indicated by SDS-PAGE analysis (Figure. 29B).

3.3.2 Purification of MBP-$V_{HH_{His6}}$ fusions and antigen binding activity

The supernatants containing the MBP-$V_{HH_{His6}}$ fusions obtained after high-speed centrifugation of the cell lysate were passed through a chromatography column packed with amylose resin and the bound proteins were eluted with 10 mM maltose (Figure 30A). SDS-PAGE analysis showed a pre-dominant band of ~60 kDa in the eluted fractions that corresponds to MBP-$V_{HH_{His6}}$ fusions (Figure 29A). The fractions containing the MBP-$V_{HH_{His6}}$ fusions were pooled and loaded onto cobalt-containing columns for IMAC. Bound MBP-$V_{HH_{His6}}$ fusions were eluted with 150 mM imidazole, pooled and analyzed by SDS-PAGE showing the presence of a single major band corresponding to the full-length MBP-$V_{HH_{His6}}$ fusions (Figure 30B). In all cases, a final yield of ~12-16 mg of purified MBP-$V_{HH_{His6}}$ fusions were obtained per L of induced culture (Table 9).

ELISA was subsequently used to test the antigen-binding activity of the purified MBP-$V_{HH_{His6}}$ fusions and different concentrations of the purified MBP-$V_{HH_{His6}}$ fusions were incubated with their respective antigens (GFP or Fib) and with a negative control antigen (BSA). Bound MBP-$V_{HH_{His6}}$ fusions were developed with anti-c-myc-mAb-POD. The generated binding curves (Figure 30C) demonstrate that these fusions recognized their specific antigens, indicating that the presence of MBP did not prevent the binding of the antigen by the VHH, which is in agreement with previous reports that MBP-scFv fusions maintain the antigen binding activity of scFvs (Bach et al., 2001). Thus, our data showed that MBP-$V_{HH_{His6}}$ fusions can be purified in high yields by two steps of affinity chromatography and they can be directly used for antigen binding or applications thereof.

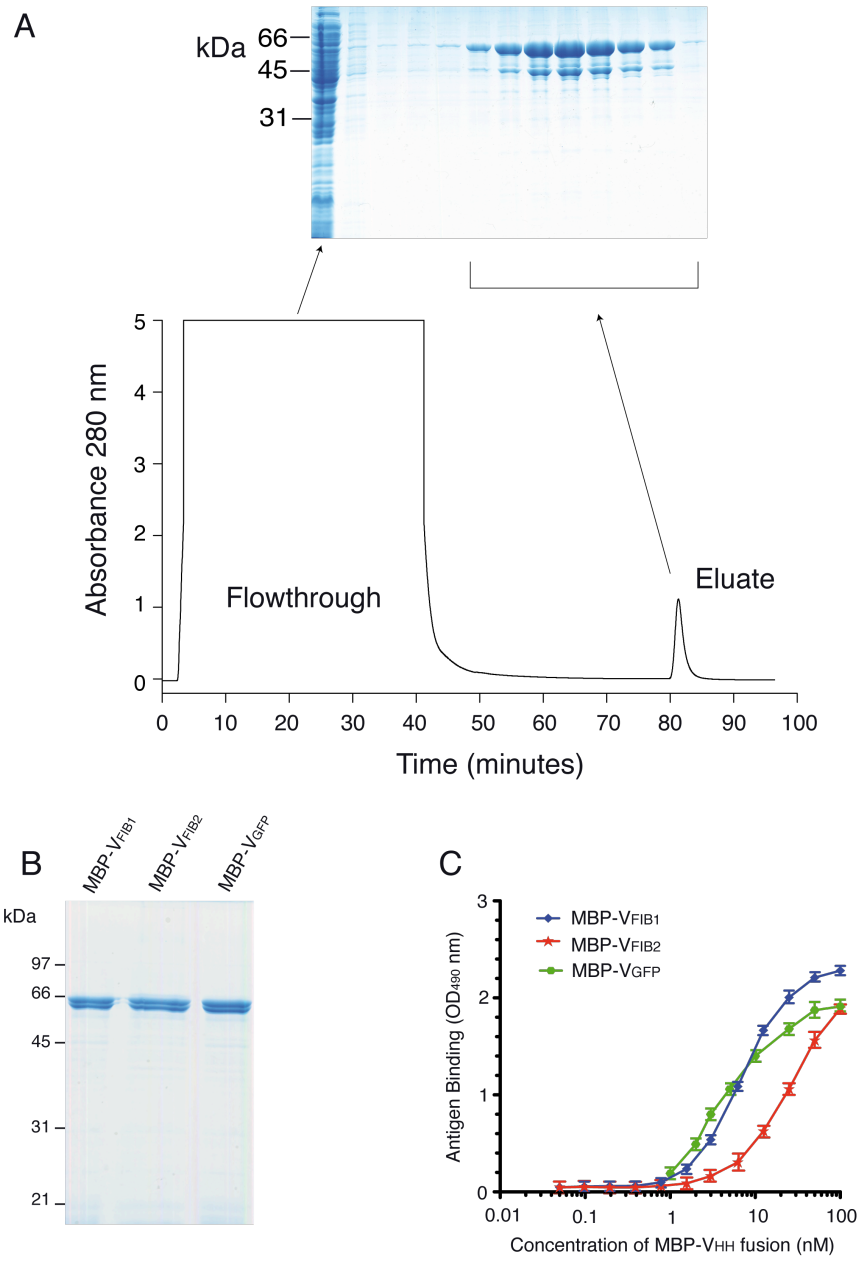

Figure 30. Purification of the MBP-fusions by Amylose affinity chromatography and their functional analysis by ELISA.

(A) Chromatogram of the purification of MBP-fusion proteins by Amylose Affinity Chromatography. The flowthrough fraction contains non-specific proteins and other impurities that do not bind the column and the elute fraction contains the purified MBP-VHH fusions. **(B)** 10% SDS-PAGE gel loaded with each of the three purified MBP-VHH fusions i.e. MBP-VFIB1 and MBP-VFIB2 are the fusions of MBP with either of two different VHHs against human fibrinogen and MBP-VGFP is a fusion of MBP with a VHH against GFP isolated from VHH libraries against GFP. **(C)** ELISA to determine the antigen binding activity of the purified MBP-VHH fusions. Different wells were coated with 5 μg/ml of GFP and human fibrinogen (positive antigens) or BSA (negative control) proteins, followed by addition of MBP-VHH solution (0.05-100 nM) to all coated wells. The presence of bound MBP-VHH fusion was detected by incubation with anti-c-myc-POD and development using a chromgenic substrate. The absorbance values reflect the specific binding of each of the MBP-VHHs to their respective antigens and have been adjusted by subtraction of the respective blank values (non-specific binding of each MBP-VHH to BSA).

3.3.3 Purification of monomeric VHH_{His6} from MBP-VHH_{His6} fusions

To purify monomeric VHH_{His6}s free of MBP, we evaluated the following purification scheme summarized in Figure 31.

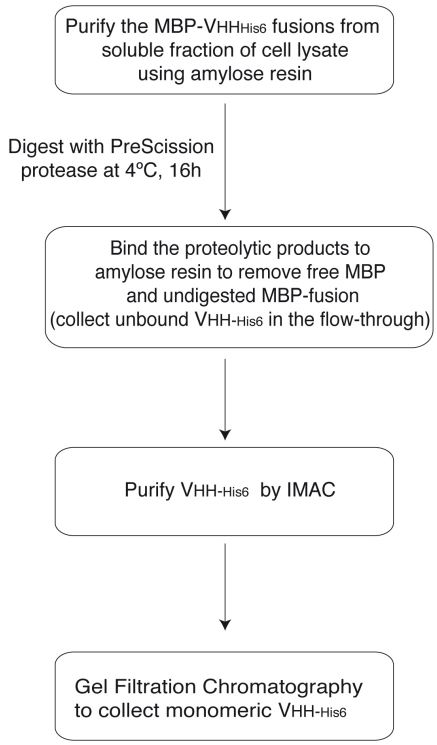

Figure 31. Expression and purification of VHHs in *E. coli*.

The scheme followed for purification of VHHs from MBP-VHH fusion proteins is illustrated.

Briefly, fractions containing the MBP-VHH_{His6} fusions eluted from the amylose resin were dialyzed to remove maltose and digested with the PreScission protease at 4 ºC for 16 h. The products of the proteolysis were analyzed on a 12% SDS-PAGE gel (Figure 32A). About 80-90% of the initial full-length MBP-VHH_{His6} fusion present in the reaction was digested into free MBP (~45 kDa) and the corresponding VHH_{His6} (~17 kDa) in all cases. The proteolytic products were subsequently loaded onto an amylose resin in order to capture the undigested MBP-fusion and free MBP, while collecting the VHH_{His6} in the flow-through. The flow-through fractions for each of the three VHHs were loaded onto a cobalt-containing column for IMAC. PreScission protease and residual free MBP, along with other impurities, were washed from the IMAC column and the purified VHH_{His6} clones were eluted with 150 mM imidazole (Figure 32B). Some residual amounts of the full-length MBP-VHH_{His6} fusion could be

detected in some cases, due to the presence of His_6-tag. The final yields of purified VHH_{His6} were ~2-3 mg per L of induced culture (Table 9).

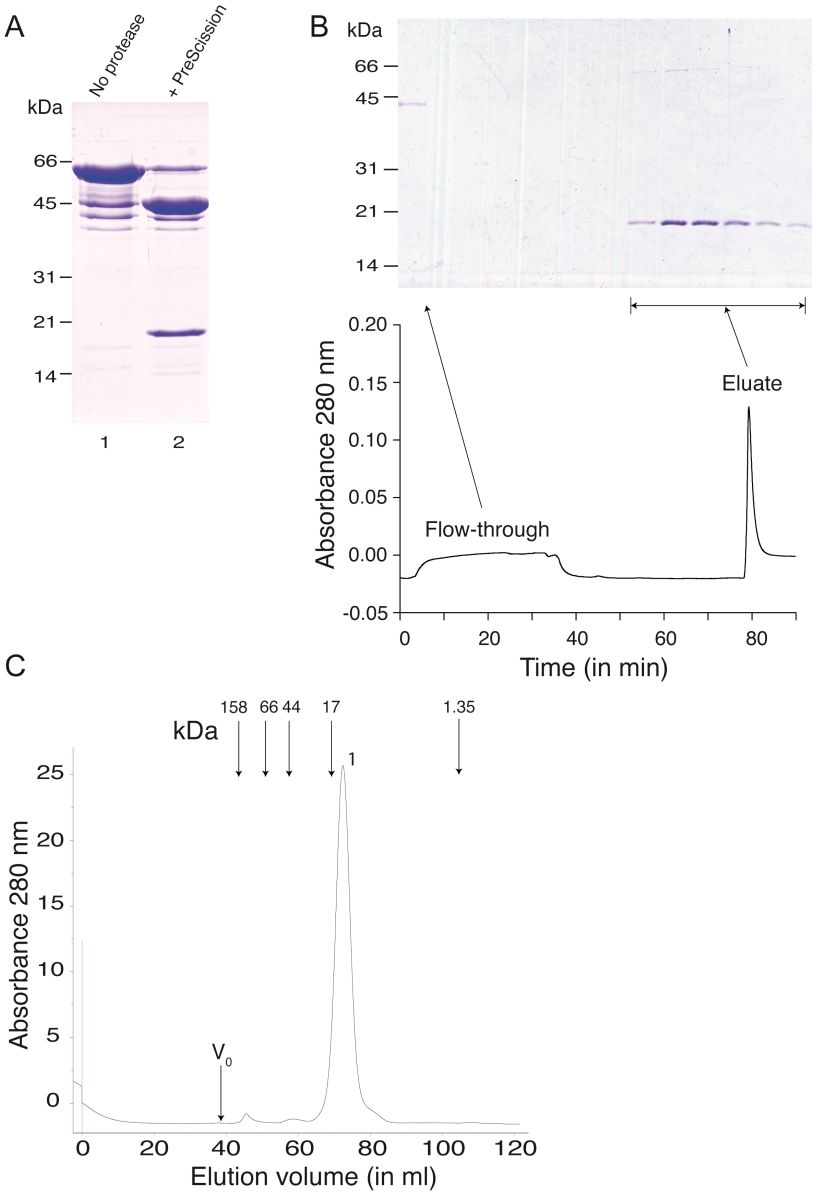

Figure 32. Protease digestion of MBP-VHH fusions, Immobilized Metal Affinity chromatography (IMAC) and Gel filtration.

A) SDS-PAGE of MBP-VHH fusions digested overnight with PreScission protease at 4ºC for 16 h. Upon observation of the gel, it can be inferred that majority of the MBP-VHH fusion was digested and separated from the VHH. Mass of protein standards is shown on the left (in kDa). **(B)** IMAC purification of VHH using Talon resin. The chromatogram of the chromatographic run is illustrated in this figure. Residual impurities like MBP and PreScision protease do not bind to the Talon resin and are found in the flowthrough, while the VHH binds to the resin and is eluted with 200 mM imidazole in the elution peak. **(C)** The VHH was loaded on to a Gel filtration column to analyze the protein for presence of multimers or dimers and separate the monomeric VHH from other forms. The exclusion volume (Vo) and the molecular weights of the gel filtration standards are indicated (in kDa). Peak 1 corresponds to the VHH in monomeric form with a molecular weight of ~16 kDa.

Table 9. Protein yields after purification from the periplasm of *E. coli* HM140.

Fusion protein	MBP- $V_{HH_{His6}}$ (mg/litre culture)	MBP-$V_{HH_{His6}}$ (mg/litre culture)
MBP-V_{HH1}	12.5	2.2
MBP-V_{HH2}	16.3	3.2
MBP-V_{HH3}	14.6	2.5

Gel filtration chromatography through a precalibrated HiLoad 16/600 Superdex 75 pg column was used to analyze the composition of the eluted V_{HHHis6} after IMAC and to purify the fractions corresponding to monomeric V_{HHHis6}. In each of the three cases, ≥95% of the protein eluted corresponded to the monomeric V_{HHHis6} as depicted by the single major peak with an apparent molecular weight of ca. 15 kDa obtained by gel filtration (Figure 32C).

Further, each purified monomeric V_{HHHis6} (namely V_{FIB1}, V_{FIB2} and V_{GFP}) was analyzed by SDS-PAGE and revealed a single protein band with molecular weights of ca. 15 -17 kDa (Figure 33A) and was found to be functional by ELISA (Figure 33B).

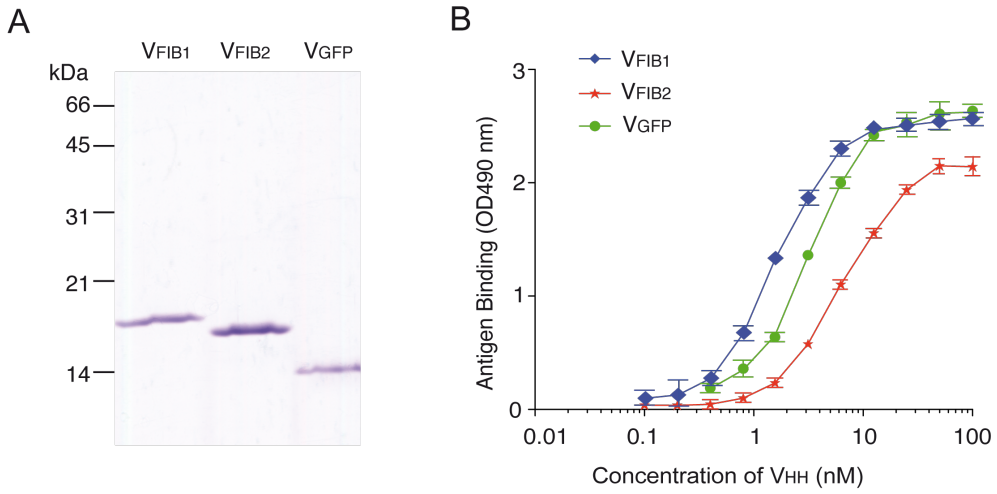

Figure 33. Monomeric VHHs and assay of functional activity by ELISA.

(A) Monomeric VHHs after gel filtration were loaded on to a 12% SDS-polyacrylamide gel and stained with Coomassie Brilliant Blue solution. The purified VHHs (Lane 1 and Lane 2 – VHHs against Fibrinogen, Lane 3 – VHH against GFP) have a molecular weight between 15 and 18 kDa. Mass of protein standards is shown on the left (in kDa). **(B)** ELISA to determine the antigen binding activity of purified monomeric VHHs. Wells were coated with 5 mg/ml of GFP, Human Fibrinogen (positive antigen) or BSA (negative control) proteins, followed by addition of VHH solution (0.05-100 nM) to the wells. The signal was developed by incubation with anti-c-myc-POD.

3.4 Determination of the affinity of VFIB1 and VFIB2 by Surface Plasmon Resonance (SPR)

In order to determine the apparent equilibrium dissociation constant (K_D) of VFIB1 and VFIB2 against Fib, their interaction was studied by SPR experiments with a Streptavidin (SA) sensor chip coated with biotinylated Fib (Materials and Methods). The change in resonance units (RU) was recorded with time at different concentrations of purified VFIB1 (from 2.5 to 40 nM) or VFIB2 (from 5 to 80 nM), and showed clear binding to Fib that reached the steady state equilibrium in ~180s (Figure 34A and 34B). No binding was observed when Vgfp (40 nM) was flown over this sensor surface, or when VFIB1, VFIB2 (40 nM) was flown over a SA flow-cell lacking biotinylated Fib (data not shown). Injection of buffer to evaluate the dissociation of VFIB1 or VFIB2 showed gradual loss of RU with time and the kinetic constants (k_{on} and k_{off}) were calculated from the sensograms. VFIB1 had a K_D of 3.2 x 10^{-9} M, with k_{on} = 6.62 x 10^5 Ms^{-1} and k_{off} = 2.1 x 10^{-3} s^{-1}. VFIB2, on the other hand, had a K_D of 24.7 x 10^{-9} M, with k_{on} = 1.02 x 10^6 Ms^{-1} and k_{off} = 2.52 x 10^{-2} s^{-1}.

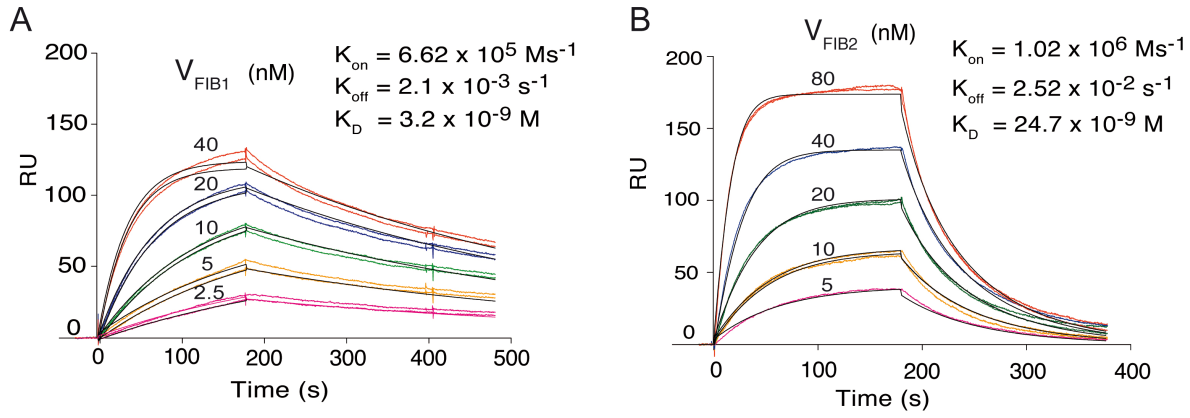

Figure 34. Determination of the equilibrium dissociation constant (KD) of clones VFIB1 and VFIB2 by SPR.

SPR sensograms monitoring real-time association and dissociation of purified sdAbs **(A)** VFIB1 and **(B)** VFIB2 (at the indicated concentrations) to biotinylated Fib immobilized onto a Streptavidin-SA sensor chip. The increase in resonance units (RU) is recorded along time (in seconds). Dissociation of VFIB1 and VFIB2 was evaluated by injection of buffer. The curve was fitted by non-linear least squares regression.

3.5 Estimation of the affinity of VFIB1 and VFIB2 by *E. coli* display

Flow cytometry analysis was used to estimate the apparent K_D of the selected VFIB sdAbs as previously performed with the VTIR1 sdAb. It was known that the sdAbs, VFIB1 had higher apparent affinity than VFIB2, therefore the final concentration range of biotinylated Fib in the assay for VFIB1 was maintained between 30 nM and 0.3 nM, while in the case of VFIB2, this range was between 300 nM and 3 nM. Briefly, *E. coli* cells (~3x10^7 CFU) with the respective sdAb on their surface were incubated with a fixed amount of biotinylated Fib (2 pmols) for 90 mins in two-fold increasing volumes of PBS (from 0.01 to 2 ml) to reach the respective final concentration ranges (as mentioned above). After this incubation, cells were washed and labeled with Streptavidin-PE as previously described.

The relative MFI of the cells was plotted against the antigen concentration used and the curve fitted by non-linear least squares regression, giving an estimated apparent K_D of 3 x10^{-9} M for VFIB1 and 35 x10^{-9} M for VFIB2 (Figure 35A and 35B). These values were consistent with the K_D determined by SPR (Figure 34A and 34B).

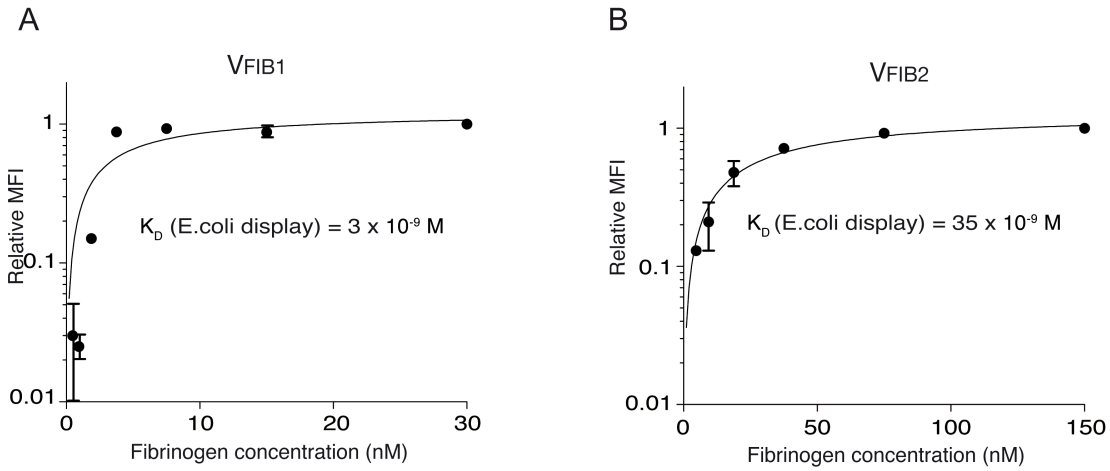

Figure 35. Estimation of the equilibrium dissociation constant (KD) of clones VFIB1 and VFIB2 against Fib by *E. coli* display.

The K_D of the selected clones (as indicated) was estimated by flow cytometry analysis of *E. coli* cells expressing NVFIB1 or NVFIB2 incubated with different concentrations of biotinylated Fib under equilibrium conditions. The mean fluorescent intensities (MFI) of bacteria, after labeling with Streptavidin-PE, were plotted *versus* the concentration of Fib used in the assays. The curve was fitted by non-linear least squares regression.

Chapter 4: Cell Selection and characterization of high affinity single domain Abs against human EGFR from immune libraries displayed on the surface of *E. coli* cells

4.1 Epidermal Growth Factor Receptor (EGFR)

The epidermal growth factor receptor (EGFR/Her1/ErbB1) is a transmembrane receptor belonging to the ErbB family of tyrosine kinases and is implicated in many human cancers (especially on squamous cancer cells), being an important target for several classes of therapeutic agents, including Ab-based drugs. These receptors are abnormally expressed in many epithelial tumors such as colorectal, lung, brain, breast, head and neck tumors etc (Gullick, 1991; Baselga and Arteaga, 2005; Huang et al., 2009) and influence their growth and survival in malignant states (Zaczek et al., 2005). The receptor comprises a transmembrane domain, an extracellular ligand-binding domain and an intracellular domain with tyrosine kinase activity (Figure 36A). Several mammalian ligands are known to activate EGFR, including EGF, transforming growth factor-α (TGF-α), heparin-binding EGF-like growth factor (HB-EGF), amphiregulin (AR), betacellulin (BTC), epiregulin (EPR) and epigen (EPI). EGFR signalling promotes angiogenesis, proliferation, invasion and metastasis of the tumor cells.

It is well established that Ab binding to the extracellular domain of EGFR can inhibit ligand-induced receptor activation and tumor growth (Sato et al., 1983; Gill et al., 1984). Various EGFR agents have been developed as anti-cancer drugs, for example, cetuximab, panitumumab (both are mAbs), gefitinib and erlotinib (small-molecule inhibitors). The mAbs target the extracellular domain of the receptor and inhibit ligand-dependent EGFR signal transduction, while the small-molecule inhibitors target the intracellular tyrosine kinase. Inactive EGFR can exist as both monomers and dimers, suggesting that the mechanism regulating EGFR activity may be subtle. Dimerization-driven activation of the intracellular kinase domains of the epidermal growth factor receptor (EGFR) upon extracellular ligand binding is crucial to cellular pathways regulating proliferation, migration, and differentiation. Molecular dynamic simulations of the membrane with the embedded EGFR

(Arkhipov et al., 2013) suggest that in ligand-bound dimers, the extracellular domains assume conformations favoring dimerization of the transmembrane helices near their N termini, dimerization of the juxtamembrane segments, and formation of asymmetric (active) kinase dimers. In ligand-free dimers, by holding apart the N termini of the transmembrane helices, the extracellular domains instead favor C-terminal dimerization of the transmembrane helices, juxtamembrane segment dissociation and membrane burial, and formation of symmetric (inactive) kinase dimers (Figure 36B).

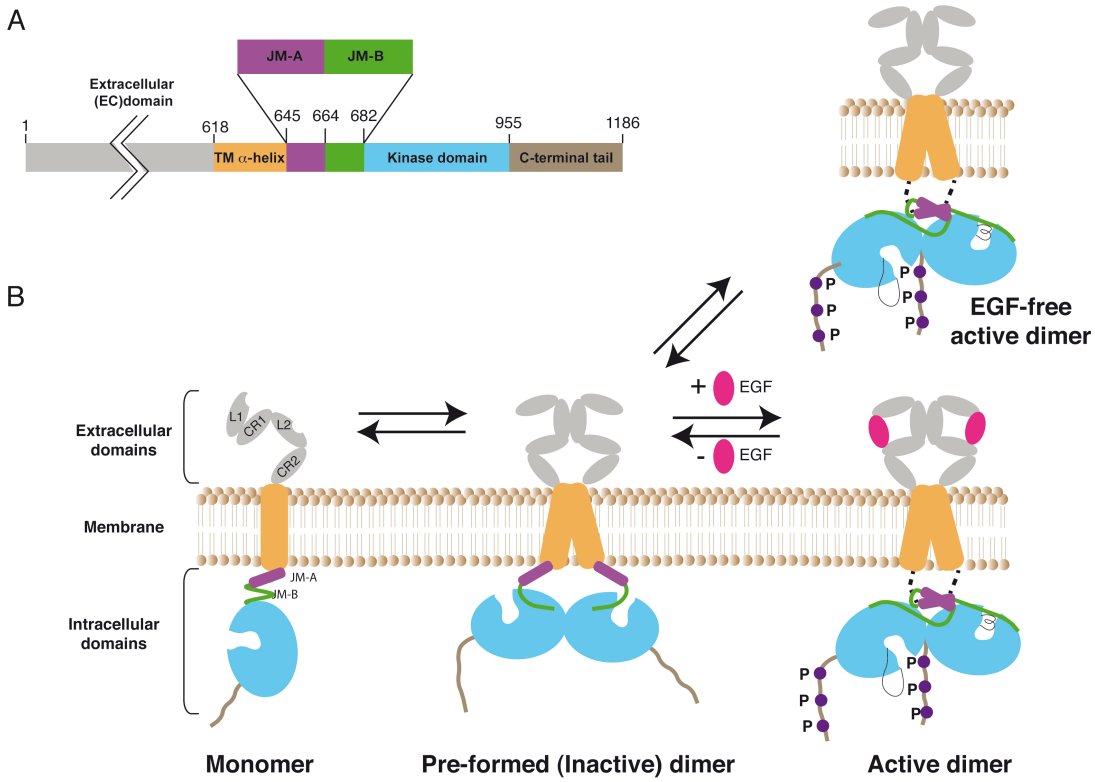

Figure 36. Schematic of EGFR and the states in which it exists.

(A) Scheme of EGFR domains (left), showing extracellular domain, transmembrane (TM) α-helix, juxtamembrane domains A&B, kinase domain, and C-terminal tail. **(B)** EGFR is present in the monomeric form or as a pre-formed dimer (inactive). Encounter of its ligand i.e. EGF, leads to phosphorylation of its C-terminal tail (active dimer) (Arkhipov et al., 2013), initiation of signalling cascades and stimulation of cell cycle machinery. Leads to secretion of growth, angiogenic and motility factors

4.2 Construction of immune sdAb library against Human EGFR

An immune sdAb library against Human EGFR cloned in a phage display vector (Roovers et al., 2007) was a kind gift from Dr Rob Roovers and Paul van Bergen en Henegouwen, University of Utrecht, Netherlands. This library contains ca. 10^7

independent clones and was constructed from VHH gene segments amplified from lymphocytes isolated from two llamas (*Llama glama*) immunized with intact human A431 cells, which overexpress EGFR (ca. $2x10^6$ molecules of EGFR/cell). . The VHH repertoire of this library was cloned into the *Sfi*I and *Not*I sites of the pNeae2 vector and transformed into EcM1 cells for *E. coli* display. A library of ~$2x10^7$ independent clones was generated.

4.3 Selection of high affinity sdAbs from the anti-EGFR immune library by MACS

To test the *E. coli* display NVHH library anti-EGFR we employed first MACS with purified rhEGFR-Fc, a recombinant protein carrying the extracellular domain of human EGFR fused to an Ig Fc region. Similar to previous selections with TirM and Fib, $2x10^8$ bacteria were incubated with biotinylated rhEGFR-Fc (100 nM) for the first selection step (MACS1) and ~0.6-0.7% of the total CFU were collected in the Bound fraction (Table 10). The colonies grown from the Bound fraction were pooled, their plasmids purified and electroporated into fresh *E. coli* EcM1 cells (≥10^7 transformants). This sublibrary was subjected to a new round of selection with 100 nM biotinylated rhEGFR-Fc under identical conditions.

Table 10. Summary of MACS with *E. coli* display libraries against rhEGFR.

Round	Antigen conc (rhEGFR-Fc)	NVHH library%
MACS1	100 nM	0.3
MACS2	100 nM	2.6

(%): Percentage of bacteria in Bound fractions with reference to total bacteria in Wash+Bound fractions (ca. 1-5 x 10^7 CFU)

The percentage of *E. coli* bacteria recovered in the Bound fractions increased to 2.6% in MACS2 (Table 10) and were analyzed by flow cytometry to test their binding to biotinylated rhEGFR-Fc (50 nM) (Figure 37), which demonstrated an enrichment of *E. coli* clones binding to rhEGFR-Fc with more than 70% positives after MACS2. No significant binding to biotinylated BSA was detected by flow cytometry in these populations. The expression levels of the NVHH fusions in the bacterial pools obtained after MACS were similar to those in the original library (Figure 37).

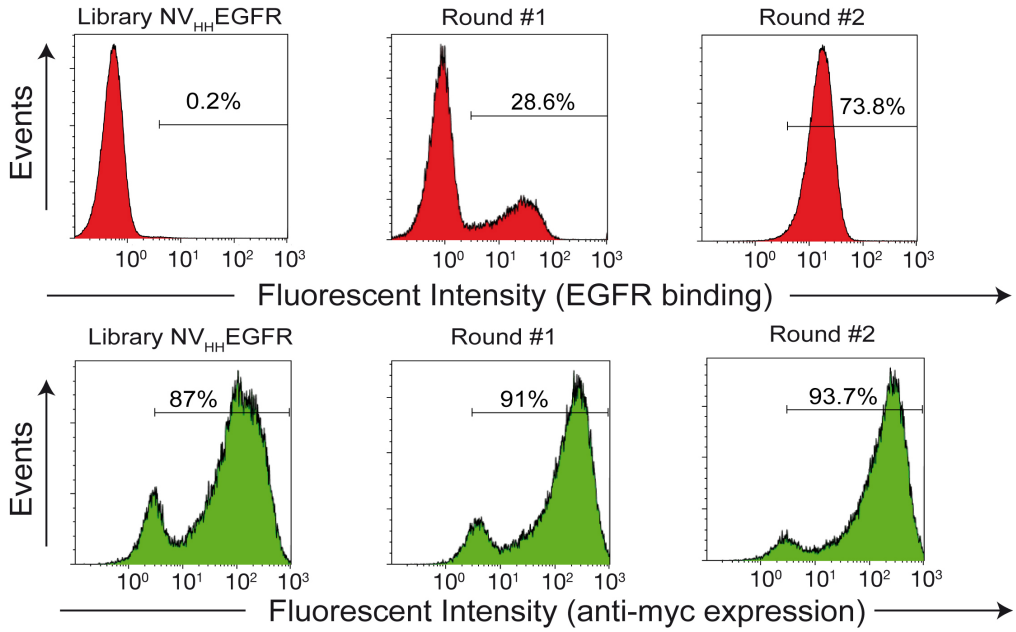

Figure 37. Magnetic cell sorting of NVHH *E. coli* display libraries with biotinylated rhEGFR-Fc antigen.

Fluorescent flow cytometry analysis of IPTG-induced *E. coli* EcM1 cells expressing NVHH immune libraries, or their respective sub-libraries enriched after the indicated round of MACS with biotinylated rhEGFR-Fc. Histograms show the fluorescence intensity of bacteria incubated with biotinylated rhEGFR-Fc and secondary Streptavidin-PE or anti-myc tag mAb and anti-mouse conjugated to Alexa 488 fluorophore.

4.4 Direct cell selection of high affinity sdAbs against EGFR using *E. coli* display.

We wanted to determine whether *E. coli* display could allow the direct selection of sdAbs from immune libraries against EGFR on live tumor cells overexpressing EGFR on its surface, instead of purified recombinant EGFR protein, previously used during MACS. Hence, we designed a simple cell selection (CellS) procedure consisting of an initial incubation step of the *E. coli* display library with a monolayer of the murine tumor cell line, NIH-3T3 2.2, which lacks expression of endogenous EGFR. This allows substractive selection of binders recognizing other cell surface antigens. Next, clones that did not bind NIH-3T3 2.2 cells were incubated with a monolayer of the murine tumor cell line HER14, which is a stably transfected NIH-3T3 2.2 clone expressing hEGFR (Honegger et al., 1987). Bacteria binding to HER14 were recovered on LB plates for plasmid isolation and subjected to subsequent rounds of selection. A schematic illustration of the methodology proposed is shown in Figure 38.

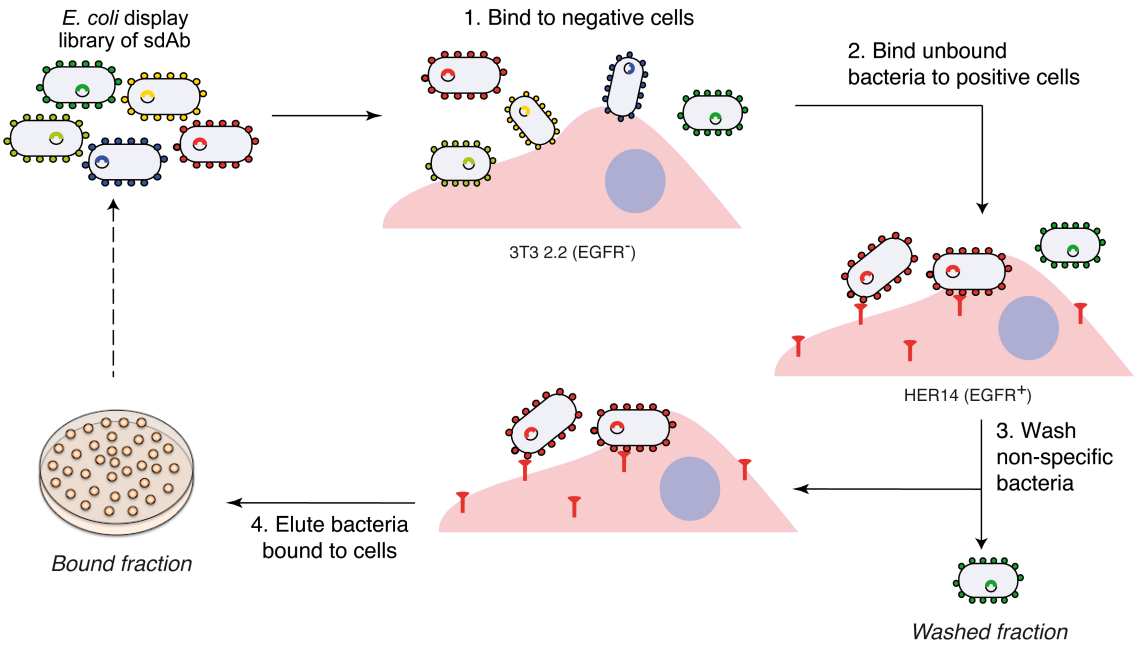

Figure 38. Direct selection of NVHH *E. coli* display libraries on cells.

E. coli cells are intially bound to eukaryotic cells not expressing EGFR i.e. NIH-3T3 2.2, and any bacteria binding non-specifically to these cells are removed. The bacteria that do not bind are recovered and incubated with eukaryotic cells that express EGFR i.e. HER14. The HER14 cells are washed to remove non-specific or loosely bound *E. coli* cells, followed by lysis of eukaryotic cells and elution of bound bacteria. The CFU of bound bacteria in the cell lysate is determined by plating.

Both cell lines were seeded in 6-well cell culture plates to attain a confluency of 50% in 24 h (≈6X10^5 cells per well). Firstly, depletion of bacteria displaying VHH clones binding to cell surface antigens but not to EGFR was carried out by incubation of induced bacteria (≈6X10^7) with NIH-3T3 2.2 cells (EGFR$^-$) at a MOI of ≈100, for 1h at 37°C. Secondly, the bacteria that were not bound to the negative cell line were recovered and incubated with HER14 cells (EGFR$^+$) for 15 mins at 37°C. Further, the cells were washed three times with HBSS to remove unbound bacteria and lysed by addition of HBSS supplemented with 0.2% SDS and 0.1% DNAse. The resulting cell lysate containing bacteria was plated.

The colonies grown in plates were pooled, their plasmids purified and electroporated into fresh *E. coli* EcM1 cells. The sublibrary was subjected to a additional round of CellS with NIH-3T3 2.2 and HER14 cell lines using identical conditions. The percentage of *E. coli* bacteria recovered in the HER14 cell-bound fractions showed an increase from the initial 0.3% in CellS1 to 1.2% in CellS2 (Table 11), suggesting an enrichment of clones binding specifically to HER14.

Table 11. Summary of Cell selections with NVHH *E. coli* display library against rhEGFR.

Round	Bacteria in input	Bacteria in output	% bacteria recovered
CellS1	6 x 10^7	2 x 10^5	0.3
CellS2	6 x 10^7	7 x 10^5	1.2

A total of 6x10^5 cells were seeded in 6 well culture plates. Bacteria were added at a MOI =100

Bacterial pools from each of the different rounds of cell selection were analyzed by flow cytometry to test their binding to biotinylated rhEGFR (50 nM) (Figure 39), which demonstrated an enrichment of *E. coli* cells binding to rhEGFR along the selection rounds, from ~0.2 % positives in the original libraries to ~35% after CellS2. No significant binding to biotinylated BSA was detected by flow cytometry in these populations. The expression levels of the NVHH fusions in the bacterial pools obtained after cell selection was similar to those of the original libraries (Figure 39).

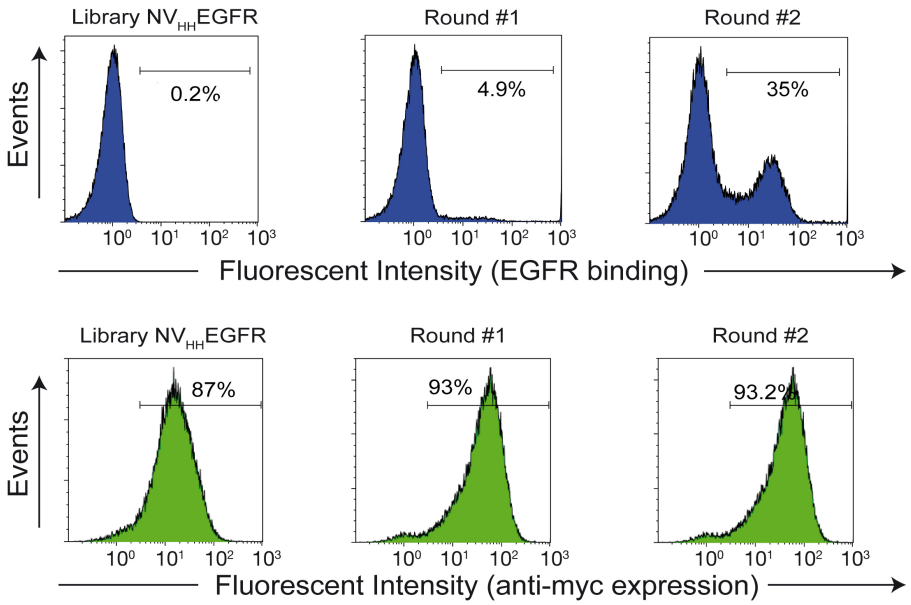

Figure 39. Flow cytometry analysis of anti-EGFR NVHH *E. coli* display libraries selected on cells.

Fluorescent flow cytometry analysis of IPTG-induced *E. coli* EcM1 cells expressing NVHH immune libraries, or their respective sub-libraries enriched after the indicated round of cell selection with biotinylated rhEGFR. Histograms show the fluorescence intensity of bacteria incubated with biotinylated rhEGFR-Fc (50 nM) and secondary Streptavidin-PE or anti-myc tag mAb and anti-mouse conjugated to Alexa 488 fluorophore.

Ninety-six colonies from the second round of selection of the NVHH library by MACS (i.e MACS2) were randomly picked for plasmid isolation and DNA sequencing. In the screening of the MACS2, a VHH sequence, named as VEGFR1, was found in 72 NVHH clones, while other clones, namely VEGFR2 (10 clones), VEGFR3 (1 clone), VEGFR4 (3 clones) and VEGFR5 (1 clone) were also found, the rest being non-EGFR binding VHH sequences.

Similarly, ninety-six clones from CellS2 were screened by visual observation under a light microscope of their specific binding to HER14 cells ($EGFR^+$), but not to NIH-3T3 2.2 cells ($EGFR^-$). Briefly, induced bacteria were added to wells containing either HER14 cells or NIH-3T3 2.2 cells at a MOI of 100 and the infection was monitored after 20 minutes by visual inspection in an inverted microscope. Clones that did not bind either cell line were classified as “Non-binders”, those that bound both NIH-3T3 2.2 cells and HER14 cells were classified as “non-specific binders” and those that bound only HER14 cells, but not NIH-3T3 2.2 cells were called “specific binders”. Out of the 96 clones screened by this method, 45 clones were non-binders, 26 clones were non-specific binders and 25 clones were specific binders. DNA sequences of all 25 specific binders were isolated and sequenced. Like previous screening of MACS2 population, VEGFR1 was found 18 times and was the major clone. VEGFR2 (3 clones), VEGFR4 (2 clones) were also found, while one new clone, VEGFR6 (2 clones) was also identified. The CDR3 sequences of all identified clones are illustrated in Table 12.

Table 12. CDR3 sequences of anti-EGFR clones selected by *E. coli* display.

Clone Name	Amino acid sequence of CDR3	Selection system	
		MACS	CellS
VEGFR1	DKWSSSRRSVDYDY	72/96	18/96
VEGFR2	TYNPYSRDHYFPRMTTEYDY	10/96	03/96
VEGFR3	RYSDVIFTLPERYAY	01/96	-
VEGFR4	STYSRDSVFTKWANYNY	03/96	02/96
VEGFR5	GPILGSSESYRSSRRYAY	01/96	-
VEGFR6	DLNFIGIVTTTSEKYDY	-	02/96

4.5 Binding of selected clones to EGFR+ tumor cells by immunofluorescence microscopy

All anti-EGFR clones isolated by *E. coli* display were further characterized for their specific binding to HER14 cells ($EGFR^+$) but not to NIH-3T3 2.2 cells ($EGFR^-$) by immunofluorescence microscopy, staining the samples with DAPI (nuclei) and fluorescent antibodies against EGFR and *E. coli*. This experiment revealed that all positive anti-EGFR *E. coli* obtained by MACS and CellS (Table 12) bound specifically to HER14 cells but not to NIH-3T3 2.2 cells (Figures 40 and 41), while one non-specific clone (number 37 from CellS, $V_{CLONE37}$) from CellS screening bound to both cell lines and a negative control *E. coli* displaying NV_{FIB1} bound to neither of the cell lines (Figure 40).

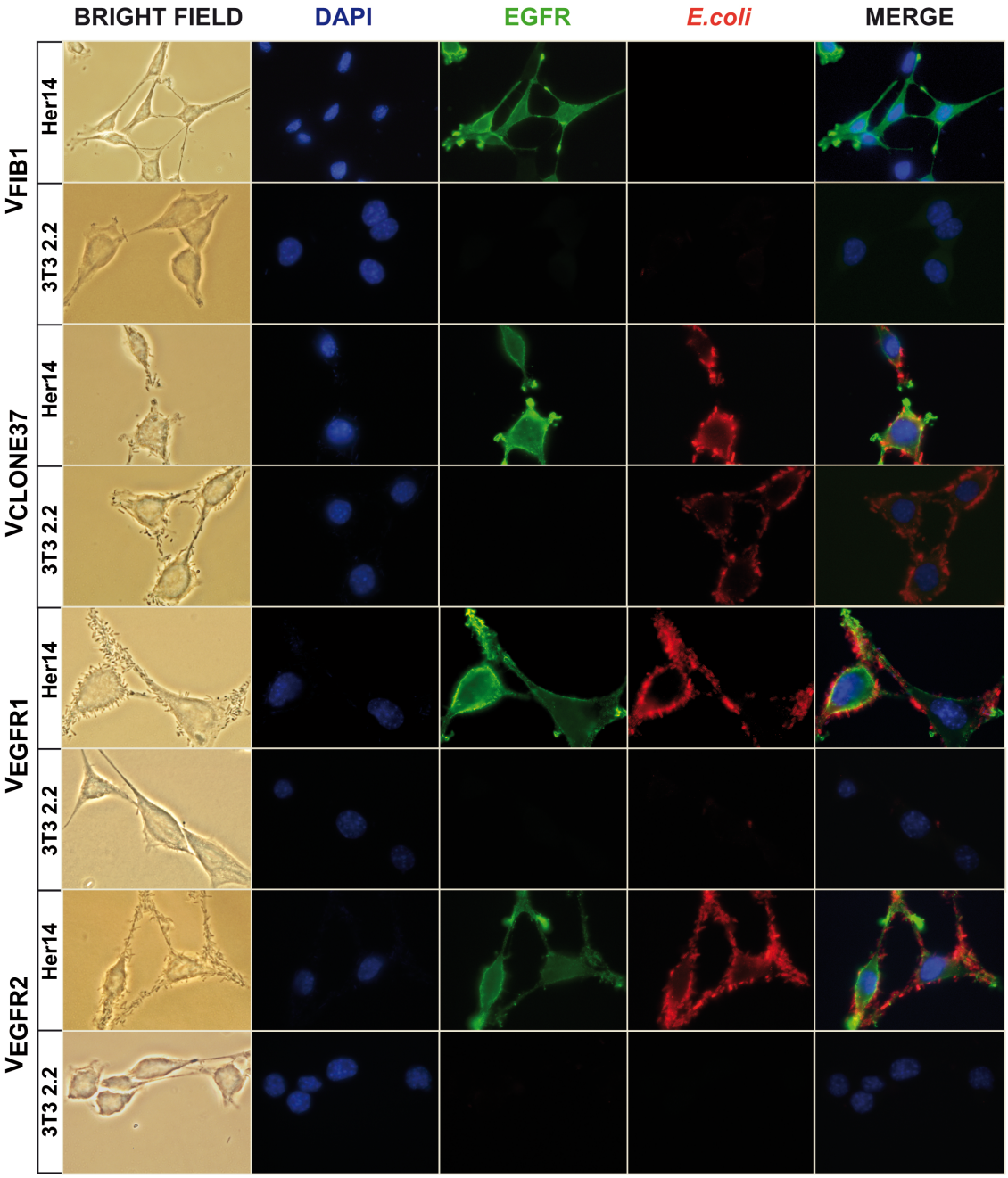

Figure 40. Bright field and immunofluorescence microscopy images of *E. coli* bacteria displaying the indicated VHH clone to HER14 and NIH-3T3 2.2 cells.

These images show the binding specificity of *E. coli* bacteria displaying the selected anti-EGFR clones VEGFR1 and VEGFR2, to HER14 and not to NIH-3T3 2.2 cells. A negative clone (VFIB1) and a non-specific clone from CellS (VCLONE 37) are also included as controls. Bacteria are labelled with anti-*E. coli* (red), EGFR is labelled with anti-EGFR mAb (green), DNA and cell nuclei labelled with DAPI (blue).

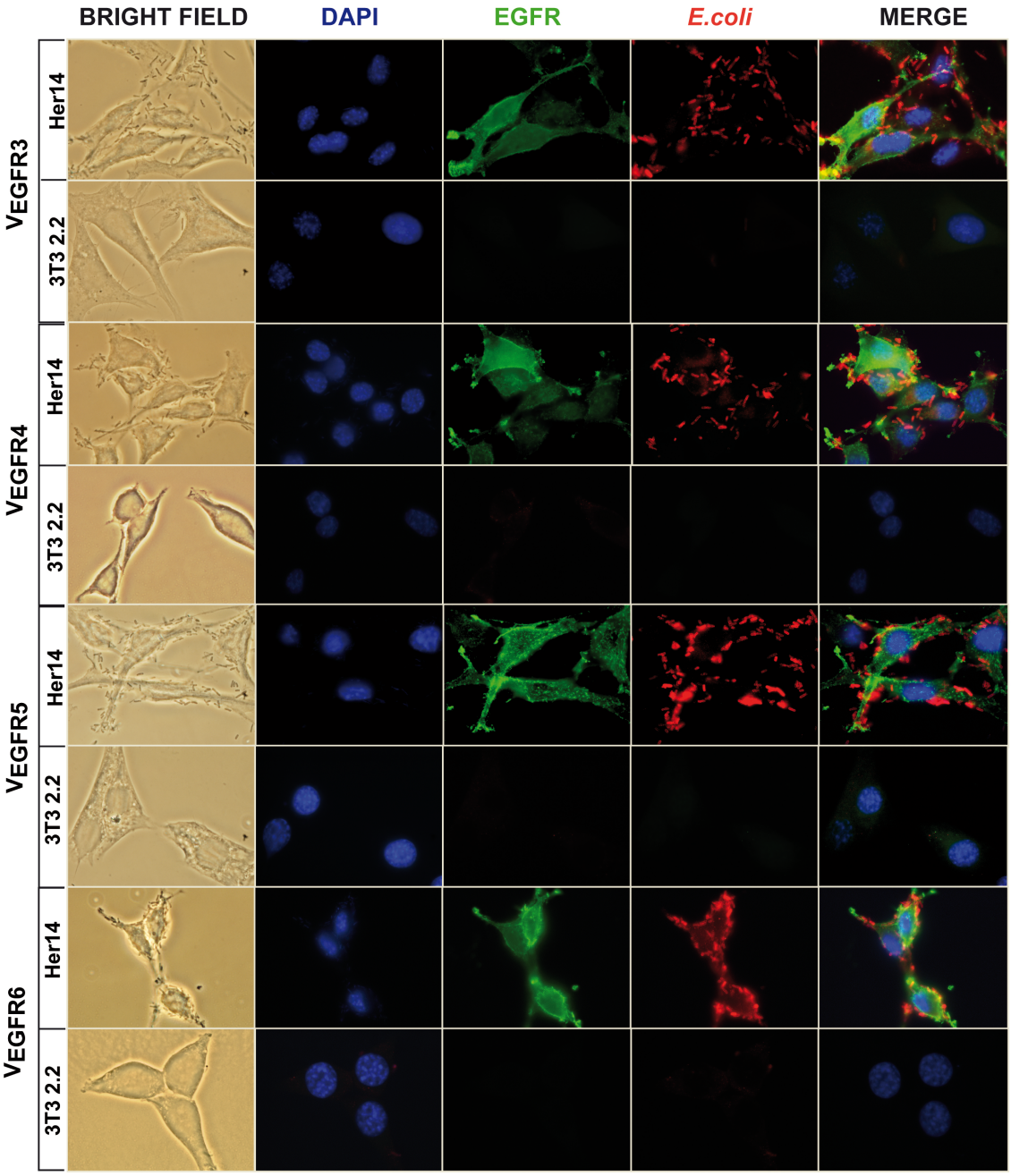

Figure 41. Bright field and immunofluorescence microscopy images of *E. coli* bacteria displaying the indicated VHH clone to HER14 and NIH-3T3 2.2 cells (continued).

These images show the binding specificity of *E. coli* bacteria displaying VEGFR3, VEGFR4, VEGFR5 and VEGFR6 to HER14 and not to NIH-3T3 2.2 cells. Samples stained as in Figure 39.

4.6 Binding of selected clones to biotinylated rhEGFR-Fc by flow cytometry.

Flow cytometry analysis confirmed the specific binding of biotinylated rhEGFR-Fc (50 nM) by *E. coli* cells displaying each of the six V_{HH} sequences, with negligible binding to biotinylated BSA. The MFI of VEGFR1 and VEGFR2 was the best and at similar levels (Figure 42A), which suggested that these clones had a high apparent

affinity for rhEGFR, while the MFI of VEGFR3-6 was found to be lower, suggesting that it had a lower apparent affinity for rhEGFR. An overlay of the binding of all selected clones to rhEGFR in flow cytometry is illustrated in Figure 42B.

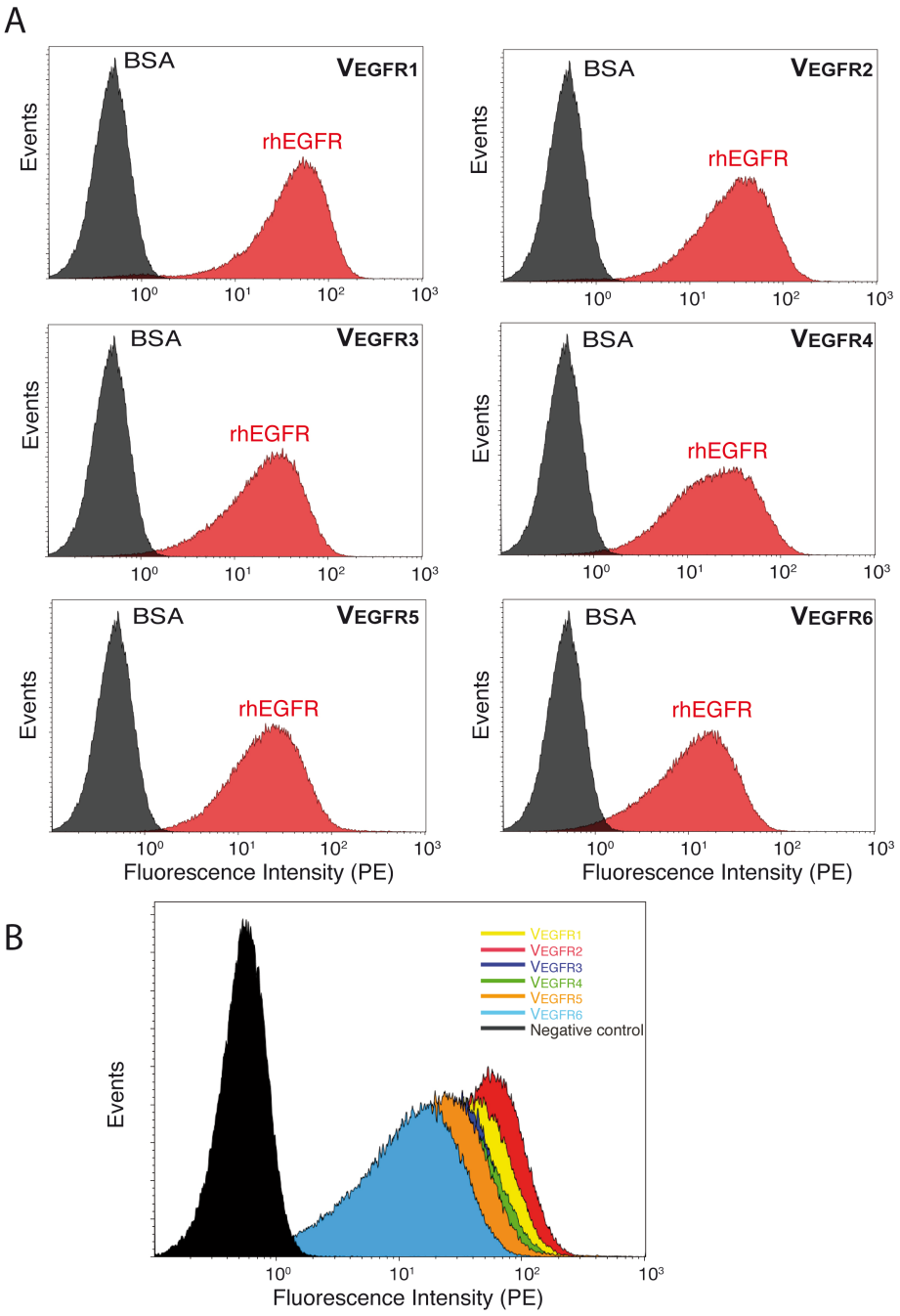

Figure 42. Binding of *E. coli* cells displaying selected clones from anti-EGFR NVHH libraries to biotinylated rhEGFR-Fc.

(A) Fluorescent flow cytometry analysis of induced *E. coli* EcM1 cells bearing the indicated plasmids selected from the anti-EGFR NVHH library. **(B)** Overlay of histograms of binding of the selected clones to biotinylated EGFR. Histograms show the fluorescence intensity of bacteria incubated with biotinylated antigens (rhEGFR or BSA, as labeled) and secondary Streptavidin-PE.

4.7 Estimation of the affinity of VEGFR1 and VEGFR2 by *E. coli* display

Flow cytometry analysis was used to estimate the apparent K_D of two V_{EGFR} clones with highest binding signals. The final concentration range of biotinylated rhEGFR-Fc in the assay for was between 100 nM and 0.8 nM. Briefly, *E. coli* cells (~$3x10^7$ CFU) with the respective sdAb on their surface were incubated with a fixed amount of biotinylated rhEGFR-Fc (1 pmol) for 90 mins in two-fold increasing volumes of PBS (from 0.01 to 2 ml) to reach the desired final concentration range (as above). After this incubation, cells were washed and labeled with Streptavidin-PE as previously described. The relative MFI of the cells was plotted against the antigen concentration used and the curve fitted by non-linear least squares regression, giving an estimated apparent K_D of 30 $x10^{-9}$ M for VEGFR1 (Figure 43A) and 12 $x10^{-9}$ M for VEGFR2 (Figure 43B).

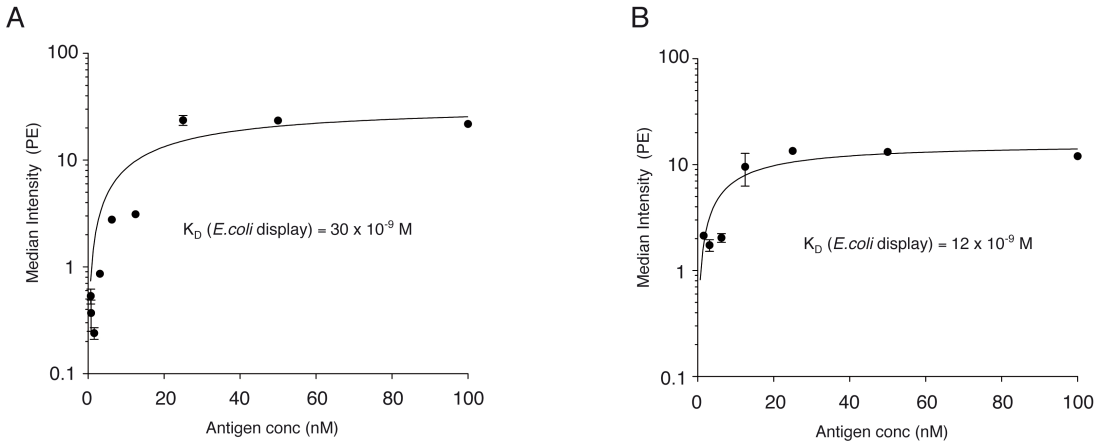

Figure 43. Estimation of the equilibrium constant (KD) of VEGFR1 and VEGFR2 by *E. coli* display.

The K_D of the selected clones (as indicated) was estimated by flow cytometry analysis of *E. coli* cells expressing NVEGFR1 or NVEGFR2 incubated with different concentrations of biotinylated EGFR (0.8-100 nM) as specified, under equilibrium conditions. The mean fluorescent intensities (MFI) of bacteria, after labeling with Streptavidin-PE, were plotted *versus* the concentration of EGFR used in the assays. The curve was fitted by non-linear least squares regression.

4.8 Binding of the selected clones to EGFR in the presence of EGF

All the clones selected by *E. coli* display were further characterized for their ability to bind EGFR in the presence of EGF using flow cytometry. It was observed that clones VEGFR2, VEGFR3, VEGFR4, VEGFR6 and to a lesser extent VEGFR1, had reduced

binding signals to rhEGFR-Fc (50 nM) when 25 μM EGF was present, while the binding of VEGFR5 was almost the same in the presence or absence of EGF (Figure 44).

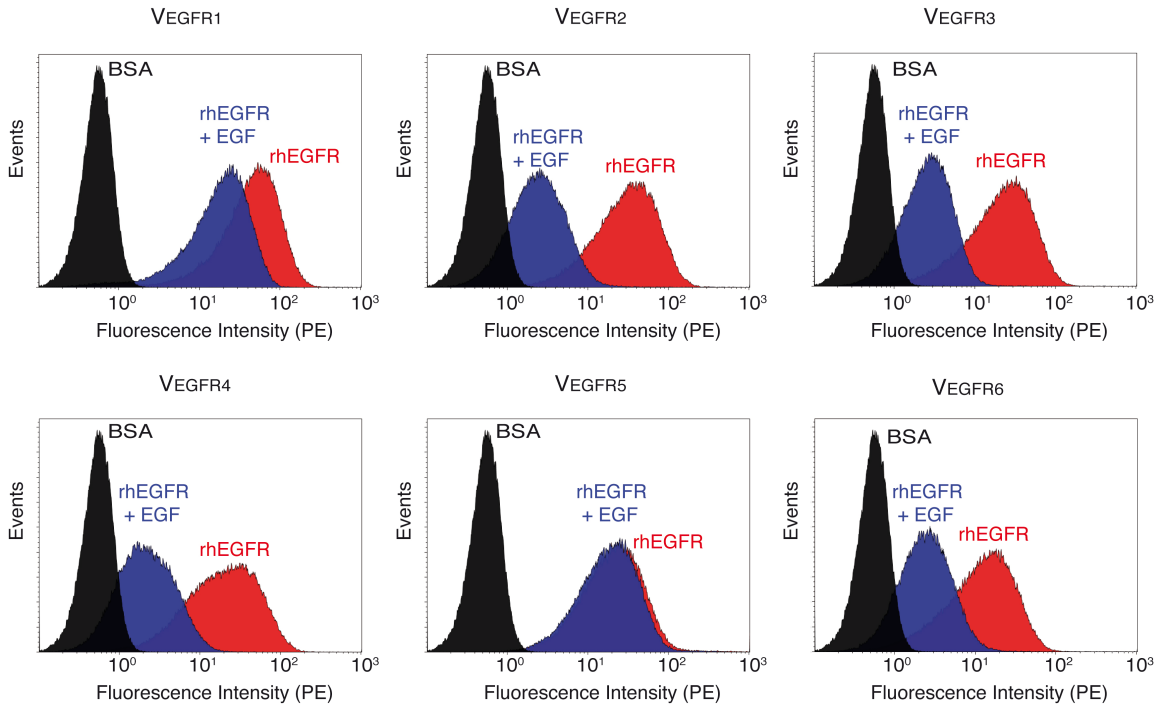

Figure 44. Flow cytometry analysis of binding to EGFR by the clones selected by *E. coli* display in the presence of EGF.

Fluorescent flow cytometry analysis of binding of the selected anti-EGFR clones to rhEGFR-Fc in the presence or absence of EGF. Histograms show the fluorescence intensity of bacteria incubated with biotinylated rhEGFR (50 nM) in the presence or absence of 25 μM EGF.

DISCUSSION

In this thesis, we have evaluated and described the application of two β-domains of EhaA and Intimin from EHEC, for the surface display of VHH clones and immune libraries against 3 different antigens of biomedical importance i.e. the extracellular domain of the translocated intimin receptor from EHEC (TirMEHEC), human fibrinogen (Fib) and epidermal growth factor receptor (EGFR). The anti-TirMEHEC and anti-Fib VHH libraries were initially used to setup the selection conditions by MACS and to compare the effectiveness of the two β-domains in selection of VHH thereof. Further, the more effective β-domain from Intimin was used to display an immune library raised using tumor cells overexpressing hEGFR and select specific high affinity binders against hEGFR using the recombinant extracellular domain of hEGFR fused to Fc and murine tumor cell lines transfected with or without hEGFR.

We have found that the β-domains of EhaA and Intimin are effective platforms for the surface display of VHH libraries on *E. coli* K-12 cells, and allow for selection of high affinity VHHs from immune libraries using biotinylated antigen and MACS (Salema et al., 2013). Despite their opposite topologies, both systems express stable fusion proteins with the native β-barrel properly folded in the OM and the VHH domain displayed to the extracellular mileu, retaining functionality and antigen binding capacity. Most clones in the immune libraries were displayed at good levels on *E. coli* with both EhaA and Intimin β-domains, with an average of 6000-8000 molecules/bacterium. From each of the immune libraries used in our studies, we obtained about 3-6 different camelid VHH sequences with different binding affinities (in the nM range) to the antigen used in the immunization, which is one of the advantages of using immune libraries. These results demonstrate that both the *E. coli* display systems can be used to retrieve high-affinity binders from immune libraries of VHH sequences. The small molecular weight, high protein solubility and stability of camelid VHH domains are likely to aid their effective translocation across the OM fused to the β-domains of either EhaA and Intimin. Similar properties have been reported with other natural sdAbs, like VNARs from sharks (Dooley, 2003), which have been engineered in synthetic libraries based on human VHs and VLs. Thus, it is likely that other types of sdAbs could also be efficiently displayed on *E. coli* cells with the EhaA and Intimin β-domains. Display of larger rAb fragments

based on a single polypeptide such as scFvs could be also possible, although the tendency to aggregate of many scFv molecules may difficult their translocation across the OM (Veiga et al., 2004). Nevertheless, this could be advantageous for the selection of highly stable and soluble scFvs from libraries. Lastly, Ab molecules with separate H and L polypeptide chains (e.g Fabs, IgGs) cannot be displayed with these β-domains (atleast in their current conformation), and either phage display or APEx (Harvey et al., 2004; Mazor et al., 2007; Mazor et al., 2010) should be used instead for their selection in *E. coli.*

Comparison of EhaA and Intimin display systems led to the observation of some important differences between them. Firstly, NVHH fusions were found to be more stable than VHHA fusions *in vivo* (to *E. coli* proteases) and *in vitro* (to externally added proteases), which could be attributed to the natural resistance of Intimin to proteolysis and denaturation (Bodelon et al., 2009); and/or due to the susceptibility of certain ATs to endogenous bacterial proteases as a part of their secretion mechanism (Bernstein, 2007; Leyton et al., 2012b). Secondly, expression of VHHA clones appeared to be more variable than NVHH fusions, with some clones showing significantly lower expression levels. This suggests that the N-terminal fragment of Intimin could have a positive effect on the expression of VHHs, as observed with other N-terminal fusion partners (i.e. MBP, Trx1, GST) used routinely for the production of recombinant proteins and Ab fragments (Jurado et al., 2006). Thirdly, the antigen binding levels determined by flow cytometry with NVHH library were found to be atleast 3 fold higher than the respective VHHA library. The lower antigen binding signals of *E. coli* cells displaying VHHA fusions could not be solely attributed to lower expression levels, and indicated the existence of additional factors. Eventhough partial misfolding of VHHA fusions cannot be totally excluded, this seems unlikely given that both EhaA and Intimin β-domains use a common secretion pathway, exposing the VHHs to the same periplasmic folding factors (e.g. DsbA) and chaperones (e.g. FkpA and Skp) that are known to participate in the folding of Ig domains (Bodelon et al., 2012). An alternative explanation could be that the longer linker region in NVHH fusions (with the D0 domain), could make the VHH domain more accessible for binding to the antigen in solution by increasing its

distance from the OM. The improved stability, higher expression levels and superior antigen binding activity could explain the reason why selection of high affinity binders from the anti-TirM$_{EHEC}$ and anti-Fib libraries was more efficient using the Intimin system than the EhaA system, with a higher percentage of positive antigen-binding clones being achieved in fewer selection rounds. The superior antigen binding signals with the Intimin β-domain also facilitates the estimation of the affinity of the selected NV$_{HH}$ clones to their antigen by flow cytometry. From our data, the only possible limitation of Intimin display could be a slight decrease in the viability of *E. coli* cultures expressing some NV$_{HH}$ fusions, which was observed for anti-TirM$_{EHEC}$ library. However, this reduction in viability of NV$_{HH}$ was not observed during the expression of anti-Fib library. We have recently tested the viability of anti-EGFR library (data not shown), and found that the viability is not affected, being ~0.9x10^9 CFU/OD_{600}. Hence, some specific attributes of the anti-TirM$_{EHEC}$ library could cause the observed toxicity in NV$_{HH}$ fusions. In any case, the observed reduction does not have a significant effect on the representation of immune libraries with a diversity of ~10^7 clones, since an excess of input bacteria over the library size is always used during MACS (≥10^8 bacteria).

The number of antigen-specific high affinity binders obtained from each immune library could be more connected to attributes of the library itself, such as the immunogenicity of antigen, number of animals used in the immunization, or size and complexity of the library (Bradbury and Marks, 2004), rather than on the effectiveness of the surface display system used for selection. In the case of the anti-TirM$_{EHEC}$ library, we obtained a single high affinity binder i.e. V$_{TIR1}$ and four other binders i.e. V$_{TIR2}$ to V$_{TIR5}$, of lower affinities. However, previous selection of the same anti-TirM$_{EHEC}$ library by phage display had failed to retreive specific high-affinity binders other than V$_{TIR1}$ isolated by *E. coli* display (data not shown). Similarly, selections of the anti-Fib and anti-EGFR libraries using *E. coli* display led to identification of a similar number of high affinity binders and essentially the same clones that were also isolated by phage display of these V$_{HH}$ libraries (Roovers et al., 2007); and data not shown. Thus, it appears that the actual diversity of binders

retreived from immune libraries is more dependent on intrinsic factors of the library rather than on the display system used for selection.

Abs are in huge demand for use in diagnosis and therapy and so is the need for inexpensive Ab expression systems for their selection and production. *E. coli* is an attractive expression system since it requires inexpensive media, has fast growing times, high efficiency of transformation (>10^{10} transformants/μg of plasmid DNA), well-characterized, versatile cloning and expression vectors. Although the purification of Nbs from the periplasm of *E. coli* is relatively straightforward owing to their high solubility and simplicity in structure, variable yields are commonly obtained among different clones (e.g. 0.1-0.5 mg/L of induced culture for Nbs). To alleviate this issue and increase the total yield of Nb produced, we investigated their production fused to the periplasmic maltose binding protein (MBP) of *E. coli*. In addition, we included a His_6 tag in the C-terminus of the fusions to allow the use of a double affinity chromatography during the purification, with amylose and immobilized metal resins. Expression of the constructs in standard *E. coli* strains such as BL21 resulted in high levels of proteolysis, and so an *E. coli* strain deficient in periplasmic proteases i.e. HM140 was used. Soluble MBP-$V_{HH_{His6}}$ fusions were consistently expressed at high levels (>12 mg/L of induced culture) in the periplasm of *E. coli*. Highly pure MBP-$V_{HH_{His6}}$ fusions were recovered by amylose and immobilized metal affinity chromatography steps. Good yields of soluble $V_{HH_{His6}}$ (between 2-3 mg/L of induced culture) were obtained after site-specific proteolysis of the fusions and their monomeric nature was confirmed by gel filtration. Both, MBP-$V_{HH_{His6}}$ fusions and free $V_{HH_{His6}}$ retained antigen binding activity and specificity (Salema and Fernandez, 2013). The anti-Fib V_{HH}, i.e. V_{FIB1} purified in this manner was successfully applied in the development of a disposable magnetoimmunosensor for detection of fibrinogen in plasma (Campuzano et al., 2014).

We chose MACS to select and recover *E. coli* cells bound to the antigen since this technology does not require expensive equipment like the fluorescent cell sorter used in FACS, and multiple samples can be processed in parallel. While we used a

manual MACS system (holding upto 8 mini-MACS columns, each with a capacity of ~10^8 bacteria), MACS is easily scalable to columns with higher loading and capturing capacities, with the possibility of being automated, thus making screening of large Ab libraries faster and more efficient than FACS.

Although MACS is an easy and fast way to select high affinity binders from an Ab library, this method relies on the availability of purified antigen, which is not always practical or feasible. Direct selection on cells expressing the antigen(s) of interest maybe required when an antigen is produced at low yields, has low solubility, or does not maintain its native conformation upon purification. It may also be an attractive approach to identify Abs against unknown antigens expressed on the surface of target cells (Ahmadvand et al., 2009; Pavoni et al., 2014). This may be challenging for antigens with low levels of expression, but it is clearly realistic with surface antigens overexpressed under certain conditions (e.g. tumor cells). In our work we used an anti-EGFR library that was obtained by immunizing llamas with whole A431 cells (EGFR+) (Roovers et al., 2007). This library was cloned into the Intimin system and selected directly on cells using a combination of negative selection cycles on cells that did not express EGFR (NIH-3T3 2.2) and positive selection cycle on cells expressing EGFR (HER14). The selection was very effective and we were able to enrich the anti-EGFR libraries in just two rounds of selection on cells. Out of the CellS, we obtained four specific binders with good affinities to EGFR (one of which was specific to this method of selection), as validated by flow cytometry analysis of binding to these clones to recombinant EGFR antigen and BSA (control). All these clones also bound specifically to HER14 cells but not to NIH-3T3 2.2 cells and competed with EGF for binding to EGFR at different levels (as demonstrated in flow cytometry assays). Further, the K_D of the two best clones (i.e V_{EGFR1} and V_{EGFR2}) was estimated by flow cytometry and was found to be 30 nM and 12 nM respectively.

In this work we have demonstrated that *E. coli* display is suitable for use with immune libraries with 10^6-10^7 clones. Nonetheless, this method is not limited to these types of libraries and could also be used with larger naïve and synthetic

libraries of ~10^9 clones (Arbabi-Ghahroudi et al., 2009; Monegal et al., 2009; Hussack et al., 2012). As mentioned previously, MACS can be scaled up with larger columns than those used in our work, hence allowing the screening of ~$5x10^9$ bacteria/column. Several of these MACS columns of large capacity can be run in parallel covering the total diversity of libraries ~10^9-10^{10} clones. In these type of MACS columns, larger volumes and densities of *E. coli* bacteria can be loaded. Importantly, *E. coli* can be manipulated with ease at a density of is ~$1x10^{10}$ CFU/ml, which is similar to the maximum size of most naïve and synthetic libraries of Ab fragments. . For large naïve and synthetic Ab libraries, phage display may appear to be more advantageous than *E. coli* display, given that bacteriophages can be produced and handled in higher densities than *E. coli* (i.e. 10^{13} PFU/ml). However, the diversity of phage display libraries is also strongly limited by intrinsic *E. coli* factors like transformation efficiency and the ability of phages to infect cultures with sufficient amount of bacteria. In addition, the percentage of phage particles actually displaying at least a single Ab molecule on the surface could be as low as less than 10% of the total infecting particles when conventional helper phages with wild type pIII (e.g. M13K07) are used to rescue phagemids (Rondot et al., 2001; Oh et al., 2007; Soltes et al., 2007). Hence, the actual density of phage-antibody particles is likely to be atleast one order of magnitude lower than the titer of phage solutions and the actual number of clones is limited by *E. coli* transformation, efficiency, as it happens with *E. coli* display. Therefore, *E. coli* display and phage display libraries are appropriate for libraries containing ~10^9-10^{10} different clones. Screening of larger Ab libraries with higher diversities will require the use of cell-free display systems (e.g. ribosome display) that avoid transformation of plasmid vectors to *E. coli* (Pluckthun, 2012; Sun et al., 2012; Kanamori et al., 2014).

One of the major benefits of *E. coli* display over phage display is the use of flow cytometry for the direct determination of the expression levels, antigen-binding specificity and affinity of the selected clones. In addition, eventhough *E. coli* cells are more sensitive than bacteriophages to extremes of pH, temperature and other strong denaturants, *E. coli* bacteria having their OM intact can be washed with most common buffers as well as tolerate significant concentrations of detergents (e.g.

0.1-0.4% w/v of TX-100, SDS or deoxycholate) marking an improvement over the washing conditions tolerated by spheroplasts in APEx. The multivalent Ab display and the less sticky properties of *E. coli* cells compared to bacteriophages makes selections to complex antigenic surfaces e.g. mammalian cells, tissues and organs, with reduced background binding possible.

We have envisaged some putative biomedical applications for the antigen-specific high affinity VHHs selected from the each of the different VHH libraries. The VHH against TirMEHEC, i.e. VTIR1 is a high affinity binder and has a very slow rate of dissociation. Such a binder could be useful in recognization and binding to Tir, thus preventing the association of EHEC to the intestinal surface and further pathogenesis of the bacteria. The VHHs against Fib can be used for diagnostic applications such as detection of fibrinogen levels in the blood using ELISA or other detection methods. In this regard, we have used V_{FIB1} in electrochemical biosensor for the measurement of fibrinogen levels in the blood plasma (Campuzano et al., 2014). Finally, the VHHs against human EGFR need further evaluation of their ability to compete and block the EGFR binding of natural ligands such as EGF, TGF-α etc, thus mimicking the mode of action of some mAbs currently in therapy e.g. Erbitux or Vectibix. This would result in the switching off of signal transduction cascades that lead to uncontrolled growth and proliferation of cells, as occurring in cancer.

CONCLUSIONS

The following are the conclusions of the doctoral thesis:

1. The *E. coli* display systems based on the β-domains of Intimin and EhaA from EHEC represent a good alternative to phage display and other cell display platforms (e.g yeast display), for the selection of high affinity sdAb binders from immune libraries of VHHs. The ability to display and select sdAbs without the need for permeabilization of the OM, along with the lower toxicity of the Neae, EhaA fusions are advantages of the two β-domains tested over other existing *E. coli* display formats.

2. *E. coli* bacteria displaying two different VHH libraries (obtained after immunization with TirMEHEC or Fib antigens) using both β-domains, were successfully screened with their respective biotinylated antigens using MACS, and facilitated the isolation of specific binders with high affinity against TirMEHEC and Fib. These studies also revealed that *E. coli* display with the Intimin β-domain is a more effective platform for selection of binders in fewer rounds. In addition, *E. coli* bacteria displaying VHHs with Intimin β-domain have higher antigen-binding signals in flow cytometry.

3. Flow cytometry of *E. coli* bacteria displaying VHH clones and libraries was used for direct determination of the expression levels, antigen binding specificity and affinity of the selected sdAbs by flow cytometry, representing a major benefit of *E. coli* display. Apparent KD values determined by flow cytometry of *E. coli* bacteria displaying sdAbs against TirMEHEC and Fib were very similar to those obtained with the purified sdAbs and state-of-the-art technologies such as SPR.

4. The multivalent nature of *E. coli* display and the less sticky properties of *E. coli* cells compared to filamentous bacteriophages, reduces background and non-specific binding and, thus makes *E. coli* display an optimal platform for selections not only with purified antigens but also on complex antigenic surfaces and cells (e.g. tumor cells) . High-affinity sdAbs binding human EGFR were selected from an *E. coli* display library of VHHs generated by immunization of llamas with human tumor cells overexpressing EGFR i.e. A431, using selections with either a

recombinant extracellular domain of hEGFR or murine tumor cell lines transfected with hEGFR.

5. Soluble sdAbs can be purified in high amounts from the periplasm of *E. coli* strain HM140 as N-terminal fusions to MBP. MBP-VHH fusions bind their cognate antigen specifically and allow purification of the soluble VHH moiety with a C-terminal His-tag after cleavage of the fusion with a site-specific protease.

Del trabajo presentado en esta tesis podemos obtener las siguentes conclusiones:

1. Los sistemas de presentación de sdAbs basados en los dominios β de intimina y EhaA de EHEC representan una buena alternativa a la presentación en fagos y otras plataformas de presentación en células (por ejemplo la presentación en levaduras), para la selección de sdAbs con alta afinidad por antígeno a partir de genotecas inmunes de V_{HH}s. La capacidad de exponer y seleccionar sdAbs sin la necesidad de permeabilizar la OM, junto con la baja toxicidad de las fusiones con Neae (intimina) o con EhaA son ventajas de estos sistemas en relación a otros formatos de presentación de sdAbs en *E. coli* actualmente existentes.

2. Se han seleccionado con éxito clones de alta afinidad a antígenos específicos desde genotecas de sdAbs presentados en la superficie de bacterias *E. coli*. Dos genotecas de V_{HH} diferentes (obtenidas después de inmunizaciones con los antígenos $TirM_{EHEC}$ o Fib) se presentaron en la superficie de E. coli con ambos dominios β y fueron rastreadas mediante MACS con sus respectivos antígenos marcados con biotina para seleccionar clones que se unían específicamente y con gran afinidad a estos antígenos. Estos estudios también revelaron que el sistema de presentación con el dominio β de la intimina es una plataforma más eficaz para el aislamiento de clones específicos realizando pocas rondas de selección. Asimismo, las bacterias *E. coli* que presentaban V_{HH}s con el dominio β de la intimina presentan señales de fluorescencia más elevadas en los análisis por citometría de flujo.

3. Hemos utilizado la técnica de citometría de flujo con bacterias *E. coli* que presentaban clones de V_{HH} individuales y colecciones de V_{HH} para la determinación directa de los niveles de expresión de los V_{HH}s, la especificidad de unión al antígeno y la afinidad de los sdAbs seleccionados, lo que representa una ventaja importante de los sistemas de presentación de sdAbs en *E. coli*. Los valores de K_D estimados mediante análisis por

citometría de flujo de bacterias *E. coli* que presentan sdAbs frente a $TirM_{EHEC}$ y Fib fueron muy similares a los valores obtenidos con sdAbs purificados aplicando tecnologías de última generación como SPR.

4. La naturaleza multivalente de la presentación de sdAbs en *E. coli* y la tendencia menor a adherirse inespecíficamente de las células de *E. coli* en comparación con bacteriófagos filamentosos, reduce la probablidad de obtener clones inespecíficos. Por ello, la presentación de sdAbs en *E. coli* es una plataforma óptima para la selección de clones específicos, no sólo utilizando antígenos purificados sino también sobre superficies antigénicamente complejas y células (ej. células tumorales). Hemos seleccionado sdAbs de afinidad frente al EGFR humano a partir de una genoteca de sdAbs presentada en *E. coli* y generada mediante inmunización con células tumorales humanas que sobreexpresaban EGFR (ej. A431). Las selecciones se realizaron con éxito utilizando tanto un dominio extracelular de EGFR humano y una línea celular murina transfectada con EGFR humano.

5. Los sdAbs pueden ser purificados en grandes cantidades y de forma soluble como fusiones amino terminal a MBP producidas en el periplasma de la cepa de *E. coli* HM140 deficiente en proteasas periplásmicas. Las fusiones MBP-V_{HH} se unen específicamente a sus antígenos respectivos y permiten la purificación del dominio V_{HH} con una cola de histidinas (His6) en su extremo C-terminal, tras la escisión de la MBP utilizando una proteasa específica de sitio.

REFERENCES

Aggen, D.H., Chervin, A.S., Insaidoo, F.K., Piepenbrink, K.H., Baker, B.M. and Kranz, D.M., 2011, Identification and engineering of human variable regions that allow expression of stable single-chain T cell receptors. Protein engineering, design & selection : PEDS 24, 361-72.

Ahmadvand, D., Rasaee, M.J., Rahbarizadeh, F., Kontermann, R.E. and Sheikholislami, F., 2009, Cell selection and characterization of a novel human endothelial cell specific nanobody. Molecular immunology 46, 1814-23.

Alvarez-Rueda, N., Behar, G., Ferre, V., Pugniere, M., Roquet, F., Gastinel, L., Jacquot, C., Aubry, J., Baty, D., Barbet, J. and Birkle, S., 2007, Generation of llama single-domain antibodies against methotrexate, a prototypical hapten. Molecular immunology 44, 1680-90.

Arbabi Ghahroudi, M., Desmyter, A., Wyns, L., Hamers, R. and Muyldermans, S., 1997, Selection and identification of single domain antibody fragments from camel heavy-chain antibodies. FEBS Letters 414, 521-526.

Arbabi-Ghahroudi, M., MacKenzie, R. and Tanha, J., 2009, Selection of non-aggregating VH binders from synthetic VH phage-display libraries. Methods in molecular biology (Clifton, N.J.) 525, 187-216, xiii.

Arbabi-Ghahroudi, M., Tanha, J. and MacKenzie, R., 2005, Prokaryotic expression of antibodies. Cancer metastasis reviews 24, 501-19.

Arkhipov, A., Shan, Y., Das, R., Endres, N.F., Eastwood, M.P., Wemmer, D.E., Kuriyan, J. and Shaw, D.E., 2013, Architecture and membrane interactions of the EGF receptor. Cell 152, 557-69.

Bach, H., Mazor, Y., Shaky, S., Shoham-Lev, A., Berdichevsky, Y., Gutnick, D.L. and Benhar, I., 2001, Escherichia coli maltose-binding protein as a molecular chaperone for recombinant intracellular cytoplasmic single-chain antibodies. Journal of molecular biology 312, 79-93.

Barbas, C.F., 3rd, Bain, J.D., Hoekstra, D.M. and Lerner, R.A., 1992, Semisynthetic combinatorial antibody libraries: a chemical solution to the diversity problem. Proceedings of the National Academy of Sciences of the United States of America 89, 4457-61.

Barbas, C.F., 3rd, Collet, T.A., Amberg, W., Roben, P., Binley, J.M., Hoekstra, D., Cababa, D., Jones, T.M., Williamson, R.A., Pilkington, G.R. and et al., 1993, Molecular profile of an antibody response to HIV-1 as probed by combinatorial libraries. Journal of molecular biology 230, 812-23.

Barnard, T.J., Dautin, N., Lukacik, P., Bernstein, H.D. and Buchanan, S.K., 2007, Autotransporter structure reveals intra-barrel cleavage followed by conformational changes. Nature structural & molecular biology 14, 1214-20.

Baselga, J. and Arteaga, C.L., 2005, Critical update and emerging trends in epidermal growth factor receptor targeting in cancer. Journal of clinical oncology : official journal of the American Society of Clinical Oncology 23, 2445-59.

Beck, A., Wurch, T., Bailly, C. and Corvaia, N., 2010, Strategies and challenges for the next generation of therapeutic antibodies. Nature reviews. Immunology 10, 345-52.

Beerli, R.R., Bauer, M., Buser, R.B., Gwerder, M., Muntwiler, S., Maurer, P., Saudan, P. and Bachmann, M.F., 2008, Isolation of human monoclonal antibodies by mammalian cell display. Proceedings of the National Academy of Sciences of the United States of America 105, 14336-41.

Berger, M., Shankar, V. and Vafai, A., 2002, Therapeutic applications of monoclonal antibodies. The American journal of the medical sciences 324, 14-30.

Bernstein, H.D., 2007, Are bacterial 'autotransporters' really transporters? Trends in microbiology 15, 441-7.

Bessette, P.H., Rice, J.J. and Daugherty, P.S., 2004, Rapid isolation of high-affinity protein binding peptides using bacterial display. Protein engineering, design & selection : PEDS 17, 731-9.

Binder, U., Matschiner, G., Theobald, I. and Skerra, A., 2010, High-throughput sorting of an Anticalin library via EspP-mediated functional display on the Escherichia coli cell surface. Journal of molecular biology 400, 783-802.

Birch, J.R. and Racher, A.J., 2006, Antibody production. Advanced drug delivery reviews 58, 671-85.

Bird, R.E., Hardman, K.D., Jacobson, J.W., Johnson, S., Kaufman, B.M., Lee, S.M., Lee, T., Pope, S.H., Riordan, G.S. and Whitlow, M., 1988, Single-chain antigen-binding proteins. Science (New York, N.Y.) 242, 423-6.

Blaise, L., Wehnert, A., Steukers, M.P., van den Beucken, T., Hoogenboom, H.R. and Hufton, S.E., 2004, Construction and diversification of yeast cell surface displayed libraries by yeast mating: application to the affinity maturation of Fab antibody fragments. Gene 342, 211-8.

Blattner, F.R., 1997, The Complete Genome Sequence of Escherichia coli K-12. Science (New York, N.Y.) 277, 1453-1462.

Blomfield, I.C., McClain, M.S., Princ, J.A., Calie, P.J. and Eisenstein, B.I., 1991, Type 1 fimbriation and fimE mutants of Escherichia coli K-12. Journal of bacteriology 173, 5298-307.

Bodelon, G., Marin, E. and Fernandez, L.A., 2009, Role of periplasmic chaperones and BamA (YaeT/Omp85) in folding and secretion of intimin from enteropathogenic Escherichia coli strains. Journal of bacteriology 191, 5169-79.

Bodelon, G., Palomino, C. and Fernandez, L.A., 2012, Immunoglobulin domains in Escherichia coli and other enterobacteria: from pathogenesis to applications in antibody technologies. FEMS microbiology reviews.

Boder, E.T., Raeeszadeh-Sarmazdeh, M. and Price, J.V., 2012, Engineering antibodies by yeast display. Archives of biochemistry and biophysics 526, 99-106.

Boder, E.T. and Wittrup, K.D., 2000, Yeast surface display for directed evolution of protein expression, affinity, and stability. Methods in enzymology 328, 430-44.

Bowley, D.R., Labrijn, A.F., Zwick, M.B. and Burton, D.R., 2007, Antigen selection from an HIV-1 immune antibody library displayed on yeast yields many novel antibodies compared to selection from the same library displayed on phage. Protein engineering, design & selection : PEDS 20, 81-90.

Bradbury, A.R. and Marks, J.D., 2004, Antibodies from phage antibody libraries. Journal of immunological methods 290, 29-49.

Bruggemann, M., Spicer, C., Buluwela, L., Rosewell, I., Barton, S., Surani, M.A. and Rabbitts, T.H., 1991, Human antibody production in transgenic mice: expression from 100 kb of the human IgH locus. European journal of immunology 21, 1323-6.

Cai, X. and Garen, A., 1995, Anti-melanoma antibodies from melanoma patients immunized with genetically modified autologous tumor cells: selection of specific antibodies from single-chain Fv fusion phage libraries. Proceedings of the National Academy of Sciences of the United States of America 92, 6537-41.

Campuzano, S., Salema, V., Moreno-Guzman, M., Gamella, M., Yanez-Sedeno, P., Fernandez, L.A. and Pingarron, J.M., 2014, Disposable amperometric magnetoimmunosensors using nanobodies as biorecognition element. Determination of fibrinogen in plasma. Biosensors & bioelectronics 52, 255-60.

Carter, P., Bedouelle, H. and Winter, G., 1985, Improved oligonucleotide site-directed mutagenesis using M13 vectors. Nucleic acids research 13, 4431-43.

Carter, P.J., 2006, Potent antibody therapeutics by design. Nature reviews. Immunology 6, 343-57.

Chester, K.A., Begent, R.H., Robson, L., Keep, P., Pedley, R.B., Boden, J.A., Boxer, G., Green, A., Winter, G., Cochet, O. and et al., 1994, Phage libraries for generation of clinically useful antibodies. Lancet 343, 455-6.

Christmann, A., Walter, K., Wentzel, A., Kratzner, R. and Kolmar, H., 1999, The cystine knot of a squash-type protease inhibitor as a structural scaffold for Escherichia coli cell

surface display of conformationally constrained peptides. Protein engineering 12, 797-806.

Clackson, T., Hoogenboom, H.R., Griffiths, A.D. and Winter, G., 1991, Making antibody fragments using phage display libraries. Nature 352, 624-8.

Colby, D.W., Garg, P., Holden, T., Chao, G., Webster, J.M., Messer, A., Ingram, V.M. and Wittrup, K.D., 2004, Development of a human light chain variable domain (V(L)) intracellular antibody specific for the amino terminus of huntingtin via yeast surface display. Journal of molecular biology 342, 901-12.

Cossins, A.J., Harrison, S., Popplewell, A.G. and Gore, M.G., 2007, Recombinant production of a VL single domain antibody in Escherichia coli and analysis of its interaction with peptostreptococcal protein L. Protein expression and purification 51, 253-9.

Cuesta, A.M., Sanchez-Martin, D., Blanco-Toribio, A., Villate, M., Enciso-Alvarez, K., Alvarez-Cienfuegos, A., Sainz-Pastor, N., Sanz, L., Blanco, F.J. and Alvarez-Vallina, L., 2012, Improved stability of multivalent antibodies containing the human collagen XV trimerization domain. mAbs 4, 226-32.

Dane, K.Y., Gottstein, C. and Daugherty, P.S., 2009, Cell surface profiling with peptide libraries yields ligand arrays that classify breast tumor subtypes. Molecular cancer therapeutics 8, 1312-8.

Daugherty, P.S., 2007, Protein engineering with bacterial display. Current opinion in structural biology 17, 474-80.

Daugherty, P.S., Chen, G., Olsen, M.J., Iverson, B.L. and Georgiou, G., 1998, Antibody affinity maturation using bacterial surface display. Protein engineering 11, 825-32.

Daugherty, P.S., Olsen, M.J., Iverson, B.L. and Georgiou, G., 1999, Development of an optimized expression system for the screening of antibody libraries displayed on the Escherichia coli surface. Protein engineering 12, 613-21.

Davies, J. and Riechmann, L., 1994, 'Camelising' human antibody fragments: NMR studies on VH domains. FEBS Lett 339, 285-90.

de Kruif, J., Terstappen, L., Boel, E. and Logtenberg, T., 1995, Rapid selection of cell subpopulation-specific human monoclonal antibodies from a synthetic phage antibody library. Proceedings of the National Academy of Sciences of the United States of America 92, 3938-42.

Deramchia, K., Jacobin-Valat, M.J., Laroche-Traineau, J., Bonetto, S., Sanchez, S., Dos Santos, P., Massot, P., Franconi, J.M., Martineau, P. and Clofent-Sanchez, G., 2012, By-Passing Large Screening Experiments Using Sequencing as a Tool to Identify scFv Fragments Targeting Atherosclerotic Lesions in a Novel In Vivo Phage Display Selection. International journal of molecular sciences 13, 6902-23.

Desmyter, A., Transue, T.R., Ghahroudi, M.A., Thi, M.H., Poortmans, F., Hamers, R., Muyldermans, S. and Wyns, L., 1996, Crystal structure of a camel single-domain VH antibody fragment in complex with lysozyme. Nature structural biology 3, 803-11.

Dooley, H., 2003, Selection and characterization of naturally occurring single-domain (IgNAR) antibody fragments from immunized sharks by phage display. Molecular immunology 40, 25-33.

Dudek, M.M., Lindahl, T.L. and Killard, A.J., 2010, Development of a point of care lateral flow device for measuring human plasma fibrinogen. Analytical chemistry 82, 2029-35.

Dumoulin, M., Conrath, K., Van Meirhaeghe, A., Meersman, F., Heremans, K., Frenken, L.G., Muyldermans, S., Wyns, L. and Matagne, A., 2002, Single-domain antibody fragments with high conformational stability. Protein science : a publication of the Protein Society 11, 500-15.

Fairman, J.W., Dautin, N., Wojtowicz, D., Liu, W., Noinaj, N., Barnard, T.J., Udho, E., Przytycka, T.M., Cherezov, V. and Buchanan, S.K., 2012, Crystal structures of the outer membrane domain of intimin and invasin from enterohemorrhagic E. coli and

enteropathogenic Y. pseudotuberculosis. Structure (London, England : 1993) 20, 1233-43.

Feldhaus, M.J. and Siegel, R.W., 2004, Yeast display of antibody fragments: a discovery and characterization platform. Journal of immunological methods 290, 69-80.

Feldhaus, M.J., Siegel, R.W., Opresko, L.K., Coleman, J.R., Feldhaus, J.M., Yeung, Y.A., Cochran, J.R., Heinzelman, P., Colby, D., Swers, J., Graff, C., Wiley, H.S. and Wittrup, K.D., 2003, Flow-cytometric isolation of human antibodies from a nonimmune Saccharomyces cerevisiae surface display library. Nature biotechnology 21, 163-70.

Fernandez, L.A., Sola, I., Enjuanes, L. and de Lorenzo, V., 2000, Specific Secretion of Active Single-Chain Fv Antibodies into the Supernatants of Escherichia coli Cultures by Use of the Hemolysin System. Applied and Environmental Microbiology 66, 5024-5029.

Flajnik, M.F., Deschacht, N. and Muyldermans, S., 2011, A case of convergence: why did a simple alternative to canonical antibodies arise in sharks and camels? PLoS biology 9, e1001120.

Fleetwood, F., Devoogdt, N., Pellis, M., Wernery, U., Muyldermans, S., Stahl, S. and Lofblom, J., 2012, Surface display of a single-domain antibody library on Gram-positive bacteria. Cellular and molecular life sciences : CMLS.

Fraile, S., Munoz, A., de Lorenzo, V. and Fernandez, L.A., 2004, Secretion of proteins with dimerization capacity by the haemolysin type I transport system of Escherichia coli. Molecular microbiology 53, 1109-21.

Francisco, J.A., Campbell, R., Iverson, B.L. and Georgiou, G., 1993, Production and fluorescence-activated cell sorting of Escherichia coli expressing a functional antibody fragment on the external surface. Proceedings of the National Academy of Sciences of the United States of America 90, 10444-8.

Frankel, G. and Phillips, A.D., 2008, Attaching effacing Escherichia coli and paradigms of Tir-triggered actin polymerization: getting off the pedestal. Cellular microbiology 10, 549-56.

Frenken, L.G., van der Linden, R.H., Hermans, P.W., Bos, J.W., Ruuls, R.C., de Geus, B. and Verrips, C.T., 2000, Isolation of antigen specific llama VHH antibody fragments and their high level secretion by Saccharomyces cerevisiae. Journal of biotechnology 78, 11-21.

Gauthier, A. and Finlay, B.B., 2003, Translocated Intimin Receptor and Its Chaperone Interact with ATPase of the Type III Secretion Apparatus of Enteropathogenic Escherichia coli. Journal of bacteriology 185, 6747-6755.

Gill, G.N., Kawamoto, T., Cochet, C., Le, A., Sato, J.D., Masui, H., McLeod, C. and Mendelsohn, J., 1984, Monoclonal anti-epidermal growth factor receptor antibodies which are inhibitors of epidermal growth factor binding and antagonists of epidermal growth factor binding and antagonists of epidermal growth factor-stimulated tyrosine protein kinase activity. The Journal of biological chemistry 259, 7755-60.

Govaert, J., Pellis, M., Deschacht, N., Vincke, C., Conrath, K., Muyldermans, S. and Saerens, D., 2012, Dual beneficial effect of interloop disulfide bond for single domain antibody fragments. The Journal of biological chemistry 287, 1970-9.

Greenberg, A.S., Avila, D., Hughes, M., Hughes, A., McKinney, E.C. and Flajnik, M.F., 1995, A new antigen receptor gene family that undergoes rearrangement and extensive somatic diversification in sharks. Nature 374, 168-73.

Griffiths, A.D., Williams, S.C., Hartley, O., Tomlinson, I.M., Waterhouse, P., Crosby, W.L., Kontermann, R.E., Jones, P.T., Low, N.M., Allison, T.J. and et al., 1994, Isolation of high affinity human antibodies directly from large synthetic repertoires. The EMBO journal 13, 3245-60.

Grodberg, J. and Dunn, J.J., 1988, ompT encodes the Escherichia coli outer membrane protease that cleaves T7 RNA polymerase during purification. Journal of bacteriology 170, 1245-53.

Gruss, F., Zahringer, F., Jakob, R.P., Burmann, B.M., Hiller, S. and Maier, T., 2013, The structural basis of autotransporter translocation by TamA. Nature structural & molecular biology 20, 1318-20.

Gullick, W.J., 1991, Prevalence of aberrant expression of the epidermal growth factor receptor in human cancers. British medical bulletin 47, 87-98.

Hall, S.S., Mitragotri, S. and Daugherty, P.S., 2007, Identification of peptide ligands facilitating nanoparticle attachment to erythrocytes. Biotechnology progress 23, 749-54.

Hamers-Casterman, C., Atarhouch, T., Muyldermans, S., Robinson, G., Hamers, C., Songa, E.B., Bendahman, N. and Hamers, R., 1993, Naturally occurring antibodies devoid of light chains. Nature 363, 446-8.

Harvey, B.R., Georgiou, G., Hayhurst, A., Jeong, K.J., Iverson, B.L. and Rogers, G.K., 2004, Anchored periplasmic expression, a versatile technology for the isolation of high-affinity antibodies from Escherichia coli-expressed libraries. Proceedings of the National Academy of Sciences of the United States of America 101, 9193-8.

Ho, M., Nagata, S. and Pastan, I., 2006, Isolation of anti-CD22 Fv with high affinity by Fv display on human cells. Proceedings of the National Academy of Sciences of the United States of America 103, 9637-42.

Holliger, P. and Hudson, P.J., 2005, Engineered antibody fragments and the rise of single domains. Nature biotechnology 23, 1126-36.

Holt, L.J., Basran, A., Jones, K., Chorlton, J., Jespers, L.S., Brewis, N.D. and Tomlinson, I.M., 2008, Anti-serum albumin domain antibodies for extending the half-lives of short lived drugs. Protein engineering, design & selection : PEDS 21, 283-8.

Honegger, A.M., Szapary, D., Schmidt, A., Lyall, R., Van Obberghen, E., Dull, T.J., Ullrich, A. and Schlessinger, J., 1987, A mutant epidermal growth factor receptor with defective protein tyrosine kinase is unable to stimulate proto-oncogene expression and DNA synthesis. Molecular and cellular biology 7, 4568-71.

Hoogenboom, H.R., 2005, Selecting and screening recombinant antibody libraries. Nature biotechnology 23, 1105-16.

Hoogenboom, H.R. and Winter, G., 1992, By-passing immunisation. Human antibodies from synthetic repertoires of germline VH gene segments rearranged in vitro. Journal of molecular biology 227, 381-8.

Hu, S., Shively, L., Raubitschek, A., Sherman, M., Williams, L.E., Wong, J.Y., Shively, J.E. and Wu, A.M., 1996, Minibody: A novel engineered anti-carcinoembryonic antigen antibody fragment (single-chain Fv-CH3) which exhibits rapid, high-level targeting of xenografts. Cancer research 56, 3055-61.

Huang, P.H., Xu, A.M. and White, F.M., 2009, Oncogenic EGFR signaling networks in glioma. Science signaling 2, re6.

Hudson, P.J. and Kortt, A.A., 1999, High avidity scFv multimers; diabodies and triabodies. Journal of immunological methods 231, 177-89.

Hussack, G., Keklikian, A., Alsughayyir, J., Hanifi-Moghaddam, P., Arbabi-Ghahroudi, M., van Faassen, H., Hou, S.T., Sad, S., MacKenzie, R. and Tanha, J., 2012, A V(L) single-domain antibody library shows a high-propensity to yield non-aggregating binders. Protein engineering, design & selection : PEDS 25, 313-8.

Hust, M. and Dubel, S., 2004, Mating antibody phage display with proteomics. Trends in biotechnology 22, 8-14.

Hust, M. and Dubel, S., 2005, Phage display vectors for the in vitro generation of human antibody fragments. Methods in molecular biology (Clifton, N.J.) 295, 71-96.

Hust, M., Jostock, T., Menzel, C., Voedisch, B., Mohr, A., Brenneis, M., Kirsch, M.I., Meier, D. and Dubel, S., 2007, Single chain Fab (scFab) fragment. BMC biotechnology 7, 14.

Jakobovits, A., Amado, R.G., Yang, X., Roskos, L. and Schwab, G., 2007, From XenoMouse technology to panitumumab, the first fully human antibody product from transgenic mice. Nature biotechnology 25, 1134-43.

Jespers, L., Schon, O., Famm, K. and Winter, G., 2004, Aggregation-resistant domain antibodies selected on phage by heat denaturation. Nature biotechnology 22, 1161-5.

Jose, J. and Meyer, T.F., 2007, The autodisplay story, from discovery to biotechnical and biomedical applications. Microbiology and molecular biology reviews : MMBR 71, 600-19.

Jurado, P., de Lorenzo, V. and Fernandez, L.A., 2006, Thioredoxin fusions increase folding of single chain Fv antibodies in the cytoplasm of Escherichia coli: evidence that chaperone activity is the prime effect of thioredoxin. Journal of molecular biology 357, 49-61.

Jurado, P., Ritz, D., Beckwith, J., de Lorenzo, V. and Fernandez, L.A., 2002, Production of functional single-chain Fv antibodies in the cytoplasm of Escherichia coli. Journal of molecular biology 320, 1-10.

Kamath, S. and Lip, G.Y.H., 2003, Fibrinogen: biochemistry, epidemiology and determinants. Qjm 96, 711-729.

Kanamori, T., Fujino, Y. and Ueda, T., 2014, PURE ribosome display and its application in antibody technology. Biochimica et biophysica acta.

Keen, N.T. and Tamaki, S., 1986, Structure of two pectate lyase genes from Erwinia chrysanthemi EC16 and their high-level expression in Escherichia coli. Journal of bacteriology 168, 595-606.

Kenny, B., DeVinney, R., Stein, M., Reinscheid, D.J., Frey, E.A. and Finlay, B.B., 1997, Enteropathogenic E. coli (EPEC) transfers its receptor for intimate adherence into mammalian cells. Cell 91, 511-20.

Kenrick, S.A. and Daugherty, P.S., 2010, Bacterial display enables efficient and quantitative peptide affinity maturation. Protein engineering, design & selection : PEDS 23, 9-17.

Kettleborough, C.A., Ansell, K.H., Allen, R.W., Rosell-Vives, E., Gussow, D.H. and Bendig, M.M., 1994, Isolation of tumor cell-specific single-chain Fv from immunized mice using phage-antibody libraries and the re-construction of whole antibodies from these antibody fragments. European journal of immunology 24, 952-8.

Koebnik, R., Locher, K.P. and Van Gelder, P., 2000, Structure and function of bacterial outer membrane proteins: barrels in a nutshell. Molecular microbiology 37, 239-53.

Kohler, G. and Milstein, C., 1975, Continuous cultures of fused cells secreting antibody of predefined specificity. Nature 256, 495-7.

Kronqvist, N., Lofblom, J., Jonsson, A., Wernerus, H. and Stahl, S., 2008, A novel affinity protein selection system based on staphylococcal cell surface display and flow cytometry. Protein engineering, design & selection : PEDS 21, 247-55.

Lai, Y., Rosenshine, I., Leong, J. and Frankel, G., 2013, Intimate host attachment: enteropathogenic and enterohaemorrhagic Escherichia coli. Cellular microbiology.

Lang, I.M., Barbas, C.F., 3rd and Schleef, R.R., 1996, Recombinant rabbit Fab with binding activity to type-1 plasminogen activator inhibitor derived from a phage-display library against human alpha-granules. Gene 172, 295-8.

Lauwereys, M., Arbabi Ghahroudi, M., Desmyter, A., Kinne, J., Holzer, W., De Genst, E., Wyns, L. and Muyldermans, S., 1998, Potent enzyme inhibitors derived from dromedary heavy-chain antibodies. The EMBO journal 17, 3512-20.

Lee, E.C., Liang, Q., Ali, H., Bayliss, L., Beasley, A., Bloomfield-Gerdes, T., Bonoli, L., Brown, R., Campbell, J., Carpenter, A., Chalk, S., Davis, A., England, N., Fane-Dremucheva, A., Franz, B., Germaschewski, V., Holmes, H., Holmes, S., Kirby, I.,

Kosmac, M., Legent, A., Lui, H., Manin, A., O'Leary, S., Paterson, J., Sciarrillo, R., Speak, A., Spensberger, D., Tuffery, L., Waddell, N., Wang, W., Wells, S., Wong, V., Wood, A., Owen, M.J., Friedrich, G.A. and Bradley, A., 2014, Complete humanization of the mouse immunoglobulin loci enables efficient therapeutic antibody discovery. Nature biotechnology.

Leo, J.C., Grin, I. and Linke, D., 2012, Type V secretion: mechanism(s) of autotransport through the bacterial outer membrane. Philosophical transactions of the Royal Society of London. Series B, Biological sciences 367, 1088-101.

Leyton, D.L., Rossiter, A.E. and Henderson, I.R., 2012a, From self sufficiency to dependence: mechanisms and factors important for autotransporter biogenesis. Nature Reviews Microbiology 10, 213-225.

Leyton, D.L., Rossiter, A.E. and Henderson, I.R., 2012b, From self sufficiency to dependence: mechanisms and factors important for autotransporter biogenesis. Nature reviews. Microbiology 10, 213-25.

Lin, S., Houston-Cummings, N.R., Prinz, B., Moore, R., Bobrowicz, B., Davidson, R.C., Wildt, S., Stadheim, T.A. and Zha, D., 2012, A novel fragment of antigen binding (Fab) surface display platform using glycoengineered Pichia pastoris. Journal of immunological methods 375, 159-65.

Little, L.E., Dane, K.Y., Daugherty, P.S., Healy, K.E. and Schaffer, D.V., 2011, Exploiting bacterial peptide display technology to engineer biomaterials for neural stem cell culture. Biomaterials 32, 1484-94.

Lofblom, J., 2011, Bacterial display in combinatorial protein engineering. Biotechnology journal 6, 1115-29.

Lowe, G.D., Rumley, A. and Mackie, I.J., 2004, Plasma fibrinogen. Annals of clinical biochemistry 41, 430-40.

Luo, Y., Frey, E.A., Pfuetzner, R.A., Creagh, A.L., Knoechel, D.G., Haynes, C.A., Finlay, B.B. and Strynadka, N.C., 2000, Crystal structure of enteropathogenic Escherichia coli intimin-receptor complex. Nature 405, 1073-7.

Ma, Y., Qian, Y. and Lv, W., 2007, The Correlation between Plasma Fibrinogen Levels and the Clinical Features of Patients with Ovarian Carcinoma. Journal of International Medical Research 35, 678-684.

Makela, A.R. and Oker-Blom, C., 2008, The baculovirus display technology--an evolving instrument for molecular screening and drug delivery. Combinatorial chemistry & high throughput screening 11, 86-98.

Marin, E., Bodelon, G. and Fernandez, L.A., 2010, Comparative analysis of the biochemical and functional properties of C-terminal domains of autotransporters. Journal of bacteriology 192, 5588-602.

Martsev, S.P., Tsybovsky, Y.I., Stremovskiy, O.A., Odintsov, S.G., Balandin, T.G., Arosio, P., Kravchuk, Z.I. and Deyev, S.M., 2004, Fusion of the antiferritin antibody VL domain to barnase results in enhanced solubility and altered pH stability. Protein engineering, design & selection : PEDS 17, 85-93.

Mazor, Y., Van Blarcom, T., Carroll, S. and Georgiou, G., 2010, Selection of full-length IgGs by tandem display on filamentous phage particles and Escherichia coli fluorescence-activated cell sorting screening. FEBS J 277, 2291-303.

Mazor, Y., Van Blarcom, T., Mabry, R., Iverson, B.L. and Georgiou, G., 2007, Isolation of engineered, full-length antibodies from libraries expressed in Escherichia coli. Nature biotechnology 25, 563-5.

McCafferty, J., Fitzgerald, K.J., Earnshaw, J., Chiswell, D.J., Link, J., Smith, R. and Kenten, J., 1994, Selection and rapid purification of murine antibody fragments that bind a transition-state analog by phage display. Applied biochemistry and biotechnology 47, 157-71; discussion 171-3.

McCafferty, J., Griffiths, A.D., Winter, G. and Chiswell, D.J., 1990, Phage antibodies: filamentous phage displaying antibody variable domains. Nature 348, 552-4.

Meerman, H.J. and Georgiou, G., 1994, Construction and characterization of a set of E. coli strains deficient in all known loci affecting the proteolytic stability of secreted recombinant proteins. Bio/technology (Nature Publishing Company) 12, 1107-10.

Monegal, A., Ami, D., Martinelli, C., Huang, H., Aliprandi, M., Capasso, P., Francavilla, C., Ossolengo, G. and de Marco, A., 2009, Immunological applications of single-domain llama recombinant antibodies isolated from a naive library. Protein engineering, design & selection : PEDS 22, 273-80.

Munera, D., Palomino, C. and Fernandez, L.A., 2008, Specific residues in the N-terminal domain of FimH stimulate type 1 fimbriae assembly in Escherichia coli following the initial binding of the adhesin to FimD usher. Molecular microbiology 69, 911-25.

Muyldermans, S., 2013, Nanobodies: natural single-domain antibodies. Annual review of biochemistry 82, 775-97.

Muyldermans, S., Baral, T.N., Retamozzo, V.C., De Baetselier, P., De Genst, E., Kinne, J., Leonhardt, H., Magez, S., Nguyen, V.K., Revets, H., Rothbauer, U., Stijlemans, B., Tillib, S., Wernery, U., Wyns, L., Hassanzadeh-Ghassabeh, G. and Saerens, D., 2009, Camelid immunoglobulins and nanobody technology. Veterinary immunology and immunopathology 128, 178-83.

Nelson, P.N., Reynolds, G.M., Waldron, E.E., Ward, E., Giannopoulos, K. and Murray, P.G., 2000, Monoclonal antibodies. Molecular pathology : MP 53, 111-7.

Nicolay, T., Vanderleyden, J. and Spaepen, S., 2013, Autotransporter-based cell surface display in Gram-negative bacteria. Critical reviews in microbiology.

Nissim, A., Hoogenboom, H.R., Tomlinson, I.M., Flynn, G., Midgley, C., Lane, D. and Winter, G., 1994, Antibody fragments from a 'single pot' phage display library as immunochemical reagents. The EMBO journal 13, 692-8.

Noinaj, N., Kuszak, A.J., Gumbart, J.C., Lukacik, P., Chang, H., Easley, N.C., Lithgow, T. and Buchanan, S.K., 2013, Structural insight into the biogenesis of beta-barrel membrane proteins. Nature 501, 385-90.

Oh, M.Y., Joo, H.Y., Hur, B.U., Jeong, Y.H. and Cha, S.H., 2007, Enhancing phage display of antibody fragments using gIII-amber suppression. Gene 386, 81-9.

Ohlin, M. and Zouali, M., 2003, The human antibody repertoire to infectious agents: implications for disease pathogenesis. Molecular immunology 40, 1-11.

Onat, A., Ozhan, H., Erbilen, E., Albayrak, S., Kucukdurmaz, Z., Can, G., Keles, I. and Hergenc, G., 2009, Independent prediction of metabolic syndrome by plasma fibrinogen in men, and predictors of elevated levels. International journal of cardiology 135, 211-7.

Oomen, C.J., van Ulsen, P., van Gelder, P., Feijen, M., Tommassen, J. and Gros, P., 2004, Structure of the translocator domain of a bacterial autotransporter. The EMBO journal 23, 1257-66.

Otto, B.R., Sijbrandi, R., Luirink, J., Oudega, B., Heddle, J.G., Mizutani, K., Park, S.Y. and Tame, J.R., 2005, Crystal structure of hemoglobin protease, a heme binding autotransporter protein from pathogenic Escherichia coli. The Journal of biological chemistry 280, 17339-45.

Palumbo, J.S., Kombrinck, K.W., Drew, A.F., Grimes, T.S., Kiser, J.H., Degen, J.L. and Bugge, T.H., 2000, Fibrinogen is an important determinant of the metastatic potential of circulating tumor cells. Blood 96, 3302-9.

Pandey, M. and Mahadevan, D., 2014, Monoclonal antibodies as therapeutics in human malignancies. Future oncology (London, England) 10, 609-36.

Pavoni, E., Vaccaro, P., Anastasi, A.M. and Minenkova, O., 2014, Optimized selection of anti-tumor recombinant antibodies from phage libraries on intact cells. Molecular immunology 57, 317-22.

Pluckthun, A., 2012, Ribosome display: a perspective. Methods in molecular biology (Clifton, N.J.) 805, 3-28.

Polterauer, S., Grimm, C., Seebacher, V., Concin, N., Marth, C., Tomovski, C., Husslein, H., Leipold, H., Hefler-Frischmuth, K., Tempfer, C., Reinthaller, A. and Hefler, L., 2009, Plasma fibrinogen levels and prognosis in patients with ovarian cancer: a multicenter study. The oncologist 14, 979-85.

Porter, R.R., 1958, Separation and isolation of fractions of rabbit gamma-globulin containing the antibody and antigenic combining sites. Nature 182, 670-1.

Rajabi-Memari, H., Jalali-Javaran, M., Rasaee, M.J., Rahbarizadeh, F., Forouzandeh-Moghadam, M. and Esmaili, A., 2006, Expression and characterization of a recombinant single-domain monoclonal antibody against MUC1 mucin in tobacco plants. Hybridoma (2005) 25, 209-15.

Rice, J.J., Schohn, A., Bessette, P.H., Boulware, K.T. and Daugherty, P.S., 2006, Bacterial display using circularly permuted outer membrane protein OmpX yields high affinity peptide ligands. Protein science : a publication of the Protein Society 15, 825-36.

Richman, S.A., Aggen, D.H., Dossett, M.L., Donermeyer, D.L., Allen, P.M., Greenberg, P.D. and Kranz, D.M., 2009, Structural features of T cell receptor variable regions that enhance domain stability and enable expression as single-chain ValphaVbeta fragments. Molecular immunology 46, 902-16.

Rondot, S., Koch, J., Breitling, F. and Dubel, S., 2001, A helper phage to improve single-chain antibody presentation in phage display. Nature biotechnology 19, 75-8.

Roovers, R.C., Laeremans, T., Huang, L., De Taeye, S., Verkleij, A.J., Revets, H., de Haard, H.J. and van Bergen en Henegouwen, P.M., 2007, Efficient inhibition of EGFR signaling and of tumour growth by antagonistic anti-EFGR Nanobodies. Cancer immunology, immunotherapy : CII 56, 303-317.

Rothbauer, U., Zolghadr, K., Muyldermans, S., Schepers, A., Cardoso, M.C. and Leonhardt, H., 2008, A versatile nanotrap for biochemical and functional studies with fluorescent fusion proteins. Molecular & cellular proteomics : MCP 7, 282-9.

Rutherford, N. and Mourez, M., 2006, Surface display of proteins by gram-negative bacterial autotransporters. Microbial cell factories 5, 22.

Ryckaert, S., Pardon, E., Steyaert, J. and Callewaert, N., 2010, Isolation of antigen-binding camelid heavy chain antibody fragments (nanobodies) from an immune library displayed on the surface of Pichia pastoris. Journal of biotechnology 145, 93-8.

Salema, V. and Fernandez, L.A., 2013, High yield purification of nanobodies from the periplasm of E. coli as fusions with the maltose binding protein. Protein expression and purification 91, 42-8.

Salema, V., Marín, E., Martínez-Arteaga, R., Ruano-Gallego, D., Fraile, S., Margolles, Y., Teira, X., Gutierrez, C., Bodelón, G. and Fernández, L.Á., 2013, Selection of Single Domain Antibodies from Immune Libraries Displayed on the Surface of E. coli Cells with Two β-Domains of Opposite Topologies. PloS one 8, e75126.

Sato, J.D., Kawamoto, T., Le, A.D., Mendelsohn, J., Polikoff, J. and Sato, G.H., 1983, Biological effects in vitro of monoclonal antibodies to human epidermal growth factor receptors. Molecular biology & medicine 1, 511-29.

Schiefner, A., Chatwell, L., Korner, J., Neumaier, I., Colby, D.W., Volkmer, R., Wittrup, K.D. and Skerra, A., 2011, A disulfide-free single-domain V(L) intrabody with blocking activity towards huntingtin reveals a novel mode of epitope recognition. Journal of molecular biology 414, 337-55.

Schmiedl, A., Breitling, F., Winter, C.H., Queitsch, I. and Dubel, S., 2000, Effects of unpaired cysteines on yield, solubility and activity of different recombinant antibody constructs expressed in E. coli. Journal of immunological methods 242, 101-14.

Schnaitman, C.A., 1973, Outer membrane proteins of Escherichia coli. I. Effect of preparative conditions on the migration of protein in polyacrylamide gels. Archives of biochemistry and biophysics 157, 541-52.

Schroff, R.W., Foon, K.A., Beatty, S.M., Oldham, R.K. and Morgan, A.C., Jr., 1985, Human anti-murine immunoglobulin responses in patients receiving monoclonal antibody therapy. Cancer research 45, 879-85.

Scott, A.M., Wolchok, J.D. and Old, L.J., 2012, Antibody therapy of cancer. Nature reviews. Cancer 12, 278-87.

Selmeci, L., Seres, L., Szekely, M., Soos, P. and Acsady, G., 2010, Assay of oxidized fibrinogen reactivity (OFR) as a biomarker of oxidative stress in human plasma: the role of lysine analogs. Clinical chemistry and laboratory medicine : CCLM / FESCC 48, 379-82.

Seymour, J.F., 2004, New treatment approaches to indolent non-Hodgkin's lymphoma. Seminars in oncology 31, 27-32.

Smith, F.B., Rumley, A., Lee, A.J., Leng, G.C., Fowkes, F.G. and Lowe, G.D., 1998, Haemostatic factors and prediction of ischaemic heart disease and stroke in claudicants. British journal of haematology 100, 758-63.

Smith, G.P., 1985, Filamentous fusion phage: novel expression vectors that display cloned antigens on the virion surface. Science (New York, N.Y.) 228, 1315-7.

Soltes, G., Hust, M., Ng, K.K., Bansal, A., Field, J., Stewart, D.I., Dubel, S., Cha, S. and Wiersma, E.J., 2007, On the influence of vector design on antibody phage display. Journal of biotechnology 127, 626-37.

Stijlemans, B., Conrath, K., Cortez-Retamozo, V., Van Xong, H., Wyns, L., Senter, P., Revets, H., De Baetselier, P., Muyldermans, S. and Magez, S., 2004, Efficient targeting of conserved cryptic epitopes of infectious agents by single domain antibodies. African trypanosomes as paradigm. The Journal of biological chemistry 279, 1256-61.

Studier, F.W. and Moffatt, B.A., 1986, Use of bacteriophage T7 RNA polymerase to direct selective high-level expression of cloned genes. Journal of molecular biology 189, 113-30.

Sun, Y., Ning, B., Liu, M., Gao, X., Fan, X., Liu, J. and Gao, Z., 2012, Selection of diethylstilbestrol-specific single-chain antibodies from a non-immunized mouse ribosome display library. PloS one 7, e33186.

Tijink, B.M., Laeremans, T., Budde, M., Stigter-van Walsum, M., Dreier, T., de Haard, H.J., Leemans, C.R. and van Dongen, G.A., 2008, Improved tumor targeting of anti-epidermal growth factor receptor Nanobodies through albumin binding: taking advantage of modular Nanobody technology. Molecular cancer therapeutics 7, 2288-97.

van Bloois, E., Winter, R.T., Kolmar, H. and Fraaije, M.W., 2011, Decorating microbes: surface display of proteins on Escherichia coli. Trends in biotechnology 29, 79-86.

van den Beucken, T., Pieters, H., Steukers, M., van der Vaart, M., Ladner, R.C., Hoogenboom, H.R. and Hufton, S.E., 2003, Affinity maturation of Fab antibody fragments by fluorescent-activated cell sorting of yeast-displayed libraries. FEBS Letters 546, 288-294.

van den Beucken, T., van Neer, N., Sablon, E., Desmet, J., Celis, L., Hoogenboom, H.R. and Hufton, S.E., 2001, Building novel binding ligands to B7.1 and B7.2 based on human antibody single variable light chain domains. Journal of molecular biology 310, 591-601.

van der Linden, R.H., Frenken, L.G., de Geus, B., Harmsen, M.M., Ruuls, R.C., Stok, W., de Ron, L., Wilson, S., Davis, P. and Verrips, C.T., 1999, Comparison of physical chemical properties of llama VHH antibody fragments and mouse monoclonal antibodies. Biochimica et biophysica acta 1431, 37-46.

Van Ewijk, W., de Kruif, J., Germeraad, W.T., Berendes, P., Ropke, C., Platenburg, P.P. and Logtenberg, T., 1997, Subtractive isolation of phage-displayed single-chain antibodies to thymic stromal cells by using intact thymic fragments. Proceedings of the National Academy of Sciences of the United States of America 94, 3903-8.

Vaneycken, I., D'Huyvetter, M., Hernot, S., De Vos, J., Xavier, C., Devoogdt, N., Caveliers, V. and Lahoutte, T., 2011, Immuno-imaging using nanobodies. Current opinion in biotechnology 22, 877-81.

Vaughan, T.J., Williams, A.J., Pritchard, K., Osbourn, J.K., Pope, A.R., Earnshaw, J.C., McCafferty, J., Hodits, R.A., Wilton, J. and Johnson, K.S., 1996, Human antibodies with sub-nanomolar affinities isolated from a large non-immunized phage display library. Nature biotechnology 14, 309-14.

Veiga, E., de Lorenzo, V. and Fernandez, L.A., 1999, Probing secretion and translocation of a beta-autotransporter using a reporter single-chain Fv as a cognate passenger domain. Molecular microbiology 33, 1232-43.

Veiga, E., de Lorenzo, V. and Fernandez, L.A., 2004, Structural tolerance of bacterial autotransporters for folded passenger protein domains. Molecular microbiology 52, 1069-80.

Vodnik, M., Zager, U., Strukelj, B. and Lunder, M., 2011, Phage display: selecting straws instead of a needle from a haystack. Molecules 16, 790-817.

Vosjan, M.J., Vercammen, J., Kolkman, J.A., Stigter-van Walsum, M., Revets, H. and van Dongen, G.A., 2012, Nanobodies targeting the hepatocyte growth factor: potential new drugs for molecular cancer therapy. Molecular cancer therapeutics 11, 1017-25.

Ward, E.S., Gussow, D., Griffiths, A.D., Jones, P.T. and Winter, G., 1989, Binding activities of a repertoire of single immunoglobulin variable domains secreted from Escherichia coli. Nature 341, 544-6.

Weaver-Feldhaus, J.M., Lou, J., Coleman, J.R., Siegel, R.W., Marks, J.D. and Feldhaus, M.J., 2004, Yeast mating for combinatorial Fab library generation and surface display. FEBS Letters 564, 24-34.

Wen, F., Sethi, D.K., Wucherpfennig, K.W. and Zhao, H., 2011, Cell surface display of functional human MHC class II proteins: yeast display versus insect cell display. Protein engineering, design & selection : PEDS 24, 701-9.

Wentzel, A., Christmann, A., Adams, T. and Kolmar, H., 2001, Display of passenger proteins on the surface of Escherichia coli K-12 by the enterohemorrhagic E. coli intimin EaeA. Journal of bacteriology 183, 7273-84.

Wernerus, H. and Stahl, S., 2004, Biotechnological applications for surface-engineered bacteria. Biotechnology and applied biochemistry 40, 209-28.

Wesolowski, J., Alzogaray, V., Reyelt, J., Unger, M., Juarez, K., Urrutia, M., Cauerhff, A., Danquah, W., Rissiek, B., Scheuplein, F., Schwarz, N., Adriouch, S., Boyer, O., Seman, M., Licea, A., Serreze, D.V., Goldbaum, F.A., Haag, F. and Koch-Nolte, F., 2009, Single domain antibodies: promising experimental and therapeutic tools in infection and immunity. Medical microbiology and immunology 198, 157-74.

Wilhelm, S., Rosenau, F., Kolmar, H. and Jaeger, K.E., 2011, Autotransporters with GDSL passenger domains: molecular physiology and biotechnological applications. Chembiochem : a European journal of chemical biology 12, 1476-85.

Winter, G., Griffiths, A.D., Hawkins, R.E. and Hoogenboom, H.R., 1994, Making antibodies by phage display technology. Annual review of immunology 12, 433-55.

Yamanaka, H.I., Inoue, T. and Ikeda-Tanaka, O., 1996, Chicken monoclonal antibody isolated by a phage display system. Journal of immunology (Baltimore, Md. : 1950) 157, 1156-62.

Yamashita, H., Kitayama, J. and Nagawa, H., 2005, Hyperfibrinogenemia is a useful predictor for lymphatic metastasis in human gastric cancer. Japanese journal of clinical oncology 35, 595-600.

Yeung, Y.A. and Wittrup, K.D., 2002, Quantitative screening of yeast surface-displayed polypeptide libraries by magnetic bead capture. Biotechnology progress 18, 212-20.

Zaczek, A., Brandt, B. and Bielawski, K.P., 2005, The diverse signaling network of EGFR, HER2, HER3 and HER4 tyrosine kinase receptors and the consequences for therapeutic approaches. Histology and histopathology 20, 1005-15.

Zell, R. and Fritz, H.J., 1987, DNA mismatch-repair in Escherichia coli counteracting the hydrolytic deamination of 5-methyl-cytosine residues. The EMBO journal 6, 1809-15.

Zou, J., Dickerson, M.T., Owen, N.K., Landon, L.A. and Deutscher, S.L., 2004, Biodistribution of filamentous phage peptide libraries in mice. Molecular biology reports 31, 121-9.

Zude, I., Leimbach, A. and Dobrindt, U., 2013, Prevalence of autotransporters in Escherichia coli: what is the impact of phylogeny and pathotype? International journal of medical microbiology : IJMM.

ANNEXURES